NASA CONTRACTOR REPORT

NASA CR-52

NASA CR-52

ELECTROTHERMAL ENGINE PROPELLANT STORAGE AND FEED SYSTEM STUDY

PHASE II

by G. E. Roos et al.

Prepared under Contract No. NAS 8-2574 *by*
BEACH AIRCRAFT CORPORATION
Boulder, Colorado
for

NATIONAL AERONAUTICS AND SPACE ADMINISTRATION • WASHINGTON, D. C. • MAY 1964

ELECTROTHERMAL ENGINE PROPELLANT STORAGE AND FEED SYSTEM STUDY

PHASE II

By G. E. Roos, J. E. Bell, J. M. Lester, L. R. Dorman,
H. E. Sutton, and B. H. Dean

Prepared under Contract No. NAS 8-2574 by
BEECH AIRCRAFT CORPORATION
Boulder, Colorado

for

NATIONAL AERONAUTICS AND SPACE ADMINISTRATION

For sale by the Office of Technical Services, Department of Commerce,
Washington, D.C. 20230 -- Price $3.00

FOREWORD

This document reports the technical data generated in compliance with NASA Contract No. NAS8-2574. The report was prepared for Lewis Research Center, NASA, Cleveland, Ohio. The following NASA personnel have managed the contract:

Mr. John E. Hickey - Contracting Office
Mr. Henry Hunczak - Technical Manager
Mr. John Deford - Contract Administrator

This document was prepared by Beech Aircraft Corporation, Boulder Division, Boulder, Colorado. Beech technical personnel contributing to the project include:

G. A. Ausburn
J. E. Bell
W. H. Bowman
L. R. Dorman
J. M. Lester
D. W. Lunsford
J. A. Pike
G. E. Roos
G. E. Ross
J. E. Schrodt
H. E. Sutton

Engine and feed system interface problems were coordinated with Plasmadyne Corporation, Santa Ana, California.

TABLE OF CONTENTS

TABLE OF CONTENTS (Cont'd)

LIST OF FIGURES

LIST OF TABLES

INTRODUCTION

This report includes work conducted on propellant storage and feed systems for electrothermal propulsion engines. The propulsion system would be used to locate and point space vehicles for various purposes. Much of the work in this report is directed toward the specific application of electrothermal thrusters to control of stationary communications satellites for periods of up to three years.

The function of the storage system is to contain and deliver a single phase fluid propellant to an engine or group of engines at specific thermodynamic conditions in a space environment. The Beech approach to solving the design problems in the most lightweight and reliable way is divided into two categories of work:

1. General design studies.
2. Specific mission design program.

The general design studies consist of detailed analyses of storage and feed system concepts. In support of this work, several testing programs were carried out.

The specific mission design program consists of lightweight designs for storage and feed systems following definite mission profile specifications. Layout drawings were made, and preliminary specifications were established for critical components.

1.0 SUMMARY

Storage and feed systems are analyzed for hydrogen and ammonia. Both propellants are stored in the liquid phase. Long-term containment of liquid hydrogen is difficult. The analysis of hydrogen storage required most of the effort expended in this study. The technical approach used for both propellants is summarized as follows:

1.1 General Design Studies (H_2 and NH_3 propellants)

A firm basis is established for detailed design of specific systems.

1.1.1 Design Approach

A. Promising storage concepts are proposed and discussed.

B. The feasibility of concepts is justified by calculations and design layouts.

C. Testing is performed to back-up theoretical studies.

D. Interface problems of various systems are coordinated with engine manufacturers.

E. Conclusions and recommendations are reached. Consideration is given to system construction with materials available at the present time, and with materials anticipated to be available two years hence.

1.1.2 Areas of Attack

Design problems are divided into several areas. These facets are studied independently at first, and then combined to form complete storage and feed systems.

A. The insulation scheme is of primary importance. A large amount of work is performed on schemes to make long-term storage of liquid hydrogen possible.

B. Structural concepts compatible with the newly derived insulation schemes are studied.

C. Zero "g" feed systems for obtaining gas from liquid storage tanks are studied. Three methods are considered:

1. Minimum surface energy liquid location.

2. Internally regenerative gas feed.
3. Thixotropic liquid location.

D. The tank system must feed a gas to the engine under specific thermodynamic conditions. The flow control, metering and other interface problems are analyzed from two standpoints:

1. Long flow pulse where start-up and shut-down characteristics are not critical.
2. Short flow pulse where start-up and shut-down characteristics are very critical.

1.1.3 Complete System Considerations

Complete storage and feed systems are analyzed. Layout drawings are made. Interactions between components of the subsystems are discussed.

1.1.4 Tank System Weight Studies

Based on work statement specifications and the foregoing studies, digital computer runs of system weights are made and presented.

1.2 Specific Mission Design Program (H_2 and NH_3 Propellants)

On the strength of the general design studies and using definite mission profile specifications, designs are established for a hydrogen and an ammonia storage system.

1.2.1 Design Approach

Systems which can be built with state-of-the-art technology about two years hence are given.

A. Concepts practical for each propellant are chosen. Selection of systems is justified.

B. Layout design is performed and drawings are made. Calculations for insulation, structure, flow system, and weights are given.

C. Specifications for critical components are established.

2.0 GENERAL DESIGN STUDIES

The objective of these studies is to generate concepts and data which will permit detailed design of specific propellant storage systems. Preliminary requirements are the same for hydrogen and ammonia propellants.

The tankage environment is hard space vacuum, (approximately 10^{-9} mm.Hg.). Tank heat inputs come from many places, but the primary source is solar radiation. Systems are subjected to boost "g" loading, high vibration, and zero gravity. Stay time in the zero gravity, high-vacuum environment is up to 3 years.

Systems deliver ammonia or hydrogen flow rates on the order of 2 (10^{-5}) lb. per second in the gaseous phase.

Flow is in bursts ranging from minutes to several days in length, and the total burst time is up to 40 days. The quantity of reactive mass or useable propellant necessary to meet the requirement is 69.12 lbs.

Systems include tanks and flow control components as needed to satisfy engine inlet conditions.

2.1 Hydrogen Storage and Feed System

In this study, the supply of hydrogen is stored in the liquid phase. It can be easily proven that high-pressure gas storage is not practical for the intended application. Gas storage volumes and tank weights are prohibitively high. While supercritical pressure storage of the hydrogen is feasible as a means of controlling gas feed in a zero gravity environment, it too imposes a relatively large weight penalty.

In order to contain liquid hydrogen efficiently in accordance with preliminary specifications, it was necessary to generate new storage methods. These methods are analyzed in the next section.

2.1.1 Technical Studies of Practical Design Concepts

Several promising storage means are proposed and discussed. The feasibility of these ideas is established by layout designs and theoretical analyses. For further proof of workability, several testing programs were carried out and the results included. Storage ideas were discussed with electrothermal engine manufacturers to obtain further system and interface design information. Conclusions and recommendations for each concept are included.

2.1.1.1 Insulation Scheme

Lightweight liquid-hydrogen tanks meeting the preliminary specifications must be very highly insulated. Liquid losses must be limited to about 0.1% per day. This is a difficult requirement for small vessels. The rate of heat flow to the liquid is roughly equal to 0.1% of the solar radiation intercepted by one square foot of area in the vicinity of the earth. These numbers are based on the assumption that all of the boil-off gases would be used in the engine and at a fairly constant rate over the three-year period.

Equilibrium Skin Temperature Control Analysis

Heat inputs to storage tanks come from many sources. The significant sources of heat during flight near the earth-moon system in space vacuum are:

Q_1 = Solar emission
Q_2 = Earth reflection
Q_3 = Earth emission
Q_4 = Moon reflection
Q_5 = Moon emission
Q_6 = Vehicle emission (not the tank)
Q_7 = Vehicle reflection (not the tank)
Q_8 = Vehicle conduction

Heat leaves the tank as:

Q_9 = Tank emission
Q_{10} = Convection in boil-off gases.

If a storage tank has a highly conductive outer covering, the temperature of this surface will tend to approach a uniform value dependent upon the balance of Q_1 through Q_{10}. The skin temperature is commonly called the "equilibrium temperature (T_{eq})". Obviously, it is desirable to obtain a low equilibrium temperature for efficient storage of liquid hydrogen.

Tank supports can be designed so that a negligible amount of heat will flow to the tank by conduction ($Q_8=0$). Efficient support designs will be discussed in a later section. If all heat inputs are considered to be by thermal radiation, tank skin temperature can be controlled by properly

coating this surface. The coating must absorb as little of the incoming radiation as possible and, at the same time, allow the surface to emit a maximum of its own thermal energy in order to reach the lowest possible equilibrium temperature. The quality of a surface by which it absorbs thermal energy is called absorptivity, and is defined as:

$$\alpha = \frac{\text{absorbed radiation}}{\text{incident radiation}}$$

The absorptivity of a given surface also depends on the nature of the incident radiation.

The quality of a surface by which it emits thermal energy is called emissivity, and is defined as:

$$\epsilon = \frac{\text{emissive power}}{\text{emissive power of a black body at the same temperature}}$$

The emissivity of a given surface also depends on the temperature of the surface. Lowest equilibrium temperatures will occur when the ratio of $\frac{\alpha}{\epsilon}$ is lowest. Table 1 shows some typical values for α and ϵ (Reference 1). Subscripts refer to solar (s), earth (E), and moon (m). The emissivities shown are roughly constant over the resulting equilibrium temperature range for spheres.

TABLE 1

Thermal Radiation Characteristics of Various Surfaces

MgO	Rutile Coating	Black Body
$\alpha_s = 0.08$	$\alpha_s = 0.27$	$\alpha_s = 1$
$\alpha_E = 0.82$	$\alpha_E = 0.82$	$\alpha_E = 1$
$\alpha_m = 0.80$	$\alpha_m = 0.80$	$\alpha_m = 1$
$\epsilon = 0.90$	$\epsilon = 0.90$	$\epsilon = 1$

Note that the magnesium oxide will produce the lowest overall $\frac{\alpha}{\epsilon}$. Several other metallic oxides have similar radiation characteristics.

The intensity of the heat flux from direct solar radiation is defined as the solar constant (C_s). This value depends almost exclusively on the

distance from the sun, and at 1 astronautical unit is 442 $\frac{B}{hr.ft.^2}$. Some solar energy striking a storage vessel is reflected from the moon and the earth. This energy is called albedo. Albedo is defined as:

$$\gamma = \frac{\text{reflected radiation}}{\text{incident radiation}}$$

Below are the relationships for Q_1 through Q_{10} written for uneclipsed spherical tanks.

$$Q_1 = \alpha_s C_s A_c$$

$$Q_2 = \alpha_s C_s A_h \gamma_E \left[\frac{R_E^2}{(R_E + H_E)^2} B_{Er}\right]$$

$$Q_3 = \alpha_E C_s (1 - \gamma_E) A_h \left[\frac{R_E^2}{(R_E + H_E)^2} B_{E\epsilon}\right]$$

$$Q_4 = \alpha_s C_s \gamma_m A_h \left[\frac{R_m^2}{(R_m + H_m)^2} B_{mr}\right]$$

$$Q_5 = \alpha_m C_s (1 - \gamma_m) A_h \left[\frac{R_m^2}{(R_m + H_m)^2} R_{m\epsilon}\right]$$

Q_6 and Q_7 These are complex functions of the vehicle configuration and cannot be determined unless specific design information is available.

$$Q_8 = \sum \left(\frac{KA\Delta T}{L}\right) \text{for all supports.}$$

$$Q_9 = \sigma \epsilon A_T T_{eq}^4$$

$$Q_{10} = \left(\frac{4\pi K_i}{\frac{1}{R_i} - \frac{1}{R_o}}\right) \left[T_{eq} - T_c\right]$$

The nomenclature applying to these equations is:

A_c = Cross sectional area of sphere

A_h = Surface area of hemisphere

A_T = Total spherical surface area

R_E = Radius of earth

H_E = Distance from tank to earth

R_m = Radius of moon

H_m = Distance from tank to moon

γ = Albedo

α = Absorptivity

ϵ = Emissivity

C_s = Solar Constant

$$B_{Er} = \frac{\text{area reflecting}}{\text{area total}} = \frac{2\pi R_E^2}{4\pi R_E^2} = \frac{1}{2}$$

This is an apparent brightness area term for earth-reflected solar radiation. Similarly, $B_{mr} = \frac{1}{2}$. This is an apparent brightness area term for moon-reflected solar radiation.

$$B_{E\epsilon} = \frac{\text{area of cross section}}{\text{area emitting}} = \frac{\pi R_E^2}{4\pi R_E^2} = \frac{1}{4}$$

This is an apparent brightness area term for earth-emitted radiation. Similarly, $B_{m\epsilon} = \frac{1}{4}$. This is an apparent brightness area term for moon-emitted radiation.

k = Thermal conductivity of solid support members.

A = Cross sectional area of solid support members.

ΔT = Temperature gradient across solid support members.

L = Length over ΔT for solid support members.

σ = Stefan-Boltzmann constant.

T_{eq} = Equilibrium temperature.

K_i = Thermal conductivity of tank insulation.

R_i = Inner radius of insulation.

R_o = Outer radius of insulation.

T_c = Temperature of stored liquid.

Subscripts:

E = Earth

m = Moon

s = Solar

r = Reflected

e = Emitted

The relationship for the heat balance which determines T_{eq} is:

$$Q_1 + Q_2 + Q_3 + Q_4 + Q_5 + Q_6 + Q_7 + Q_8 = Q_9 + Q_{10} \qquad \text{(Eq. 1)}$$

To obtain preliminary design information, this equation was solved using the following assumptions:

1. The tank is at a constant distance from the sun. (1 astronautical unit)
2. The tank "sees" a lighted hemisphere of sun, moon and earth all at the same time. This is an impossible situation but the error produced by this assumption is negligible.
3. The tank skin is infinitely conducting.
4. Absorptivity and emissivity are constant over the temperature range considered.
5. Heat inputs from the vehicle, i.e. Q_6, Q_7, and Q_8 are assumed to be zero.
6. Heat input to the liquid is assumed to be zero (Q_{10}). Small values of Q_{10} for highly insulated tanks will not significantly control T_{eq}.

T_{eq} is plotted versus distance from the earth in Figure 1. Note that the minimum obtainable T_{eq} is 274°R. Above a distance of 20,000 miles from the earth, earth albedo and emission influence T_{eq} very little. Above a distance of 9,000 miles from the moon, moon albedo and emission influence T_{eq} very little. The validity of the Figure 1 for use as design information for actual systems depends largely on the specific vehicle configuration. All additional heat inputs from the vehicle will tend to raise T_{eq}.

FIGURE 1
DISTANCE IN EARTH-MOON SYSTEM VS.
EQUILIBRIUM TEMPERATURE

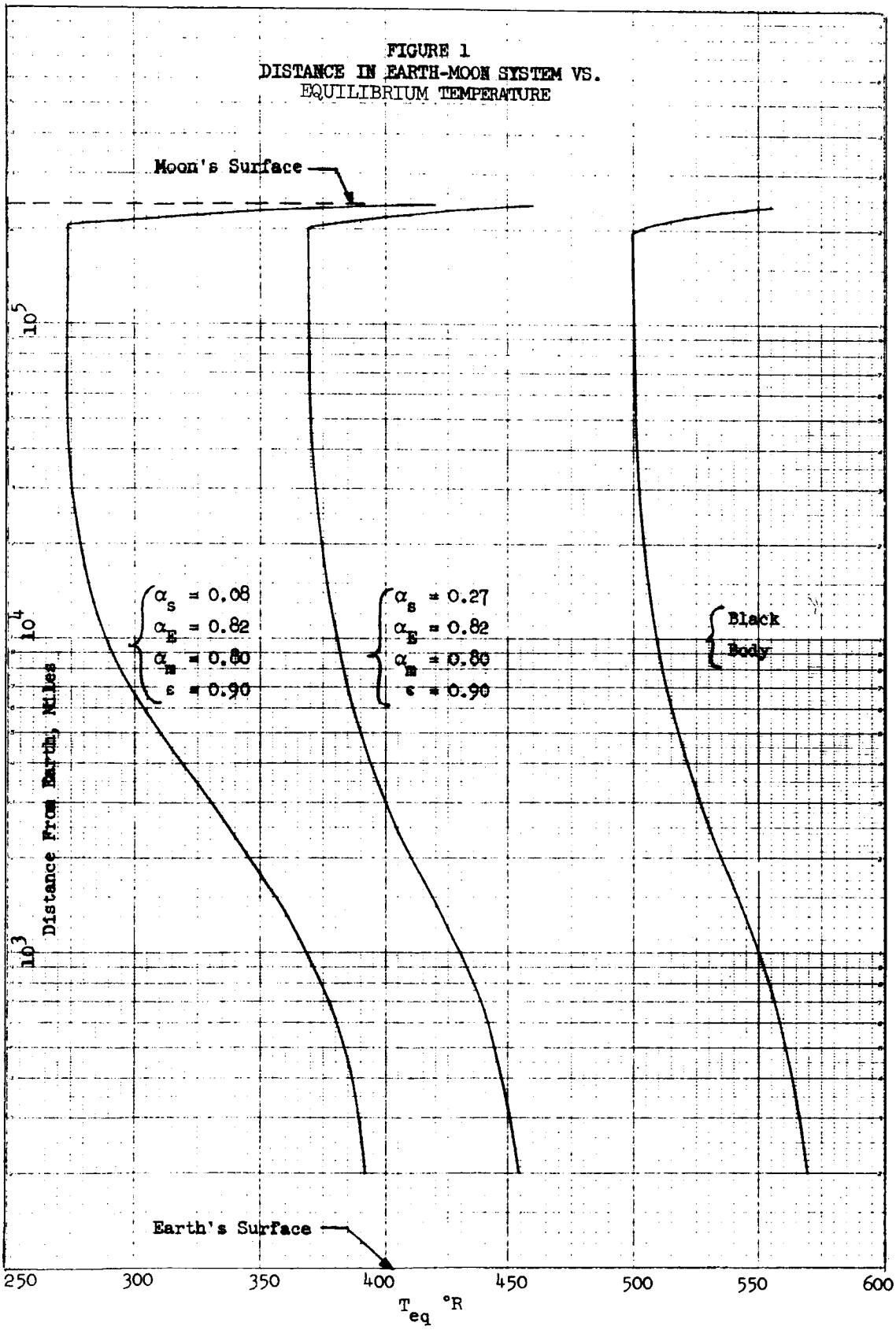

Local shadow shielding or insulation sections can be used to reduce vehicle heat inputs since their orientation is fixed with respect to the tank. Weight penalties associated with this kind of thermal protection will probably be very small in comparison to over-all tank weight for most electrothermal engine controlled communications systems. In any attitude where the tank is shaded from the sun by the vehicle, the presence of the vehicle can be an aid to reduction of T_{eq}. Any eclipsing of the tank from the sun by the earth or moon would provide a great reduction of T_{eq}.

The stability of the thermal radiation characteristics of surfaces must be maintained over the three-year period in a hard vacuum. Inadequate data is available to make estimates of the deterioration of various coatings. Testing is required in this area before final designs are made. It is expected that characteristics will change and cause T_{eq} to change gradually.

Composite Insulations

A highly efficient, easy to construct, insulation scheme has been devised. Two different kinds of insulation are used for different reasons. Figure 2 shows this concept. The purpose of insulating a tank in this manner is to make use of the best qualities of load-bearing and nonload-bearing insulations to obtain an optimum design.

The pressure vessel is completely covered by a thin layer of load-bearing multilayer insulation. A vacuum shell covers the insulation and serves as a support for the pressure vessel. Filler strips next to the closure weld allow this joint to be made without destroying the load-bearing insulation. Highly efficient nonload-bearing multilayer insulation covers the vacuum shell. A vapor-cooled shield is included in this layer. Filler strips placed next to the circumferential support ring allow the nonload-bearing insulation to have a constant thickness. A metallic, highly conductive outer covering surrounds the nonload-bearing insulation and provides a base for the equilibrium temperature coating.

Retractable supports hold the tank at the lugs in the support ring. Heat leaks through discontinuities are largely eliminated by slide doors which cover these areas. Two extension springs attached to the outer covering at each support retain the tank in the near zero gravity environment. Fill and vent lines are removed and capped off inside of the nonload-bearing insulation before launch.

The purpose of the load-bearing insulation is to prevent excessive boil-off during ground standby and launch. The gas pressure between the pressure vessel and vacuum shell is reduced to approximately (10^{-6}) mm. of mercury to obtain good insulation efficiency. A highly desirable characteristic

of load-bearing insulation is that it is capable of firmly supporting and shock-mounting the pressure vessel. In doing this, it does not subject the pressure vessel to point loading. The resulting even stress distribution allows the vessel to be constructed in the lightest possible way. Suitable load-bearing insulation is capable of supporting nonrigid vacuum shells under an atmospheric load of 14.7 pounds per square inch in addition to the vibration and acceleration loads. For many small tanks minimum gage vacuum shells are rigid enough to support the atmospheric load. Loads applied to the insulation in these cases are usually considerably less than 14.7 pounds per square inch.

To date, it has not been possible to develop a load-bearing insulation with insulating qualities which are superior to the best nonload-bearing varieties. Apparent thermal conductivities of load-bearing insulations are characteristically an order of magnitude higher. Table 2 shows some typical values of thermal conductivity for Beech-developed load-bearing insulations.

Filler strips are made of load-bearing fiberglass mat. No reflective shields are included in these pieces. The filler strips act as spacers which allow the nonload-bearing insulation to maintain a constant thickness and have a minimum of discontinuities. The insulating value of the fillers is low.

The purpose of the nonload-bearing insulation is to reduce the boil-off to a very low level during the three-year stay time in space. Just after launch, the pressure in this layer starts to decrease rapidly as air is vented to the rarified atmosphere. After a short time in space, the pressure in the insulation reaches a value which approaches the hard space vacuum. The insulation temperatures stabilize gradually as heat flows from the inner layers to the tank and environment. The nonload-bearing insulation layer is not required to support any appreciable loads. This circumstance allows use of the best of the multilayer insulations which characteristically cannot support significant loads without sustaining serious deterioration of insulating qualities and permanent set. Table 3 shows some typical values of thermal conductivities for nonload-bearing multilayer insulations. No solid support members or large lines go through the nonload-bearing insulation during the three-year stay time in space. This is a very important design point. The often overlooked discontinuities in insulation produced by support members and lines can have disastrous effects in otherwise highly efficient storage systems.

FIGURE 2

COMPOSITE INSULATION CONCEPT

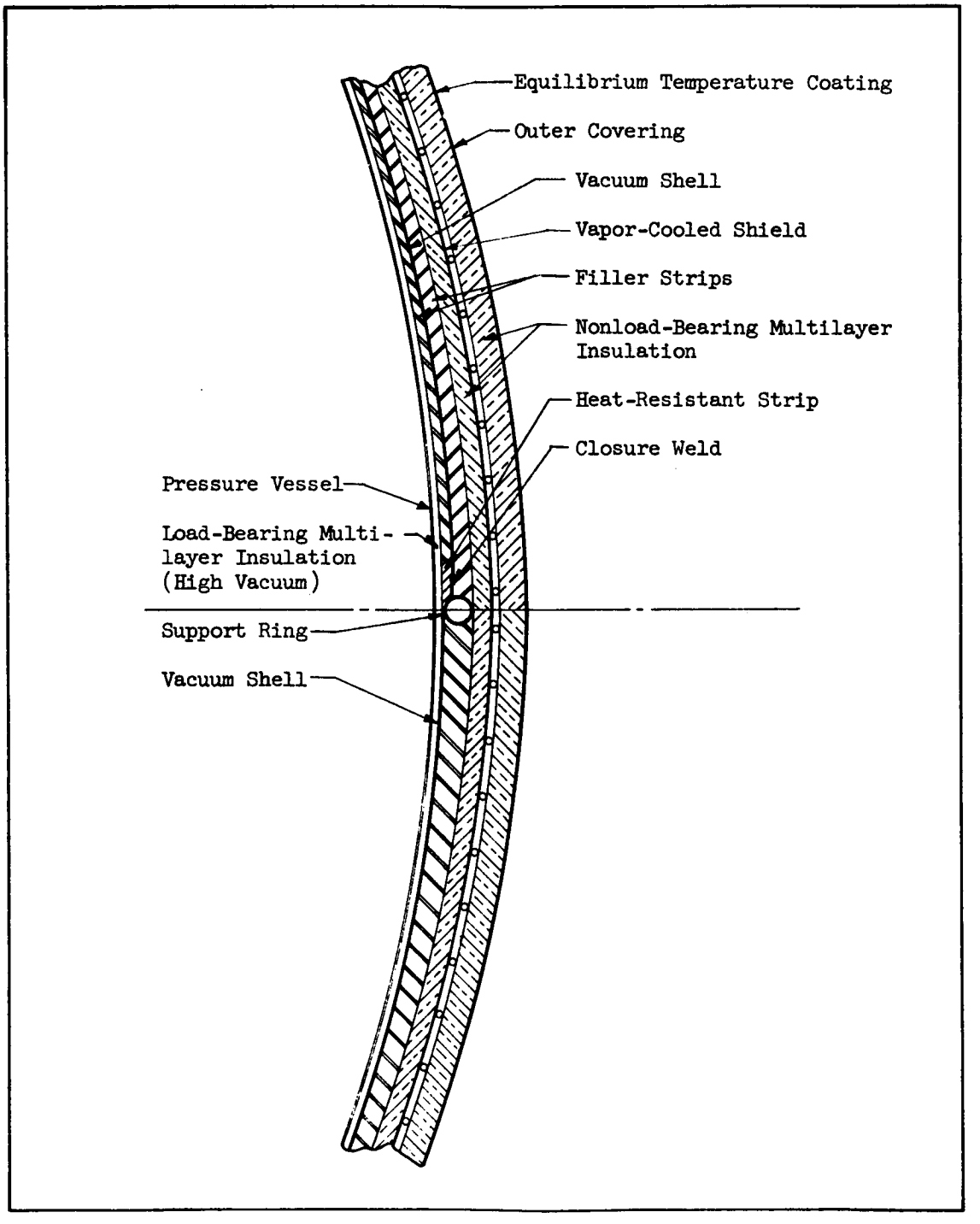

TABLE 2

APPARENT THERMAL CONDUCTIVITIES
OF LOAD-BEARING INSULATIONS

Type	Composition	Δt	ρ #/ft^3	Load	$\bar{k}$ $\frac{B \text{ In}}{\text{hr-ft}^2\text{°F}}$
Min. K-504 (Ref. 2a)	Glass Fiber Carbon	300-76°K	--	1 atm	.07
Sta Foam A-A602		300-76°K	--	1 atm	.13
LBI-A4 Beech Developed (Ref. 2a)	Multilayer Fiberglass Mat Aluminum Foil Mylar Film	300-76°K	--	1 atm	.0042
LBI-A2 Beech Developed (Ref. 2a)	Multilayer Titanium Sheet Fiberglass Mat Aluminum Foil Mylar Film	300-76°K	--	1 atm	.0035
LBI-A6 Beech Developed (Ref. 2a)	Multilayer Titanium Sheet Fiberglass Mat Mylar Film	300-76°K	--	1 atm	.0010
TG-15,000 (Ref. 2b)	Fiberglass "A" Fiber Silicon Bond	288-76°K	6.0	3 psi	.0027
TG-15,000 (Ref. 2b)	Fiberglass "A" Fiber Silicon Bond	288-76°K	6.0	15 psi	.0028

TABLE 3

APPARENT THERMAL CONDUCTIVITIES
OF NON-LOAD-BEARING INSULATIONS

Type	Composition	Δt	ρ #/ft^3	$\bar{k}$ $\frac{\text{B-In}}{\text{hr.ft}^2\text{°F}}$
Silica (Ref. 3a)	Chemically Prepared at $<10^{-4}$ Torr	304°-76°K	6.24	.0145
Perlite (Ref. 3a)	Expanded, +30 Mesh at $<10^{-4}$ Torr	304°-76°K	3.75	.0145
	-80 Mesh at $<10^{-4}$ Torr	304°-76°K	8.74	.0069
Diatomaceous Earth (Ref. 3a)	1-100 microns	304°-76°K	14.98	.0110
Alumina Fused (Ref. 3a)	-50+100 mesh at $<10^{-4}$ Torr	304°-76°K	124.80	.0124
Mica Expanded (Ref. 3a)	-20+30 mesh 30% -30+15 mesh 70% at $<10^{-4}$ Torr	304°-76°K	9.36	.0124
Phenolic Spheres (Ref. 3a)	25-100 microns at $<10^{-4}$ Torr	304°-76°K	12.49	.0089
Calcium Silicate (Ref. 3a)	Synthetic .02-.07 Microns at $<10^{-4}$ Torr	304°-76°K	22.47	.0038
NRC-2 (Ref. 3b)	Multilayer Shields	300°-76°K	2.0-3.0	.0002
Linde CS-5 (Ref. 3c)	Copper Flakes Santocel	540°-163°R	11.0	.0026
Linde SI-12 (Ref. 3c)	Aluminum Foil Glass Fiber Mat	540°-163°R	2.5	.0013
Linde SI-4 (Ref. 3c)	Aluminum Foil Glass Fiber Paper	540°-163°R	4.7	.0003
Linde SI-4 (Ref 3c)	(Theoretical)	300°-37°R	4.7	.00014

Single Vapor-Cooled Shield

The concept of the vapor-cooled shield is recognized as a highly reliable means of reducing vent losses from cryogenic storage vessels.

There are no moving mechanical parts in the system. Construction of vapor-cooled shields is simple and weight penalties are very low. Vapor-cooled shields can be installed in the best of the multilayer insulations.

Figure 3 shows how a shield is applied to a storage vessel. Boil-off gases resulting from insulation heat leak are passed through cooling coils. The cooling coils are attached to or built into a highly conducting shield. As the cold gas passes through the coils, the shield is cooled, insulation heat leak is intercepted and carried overboard, and the efficiency of the insulation system is greatly improved.

There is an optimum location in the insulation for the cooled shield. At the optimum location between the cold wall and the outer covering, the heat leak to the tank reaches a minimum value. A recent Beech report (Reference 4) outlines the analytical method for determining the optimum location and temperature of shields installed in the insulation of spherical tanks. Shield analysis has been expanded in this report. The objective of this work was to establish further information which will enable detailed design of actual systems. It was desired to establish general rules and simplified parameters for the design of shields installed on spherical liquid-hydrogen tanks. It was also desired to know if the addition of a second concentric shield would reduce boil-off losses significantly more than one shield.

Two approaches are taken in the analytical study of single vapor-cooled shields. These methods are presented in Appendix A.

Single Vapor-Cooled Shield Analysis Based on the Fourier Equation

Fourier equation for heat transfer through a solid conductor is applied to spherical tanks in Section 1.1 of Appendix A. The basic relationship is:

$$Q = \frac{kA\Delta T}{L} \qquad \text{(Eq. 2)}$$

where:
- Q = Heat flow rate
- k = Insulation thermal conductivity
- A = Insulation area normal to heat flow
- ΔT = Temperature difference across insulation
- L = Thickness of insulation in the direction of heat flow.

FIGURE 3
VAPOR-COOLED SHIELD

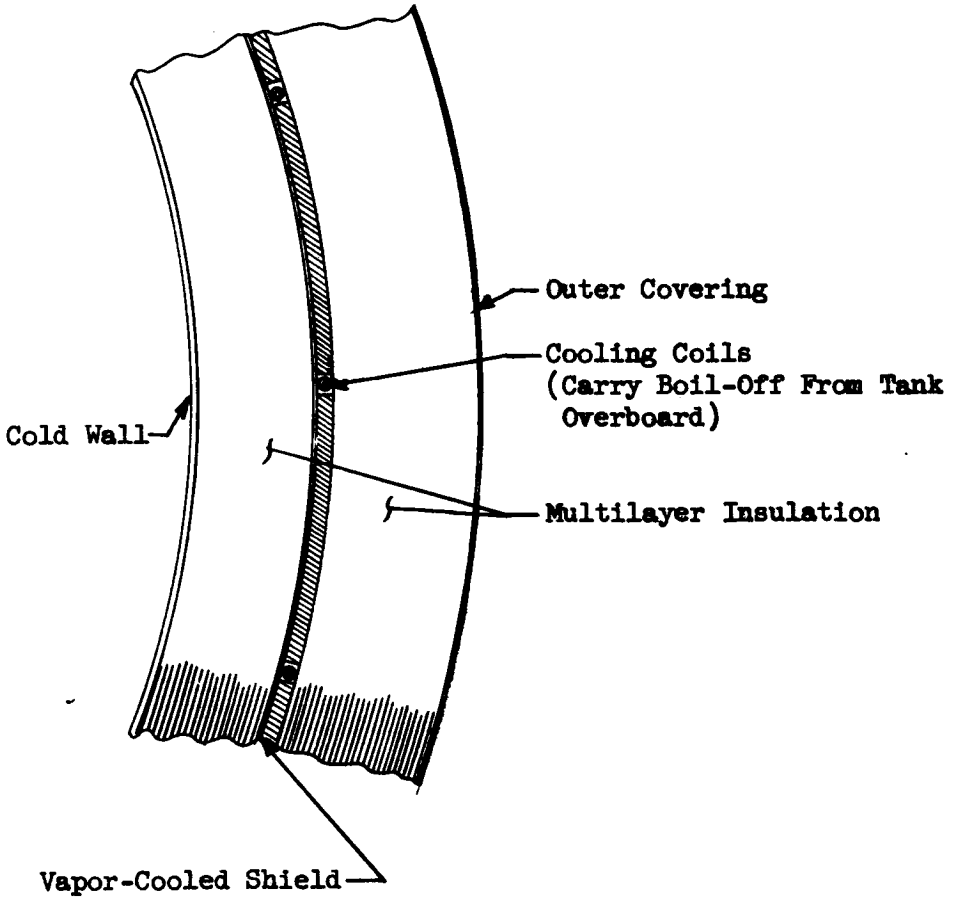

In the study, insulation thickness and tank curvature are low enough so that the resulting values approach those for the flat plate condition. Figures A2 through A7 summarize the results of the calculations for one shield. The following conclusions are drawn:

1. The optimum location for the vapor-cooled shield is close to halfway through the insulation layer for spherical tanks. This is true for tanks where the ratio of outer insulation radius to inner insulation radius does not exceed 1.1.

2. The shield location is not critical for good efficiency. The flat bottoms of the boil-off curves in A2, A2, and A6 are evidence of this.

3. It is not necessary to maintain closely controlled shield temperature for good efficiency. This can be seen by noting the wide temperature range corresponding to near optimum boil-off rates.

4. Vapor-shields are effective over a wide range of ambient temperatures and tank pressures.

5. Shield effectiveness increases as ambient temperature increases.

6. Shield effectiveness increases as tank pressure increases.

Single Vapor-Cooled Shield Analysis Based on the Stefan-Boltzmann Equation

In the Fourier analysis, the thermal conductivity through the insulation is assumed to be constant. This is hardly ever true because thermal conductivity is a complex function of temperature, and will almost always decrease with decreasing temperature. Multilayer insulation values are highly dependent on temperature level. This is because the mode of heat transfer is primarily by radiation. The law which governs radiant heat transfer is given by the Stefan-Boltzmann equation which is of the form:

$$Q = \sigma E A (T_2^4 - T_1^4) \qquad \text{(Eq. 3)}$$

where:
- Q = Heat flow rate
- σ = Stefan-Boltzmann constant
- E = Emissivity of radiating surfaces
- A = Area of radiating surfaces
- T_1 = Temperature of cold surface
- T_2 = Temperature of warm surface or equilibrium temperature

An analysis of vapor-cooled shields was made based on Equation 3 and is given in Section 1.2 of Appendix A. Figures A8 through A16 summarize the results of the calculations. It was found that:

1. The optimum location for the vapor-cooled shield is close to 0.27 of the way from the cold side to the hot side of the insulation. This is true where radiation reflectors are equally spaced and nearly flat.

2. The shield location is not critical for good efficiency.

3. It is not necessary to maintain closely controlled shield temperature.

4. Vapor-shields are effective over a wide range of ambient temperature and tank pressures.

5. Shield effectiveness increases as ambient temperature increases.

6. Shield effectiveness increases as tank pressure increases.

Summarized Results of Fourier and Stefan-Boltzmann Shield Analyses

Boil-off reduction factors for optimum shielded tanks are plotted in Figure A17. Boil-off reductions are much greater where the mode of heat transfer is considered to be by radiation. Actual multilayer vacuum insulations act as a combination of radiation and conduction barriers. It is expected that the decrease in boil-off will lie between the values obtained from the Fourier and Stefan-Boltzmann analyses in these cases. A comprehensive testing program is underway to establish accurate design values for real insulations.

The curves of Figures A17 greatly simplify the weight and size analyses for specific designs. If the apparent thermal conductivity for a real insulation, tank pressure, and equilibrium skin temperature are known for a liquid-hydrogen storage tank, the heat flow to the liquid can be calculated by the modified Fourier equation:

$$Q = \frac{kA\Delta T}{\frac{L\,\dot{M}\ \text{Unshielded}}{\dot{M}\ \text{Shielded}}} \qquad \text{(Eq. 4)}$$

where: $\frac{\dot{M}\ \text{Unshielded}}{\dot{M}\ \text{Shielded}}$ = The boil-off reduction factor for the particular insulation in question.

Note that the optimum shield location can be considered to be 0.4 of the way between inner insulation radius and the outer insulation radius in spherical tanks where insulation is not excessively thick in relation to the diameter. At this location, the shield is very close to the optimum established by both the Fourier or Stefan-Boltzmann Analyses.

Dual Vapor-Cooled Shields

The temperature of the gas leaving a shield is approximately equal to the temperature of the shield. By examining the shield temperature curves such as A3, it can be seen that this temperature is always far below the equilibrium skin temperature for optimum designs. The exit gas, therefore, still retains the capacity to remove heat from warmer insulation layers. It is reasonable to expect that additional vapor-cooled shields could further reduce boil-off losses. This discussion deals with the analysis of two concentric shields on tanks where the walls are assumed to be flat.

Dual Vapor-Cooled Shields Analysis Based on Fourier Equation

The detailed analysis is given in Section 2.1 of Appendix A. The plotted curves are limited to the case where the tank pressure is 50 psia and the equilibrium temperature 300°R. The range of variables is purposely limited in this way so as to illustrate the point without excessive calculation. Curves A18 through A23 show boil-off reductions for dual shields placed at various locations. Note that for one shield, the boil-off is reduced to 0.62 of the unshielded value as shown in Figure A18. For two shields, the optimum locations are 1/3 and 2/3 of the way through the insulation and the boil-off is reduced to 0.53 of the unshielded value.

The optimum locations are shown approximately in Figure A21. For small tanks it is questionable whether the small additional boil-off reduction is worth the extra complications accompanying the installation of the second shield. For large tanks, the resulting weight savings could be quite significant.

Dual Vapor-Cooled Shields Analysis Based on Stefan-Boltzmann Equation

In this case, as in the preceding paragraph, the plotted curves shown in Section 2.2 of Appendix A are limited to 50 psia tank pressure and 300°R equilibrium skin temperature. Curves A24 through A27 show boil-off reductions for tanks with dual shields placed at various locations. Note

that the boil-off is reduced to 0.40 of the unshielded value for one shield as shown in Figure A24. For two shields the optimum locations appear to 0.14 and 0.50 from the cold wall to the hot wall for the colder and warmer shields respectively. At the optimum situation which is shown in Figure A26, the boil-off is reduced to 0.32 of the unshielded value.

It appears that it would not be worthwhile to attempt to expand the analysis to 3 concentric shields. Any further boil-off reductions for 3 shields would be very small and hardly worth the added system complication.

Removable Launch Supports

Solid support members contribute a major portion of the total heat leak in highly insulated liquid-hydrogen storage tanks. This fact is not always evident when preliminary design calculations are made based purely on the solid conduction component of heat leak through the supports. A more elusive and difficult to estimate heat leak always accompanies the pure conduction component when the insulation discontinuities around the supports are considered. Any holes or slots in the insulation tend to act as absorbers for thermal radiation. At all points where insulation comes into contact with solid support members, "thermal shorts" are produced and the layers of insulation are fed with heat. Potentially efficient support systems using long rods or wires require long holes or slots in the insulation. In these cases, more areas of hot support members "see" the colder insulation and the radiation component is increased. The result of all of the effects discussed above is that the normally uncalculated discontinuity heat leak becomes a larger share of the total while the calculated pure conduction component becomes smaller.

Because of the relatively poor dimensional stability of nonload-bearing insulations, it is difficult to maintain consistency in the support discontinuity heat leaks from unit to unit. This fact makes it very difficult to calculate the optimum amount of insulation required. The designer is forced to rely on a testing program to establish an optimum design.

Tension support members made of plastic materials such as Dacron or nylon appear to be highly efficient. The ratio of allowable tensile strength to thermal conductivity is a good indicator. Table 4 shows some typical values for various materials (Reference 5).

It appears that the plastic materials, especially Dacron, are the obvious choice. These materials, however, have several drawbacks. Because of their lower tensile strengths, the cross sectional area must be greater than metallic wires or rods. The surface area of the plastic member is, therefore, greater. When insulation contacts these members, more contact points, or thermal shorts, are established. Plastics have high emissivity values by comparison to metallic wires, and can more effectively radiate heat from their greater area to the surrounding insulation. Holes or slots in the insulation must be larger to accommodate the larger plastic members. The designer can easily be fooled into thinking he has solved the problem by using plastic supports while he has only transferred much of the heat leak into a form for which he cannot make accurate estimates. Plastic support members have poor creep properties by comparison to metals. Any slack which might develop in a support system before launch would have a very bad effect during the high vibration period after launch. The supports are likely to creep during the period of evacuation when it is necessary to maintain high insulation temperatures (300 to 500°F). At the cold end of the supports, the plastic material becomes hard, brittle, and becomes a poor structural member under high vibration.

TABLE 4

SELECTED SUPPORT MATERIAL PROPERTIES

	Allowable Tensile Strength (F Ty) KIPS/SI	Apparent Thermal Conductivity (k) B/Hr.Ft.°R	$\frac{F\ Ty}{k}$
Drawn Stainless Steel	150	5.2	29
Ti Alloy 4Al-4MN	145	3.5	41.4
Dacron	20	0.088	227
Nylon	20	0.18	111

The Beech approach to the problem is to remove main load-carrying structural supports when they are not needed. If a tank is subjected to near zero gravity conditions for most of its mission, there is no need to retain supports which carry large loads. Removal of supports is accomplished by the device shown in Figure 4. This part is an explosively actuated, fully retractable support pin. It belongs to a class of highly reliable hardware which also includes explosive squib valves, and explosive latch pins. These devices are frequently used in "must work" situations in aircraft and spacecraft.

Several retractable supports are spaced around a spherical tank and index by slip-fit into the support lugs. The support lugs are welded into the circumferential support ring. The support assemblies are bolted to the primary vehicle structure. After the vehicle is launched into a zero-gravity environment, an electrical signal activates the explosive charge. The latch fork is propelled from the pin, and the pin is driven back into the housing. The pin is purposely retained in the housing so as not to induce an unwanted acceleration into the vehicle. Additional explosive charges can be added to the housing to improve reliability. Two charges are often used in explosive squib valves to obtain reliability of 0.9999 or better.

The tank is retained against small forces arising from reorientation or relocation of the vehicle by two extension springs at each support. These springs attach to the outer covering and provide support with a long heat path should the structure become warmer than the tank.

With the pin in the retracted position, only a small cylindrical hole is left in the insulation. This hole is automatically capped by a spring-loaded slide door when the pin retracts. The door is coated on the outside and inside to reduce radiation heat leak to a minimum.

Removable Fill and Fill-Vent Lines

In keeping with the concept of minimum discontinuity heat leaks, the fill and fill-vent transfer lines are also removable. For tanks of the size range studied in this report, it is estimated that a 3/8 O.D. liquid fill line and 5/8 O.D. fill vent line of thin-wall construction are required. For gas supply during the mission, however, the required supply line size is so small that plugging probabilities will control. A minimum line size of about 0.050 O.D. will be used at the tank outlet.

FIGURE 4
REMOVABLE LAUNCH SUPPORT

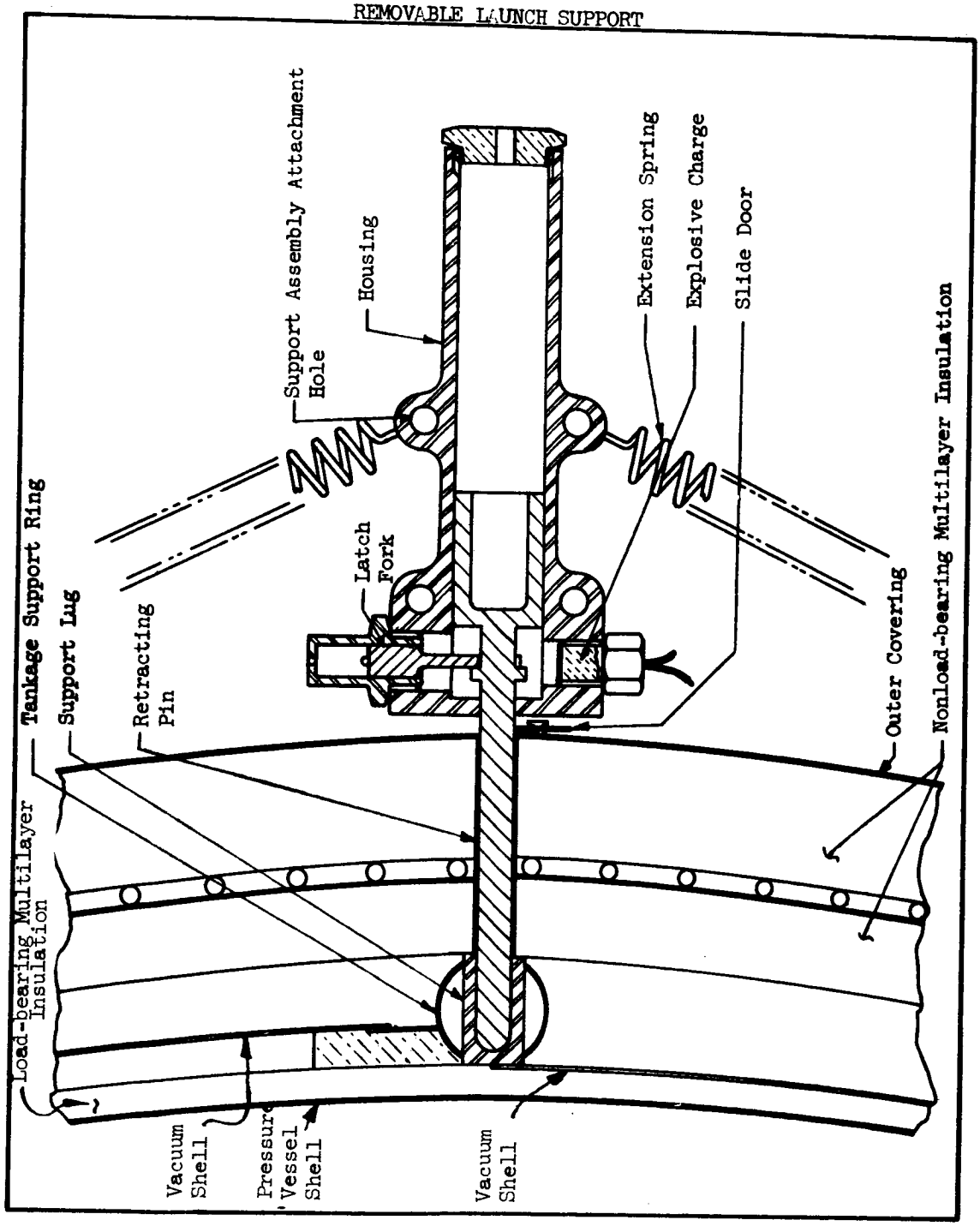

Since the large fill lines are not required during the mission, it is logical to remove the source of heat leak before launch. Table 5 gives an indication of the magnitude of heat leak reduction possible. In addition, there will be a small weight saving since less insulation and no long fill and fill-vent lines will be carried with the vehicle. Figure 5 shows a concentric fill-vent connector which is installed in the tank. This unit is placed on the cold side of the non-load-bearing insulation. The concentric configuration serves to reduce the size of the required access hole in the non-load-bearing insulation. The connector is installed in the bottom of the pressure vessel to prevent the collection of an excessive amount of frost or liquid air. For complete elimination of frost or liquid air, the area can be flooded with a light gas such as helium which will rise into the cavity during the fill procedure. The bottom connector position also facilitates the installation of the thermal standoff. This standoff is required for reduction of heat input during ground standby and launch. The connector is actuated by the adjoining ground support equipment. Both of the internal poppets are opened against a single spring. When the tank is filled and the ground support equipment removed, the poppets will partially check the outflow of gas. A manual cap is placed over the connector before launch to provide a positive, leak-proof seal. Before the cap is installed, boil-off gas may leak slowly through the connector. The poppets serve only to prevent circulation of air and other gases up the fill and vent lines by stray connection currents. Note that leak-proof seal is not required between the fill and vent side of the connector. All that is required is a seal which will allow orderly filling and venting without a great amount of liquid leakage to the vent side. Before launch, and after the outlet is tightly capped, a cover is placed over the open hole in the non-load-bearing insulation to reduce radiation heat leak in this area.

Insulation Discontinuity Protection

Discontinuities in the proposed insulation system are limited to the following places during the three-year stay time in the zero gravity space environment:

1. Several small cylindrical holes perpendicular to the insulation for support pin access.

2. A small cylindrical hole for removal of fill and fill-vent lines.

3. One small cylindrical hole for heat input purposes. (See Section 2.1.1.3 on metering and control).

4. One coiled thin-wall feed line of about 0.050 O.D.

5. Joints in the insulation. At best there will be one circumferential joint for two insulation hemispheres.

TABLE 5

HEAT LEAK THROUGH FILL AND VENT LINES
ON LIQUID-HYDROGEN TANKS

Alloy	Heat Leak Per Foot B/hr		%/ft of Total Allowable Heat Leak Based on 69.12 lb Vented in 3 yrs @ 50 psia	
	300 - 37°R	540 - 37°R	300 - 37°R	540 - 37°R
Titanium 4.7% M_n, 3.99% Al, 0.14%C 3/8 x 0.006 wall	0.033	0.081	7.3%	17.62%
Titanium 4.7% M_n, 3.99% Al, 0.14%C 5/8 x 0.008 wall	0.075	0.181	16.4%	39.5%
Stainless Steel Avg value for type 303, 304 316, 347 st.steel as compiled in N.B.S. Circular 556. 3/8 0.006 wall	0.060	0.149	13.1%	32.5%
Stainless Steel Avg value for close curve of type 303, 304, 316, 347, st.steel as compiled in N.B.S. Circular 556 5/8 x 0.008 wall	0.134	0.334	29.3%	72.9%

FIGURE 5

FILL-VENT-CONNECTOR

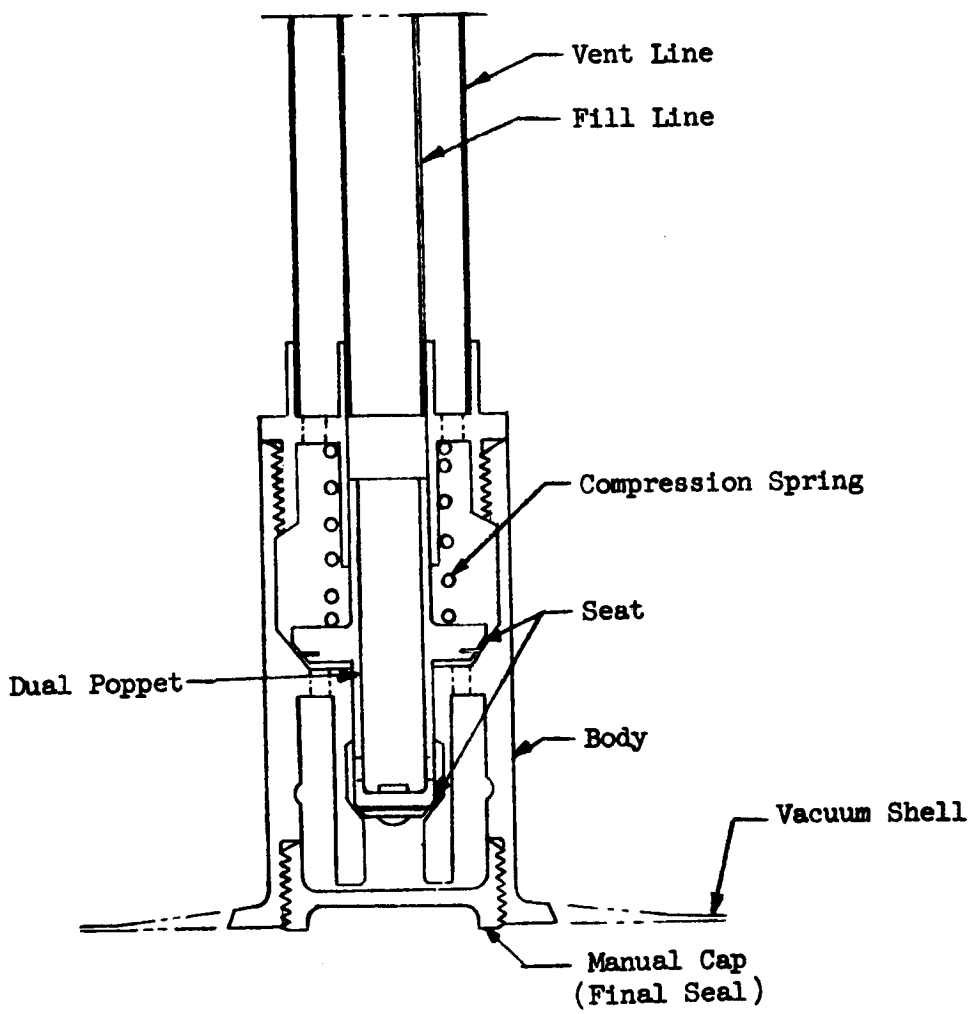

It is possible to combine discontinuities 1 and 5 by placing the support pin access holes at the insulation joints. As explained in preceding sections, all holes will be covered to reduce radiation heat leak. Where possible, the discontinuities will be placed in the most shaded or coolest areas.

The amount of radiation absorbed at the cold wall through a hole can be roughly estimated by the Stefan-Boltzmann equation.

$$Q = \sigma E A (T_2^4 - T_1^4) \qquad \text{(Eq. 5)}$$

Where:

Q = Heat absorbed - $\frac{B}{Hr.}$

σ = Stefan-Boltzmann constant = $1.71\ (10^{-9})\ \frac{B}{Hr.Ft.^2 °R^4}$

A = Cross sectional area of hole - ft^2

T_1 = Temperature of cold wall - °R

T_2 = Temperature of hot wall - °R

$E = \frac{\epsilon_1 \epsilon_2}{\epsilon_2 + (1-\epsilon_2)\epsilon_1}$ (Reference 6)

ϵ_1 = Emissivity of cold wall

ϵ_2 = Emissivity of hot wall

Example: Estimate the radiation heat leak through a 1-inch-diameter insulation hole bounded by 300°R and 37°R surfaces. Both surfaces are shiny aluminum.

$\epsilon_2 = 0.025$

$\epsilon_1 = 0.014$

$$E = \frac{(0.014)(0.025)}{(0.025) + (1-0.025)(0.014)} = 0.00906$$

$$A = \frac{\pi D^2}{(4)(144)} = 5.45\ (10^{-3})\ ft.^2$$

$$Q = \sigma E A (T_2^4 - T_1^4)$$

$$Q = (1.71)(10^{-9})(0.00906)(5.45)(10^{-3})(300^4 - 37^4) = 0.00068\ \frac{B}{Hr.}$$

This is only 0.15% of the allowable average heat leak to a liquid-hydrogen tank at 50 psia supplying 69.12 pounds of liquid in three years.

Actually, the direct radiation is only part of the heat leak caused by the hole because radiant energy is being absorbed, reflected, and emitted in all directions by the walls of the hole. (See Figure 6). Some of this energy arrives at the pressure vessel in the form of radiation and some

INSULATION HOLE

FIGURE 6

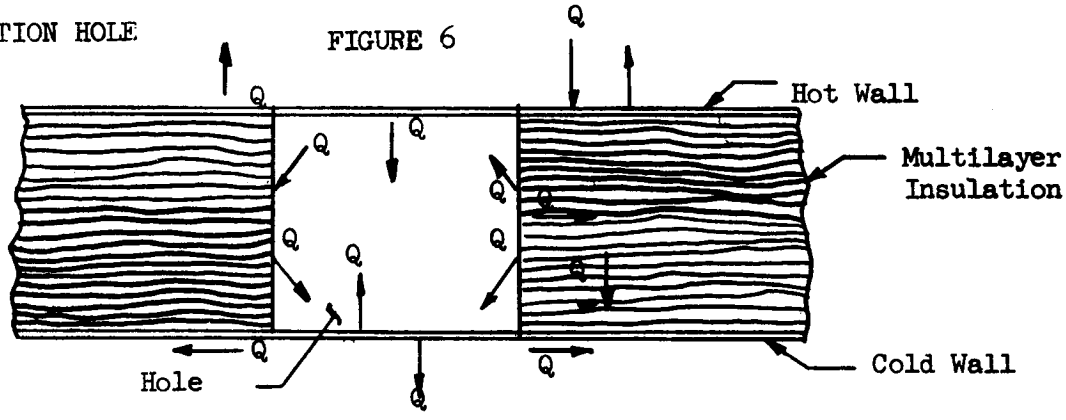

is conducted through the insulation. This unaccountable heat leak can be expected to be less than the direct radiation component for most holes.

Insulation joints should be arranged in such a way that the corresponding layers line up as much as possible. The dimensional instability of multilayer insulations often allows a situation such as is shown in Figure 7 to exist. Warmer layers are displaced on one side of the joint and contact colder layers on the other side. The resulting thermal shorts

FIGURE 7
BUTT JOINT

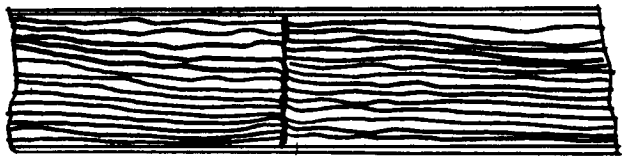

tend to increase the overall heat leak at the joint. A lap joint or scarf joint improves the insulation. Layers are most accurately located and some of the thermal shorts are eliminated. See Figure 8.

FIGURE 8
IMPROVED JOINTS

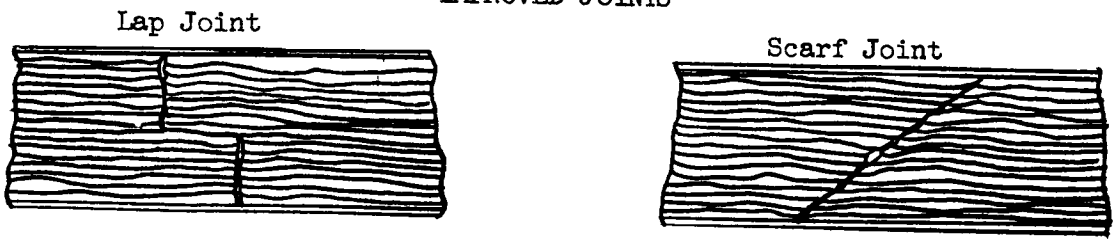

By using care at the joints and holes on a tank, the apparent thermal conductivity of the entire insulation scheme very closely approaches laboratory insulation sample values. In the weight studies presented on hydrogen tanks in this report, a small allowance is made for discontinuities in the assumption of an apparent thermal conductivity.

2.1.1.2 Zero Gravity Gas Feed Concepts

The behavior of gas and liquid mixtures in a zero gravity environment has been the subject of several recent reports. (Reference 7) Much study and testing time has been devoted to the problem of venting or feeding either liquid or gas from a storage tank. In electrothermal propellant supply systems, the feed requirement is for gas. This requirement is determined by these factors:

1. The liquid must be allowed to boil in the tank and carry away insulation heat leak for maximum storage efficiency.

2. Downstream pressure requirements are low enough (1 to 3 atmospheres) to eliminate the need for efficient liquid pumping.

3. The fluid must be supplied to the engine as a superheated vapor.

Of the many proposed systems for providing gas feed in zero gravity, three are singled out for study in this report. These systems are considered to be the most practical and reliable for low flow rate delivery.

1. Minimum surface energy liquid location.

2. Regenerative gas feed system.

3. Thixotropic liquid location.

The system principles, component design, advantages, and disadvantages are discussed in the following sections.

Minimum Surface Energy Liquid Location

The most reliable method of obtaining gas feed from a tank is to locate the outlet in a place where gas is always present. It has been proposed, but it is not certain, that a tank could be constructed in such a way that the location of the gas and liquid would always be known to a degree in a near zero gravity environment. The system would make use of the surface energy forces of the liquid to obtain the desired gas location. One report (Reference 8) gives analyses and shows actual photographs of liquid hydrogen in zero gravity environment. In the photographs, the liquid was shown clinging to the walls with the gas located away from the walls. High heating rates were capable of separating the liquid from the wall.

A gas feed system for a true zero gravity environment is shown in Figure 9. The liquid hydrogen wets the wall and the gas is formed into a single spherical bubble by the natural liquid requirement for minimum surface energy or minimum gas-liquid interface area. The initial ullage is sized so that for any location of the gas sphere the outlet will always be inside the gas sphere. For spherical tanks the minimum allowable ullage (V_2) volume is exactly 1/8 of the tank volume (V_1). This ullage is determined as follows:

$$V_1 = 1/6\ \pi\ D_1^3 \qquad \text{(Eq. 6)}$$

$$V_2 = 1/6\ \pi\ D_2^3 \qquad \text{(Eq. 7)}$$

$$D_2 = \frac{D_1}{2} \qquad \text{(Eq. 8)}$$

Where:
- V_1 = Tank volume
- V_2 = Initial ullage volume
- D_1 = Tank diameter
- D_2 = Zero "g" ullage volume diameter

$$\frac{V_2}{V_1} = \frac{\frac{1}{6}\ \pi\ D_2^3}{\frac{1}{6}\ \pi\ D_1^3} = \left(\frac{D_2}{D_1}\right)^3 = \left(\frac{D_1}{2D_1}\right)^3 = \frac{1}{8} \qquad \text{(Eq. 9)}$$

FIGURE 9
MINIMUM SURFACE ENERGY GAS FEED SYSTEM

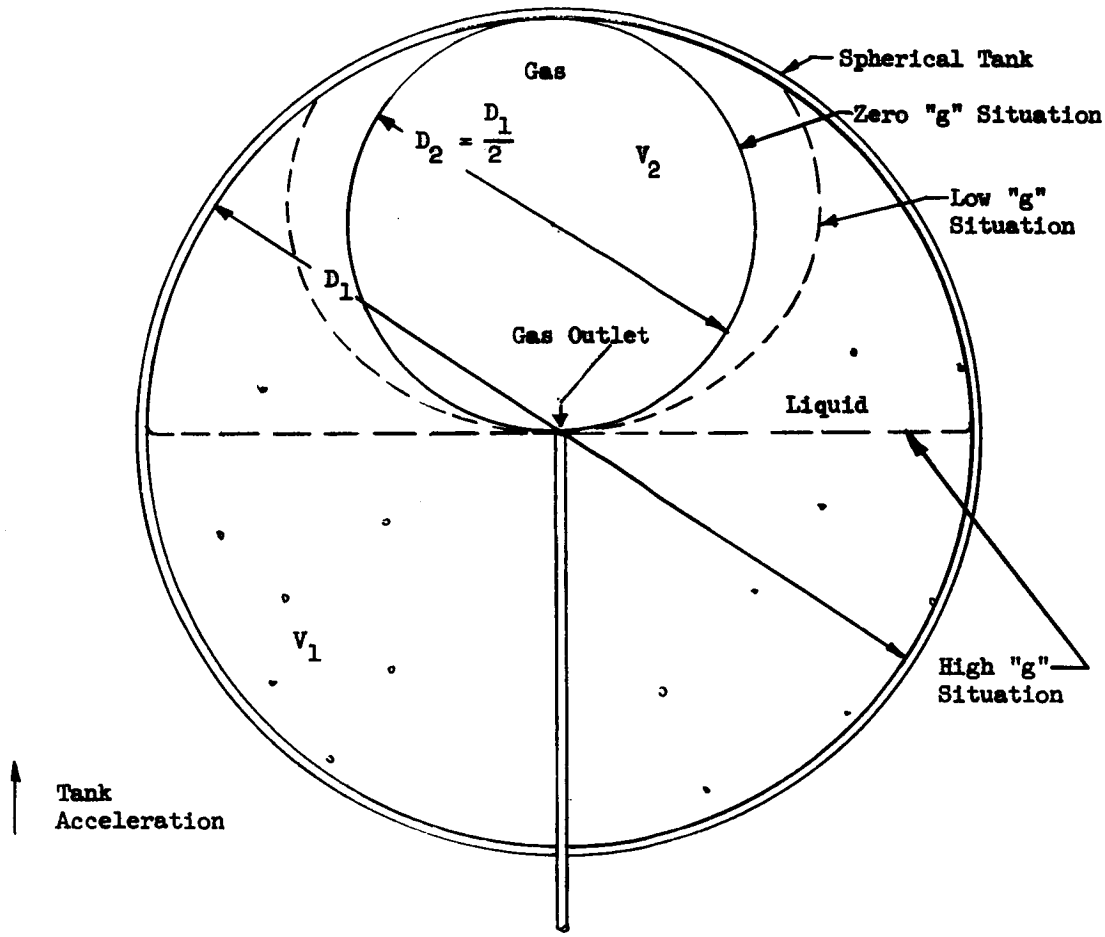

Additional ullage must be included to account for small accelerations which tend to deform the gas sphere. For large accelerations the liquid surface would be nearly flat with very small menisci at the walls. If this occurs, the initial ullage volume must be at least 1/2 of the total volume. For low accelerations the initial ullage volume required would be between 1/8 and 1/2 of the total volume.

The shape of the liquid near the exit tube will depend on the shape of the outlet. For small tubes it is expected that a small additional ullage would be required because the outlet cannot practically be placed exactly at the unpunctured gas-liquid interface.

An alternate approach would provide for liquid withdrawal only. Figure 10 shows the system. An outlet trap is located in the tank wall such that the direction of normal acceleration is away from the trap. The contact angle between a solid surface and liquid hydrogen is near zero. A single vapor bubble will form in the interior when the system is in a zero G environment (Reference 15). See Figure 10 a. The diameter of the gas sphere, having a volume equal to the initial ullage, is greater than the diameter of the cylindrical trap. To enter the cylindrical trap, the gas bubble (sphere) would have to deform. Entry is prevented because the gas bubble will remain in a spherical shape which is the condition for minimum surface energy. The bubble may tend to obstruct the outlet trap, however, a liquid path to the trap is provided because the solid surfaces are wetted by the liquid hydrogen. When an acceleration is encountered, the gas bubble will move in the direction of the acceleration. See Figure 10 b. If the direction of acceleration is away from the outlet trap, liquid will then flow from the outlet. Acceleration in random directions will not disturb the liquid in the outlet trap until some critical acceleration magnitude is attained. Then the liquid will leave the trap and gas flow will occur. This is an unstable condition, because the minimum surface energy condition does not exist. The return to a stable condition of fluid in the outlet trap will occur in a short time. If the quantity of remaining liquid is small, the refilling of the outlet trap would take longer because the fluid path would be only along the wetted container walls.

The outflow liquid must be vaporized. This is accomplished by a fixed pressure drop device which causes a corresponding temperature drop in the outlet fluid. At the lower temperature the outlet liquid is boiled using heat from the liquid still in storage. A more complete explanation of the vaporization technique is given in the section on regenerative gas feed systems.

Much analytical work has been done on zero "g" liquid behavior. Possibly an arrangement of baffles or a certain tank shape would promote the desired action under small accelerations. The systems described above have not been investigated thoroughly in actual zero "g" conditions. Even if the phenomena described above do exist, as speculated, valid qualification testing of units using these principles would require extended zero gravity test times. A complete program could become very expensive and time consuming.

FIGURE 10

MINIMUM SURFACE ENERGY LIQUID FEED SYSTEM

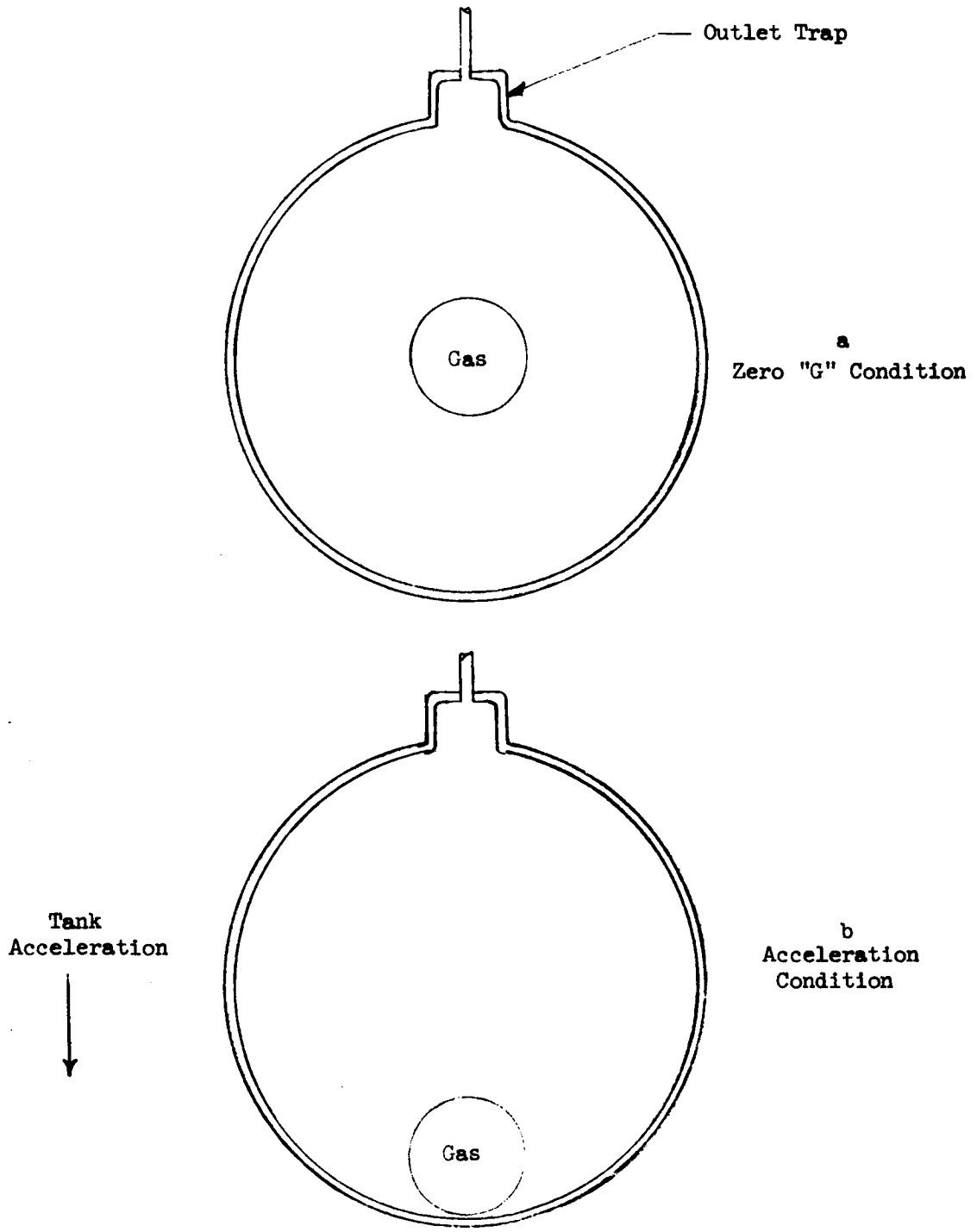

Regenerative Gas Feed System

A recent report (Reference 15) shows evidence that minimum surface energy liquid location systems may be feasible. The tank geometry and contact angle of the liquid are the controlling factors in determining placement of the outlet. Until such time as more conclusive test data becomes available, an alternate system shall be considered. In this section, a system is discussed which is capable of providing gas feed from a tank containing liquid and gas regardless of the natural pattern of liquid location, g loading, or sloshing present.

Figure 11 shows the system schematically. The principle of operation is as follows:

Either gas or liquid can arrive at the valve inlet at any time. The purpose of the valve is to produce an isenthalpic expansion as shown in Figure 12. After the expansion, part of the fluid is always in the form of a gas. All of the expanded fluid is at a lower temperature than the surrounding tank contents. When this fluid is passed through a heat exchanger which is inside the tank, it boils and provides a pure gas stream at the tank outlet. The boiling process removes heat from the tank. This heat removal is necessary if high storage efficiency is to be maintained.

The maximum heat requirement to maintain saturated vapor at the tank outlet is shown in Figure 13. This heat flow must be present across the heat exchanger when the expansion valve is fed by 100% liquid.

The heart of the gas delivery system is the specialized component shown in Figure 14. This module includes expansion valve, heat exchanger and downstream check valve. The basic requirement of the module is that it must supply gas at the outlet regardless of the phase of the inlet fluid. In addition to the former requirement, it must not cause too great a variation in downstream pressure resulting from fluid phase changes at the inlet. The functions performed by the various parts are described below:

The bellows senses the difference in pressure between the tank and the downstream outflow gas and adjusts the poppet to maintain a constant differential pressure when fluid is flowing.

The porous plug acts as a snubber for variable inlet phase conditions, a pressure dropping device, a liquid retainer, and a boiler. The heat exchanger aids the transfer of heat from the surrounding tank fluid to the expanded fluid in the porous plug. Liquid hydrogen can collect between the fins of a heat exchanger as shown in Figure 14, and this would tend to insulate the porous plug. The placement and cross-sectional area of heat exchange surface must be carefully considered to insure adequate heat conduction to the porous plug. The check valve prevents the return of hot gas from the downstream lines when no flow is present.

FIGURE 11

REGENERATIVE GAS FEED SYSTEM

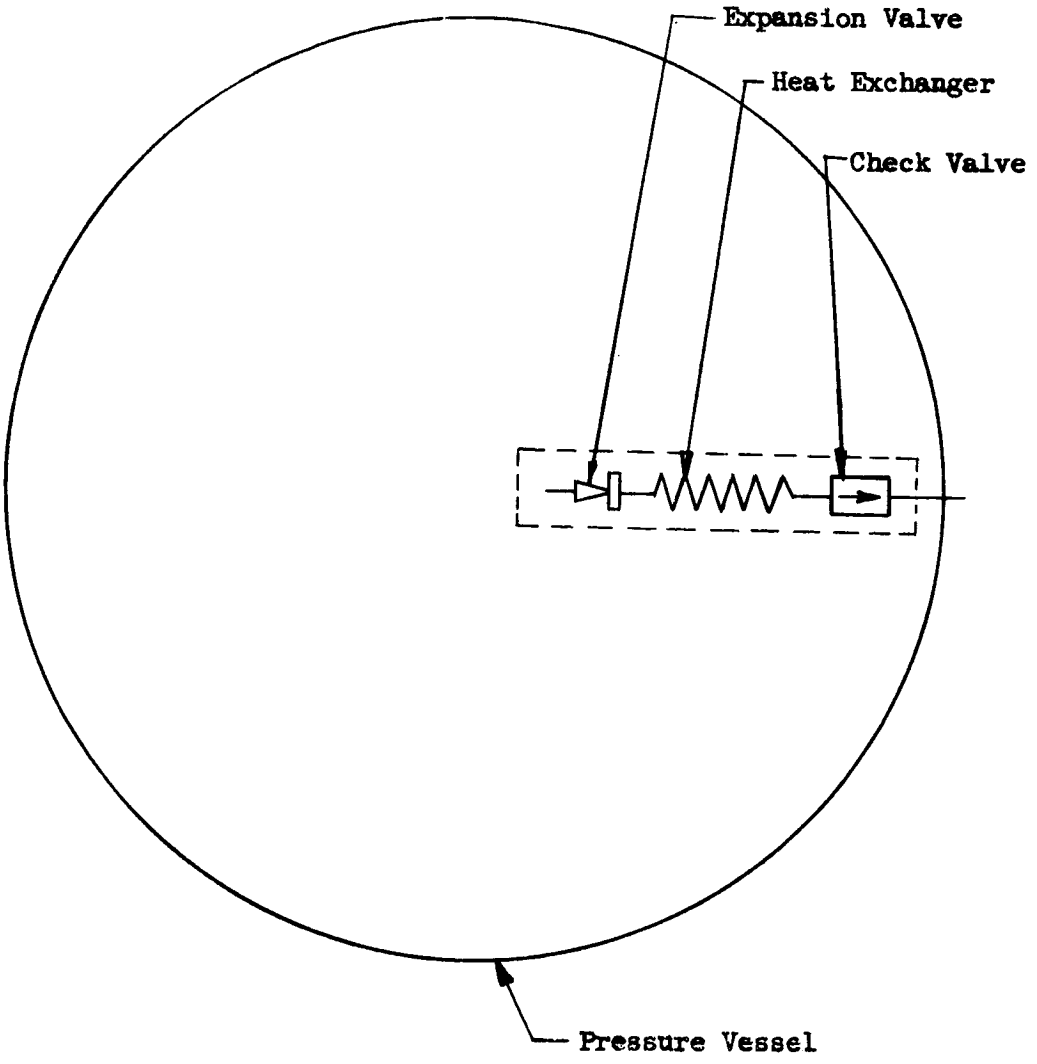

FIGURE 12
TEMPERATURE ENTROPY DIAGRAM
(REGENERATIVE GAS FEED SYSTEM)

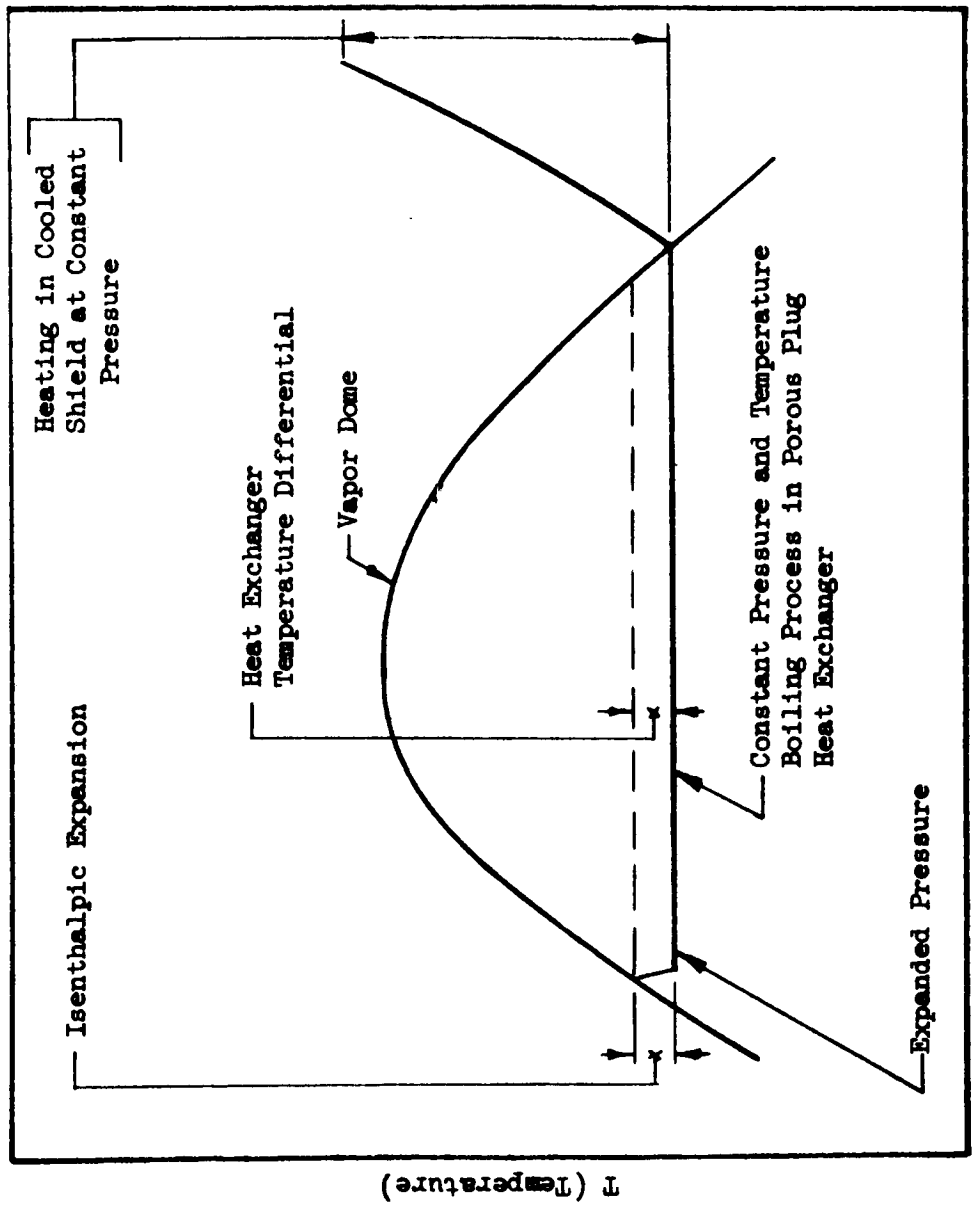

FIGURE 13

HYDROGEN VAPORIZATION HEAT REQUIREMENT ACROSS HEAT EXCHANGER

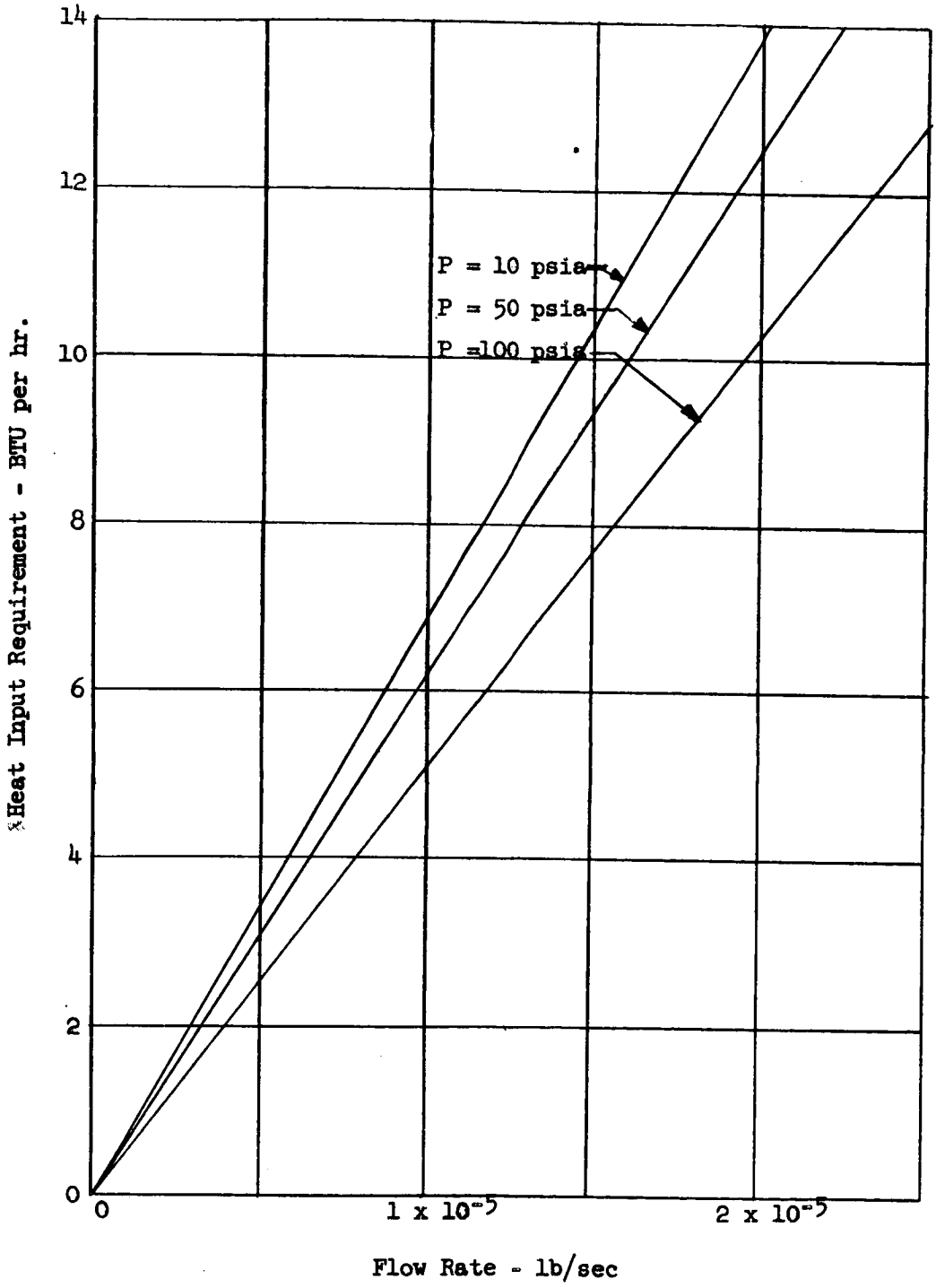

Heat Input Requirement Versus Flow Rate

FIGURE 14

GAS DELIVERY MODULE

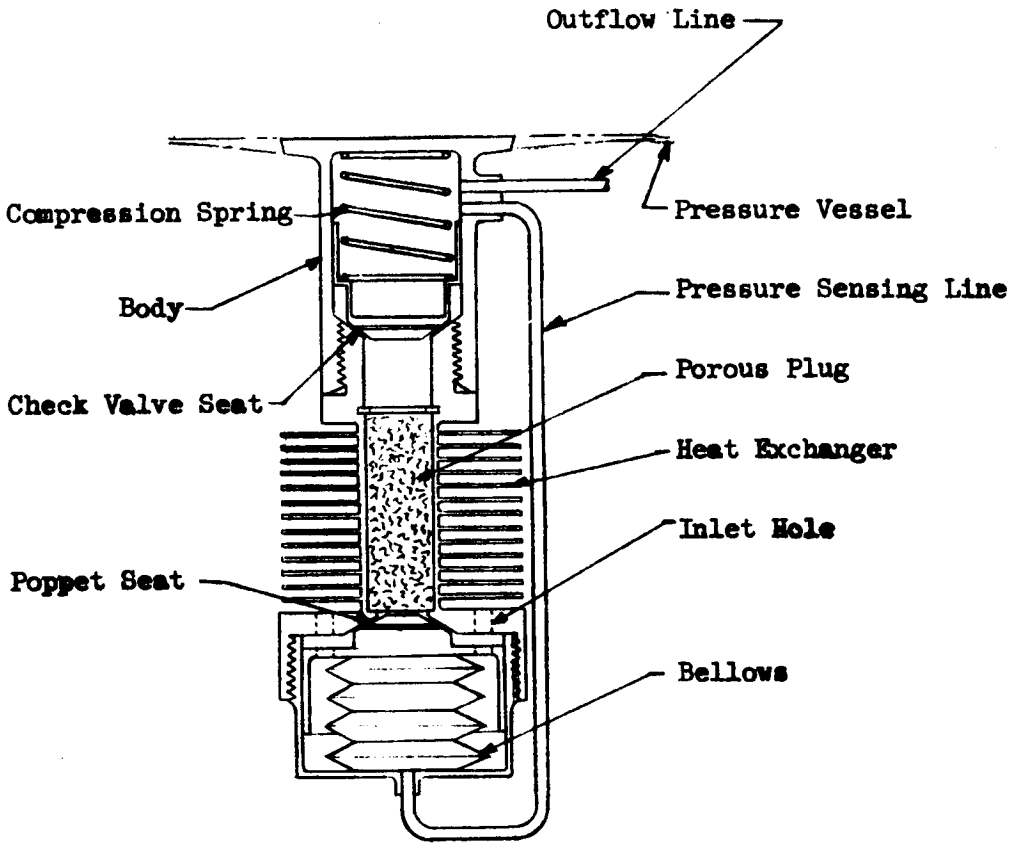

Case 1 - Pure Gas at Inlet

When pure gas enters the module, there is no need for the expansion process because the desired phase separation has occurred by chance in the tank. Nevertheless, the downstream pressure must not fall too low under this condition. The poppet will be adjusted to the full open position exposing the most inlet area to the porous plug. A small amount of refrigeration will be supplied to the hydrogen tank, and the expanded gas will tend to become superheated to the tank content's temperature.

Case 2 - Pure Liquid at Inlet

When pure liquid enters the module, the poppet will be adjusted nearly closed exposing a small amount of porous plug inlet area. The corresponding drop in pressure across the plug will cause a sufficient isenthalpic temperature drop to allow complete boiling of the liquid before it reaches the end of the plug.

Case 3 - Slugging Flow

In this case, gas is flowing into the inlet when suddenly a glob of liquid becomes entrained in the gas stream and impinges against the inlet. In order to comprehend the usefulness of the porous plug under this condition, it is necessary to imagine the action of an alternate pressure dropping device, the controlled flat plate orifice. If an orifice is adjusted to control pressure drop when liquid suddenly arrives at this place, the inertia of the entrained liquid will appear as an instantaneous increase in upstream total pressure. The control, seeing only the tank-line differential, will not readjust quickly and will allow a momentary increase in mass flow into the downstream boiling section. Since the downstream demand for mass flow is unchanging, the pressure in the boiler will start to increase as the slug of liquid is boiled. It is conceivable that too large a slug could be taken into the boiler before the valve can readjust. This action would completely eliminate the pressure differential (and the boiling) momentarily and allowing the possibility of liquid passing out of the tank.

The porous plug would allow the valve to readjust in time to prevent liquid delivery. If a slug arrives at the plug inlet, it too will enter at increased mass flow and total pressure. The plug, however, acts like a series of small flow restrictions spread out over a great length. When the slug enters the plug, it is a relatively long time before the downstream pressure sensing tap will feel an increase in pressure resulting from the flow of the slug. The valve, then, will close gradually over a

relatively long period of time. If the plug is of sufficient size, all of the liquid can be retained before the valve can completely readjust to the steady-state liquid flow condition.

If liquid is flowing through the module when gas appears at the inlet, the reservoir of boiling liquid in the porous plug will supply the outlet mass flow demand while the valve is opening.

Case 4 - No Flow

If gas is flowing into the module inlet when flow is stopped, the inlet poppet will close. The gas between the poppet and the check valve will be superheated in a constant density process until the check valve opens. At this time, any further superheating will cause gas in the module to expand as a constant pressure process.

If liquid is flowing into the module inlet when flow is stopped, the inlet poppet will close. Some of the liquid remaining in the porous plug will boil and the pressure in the module will increase. Since the porous plug is not full, all of the liquid remaining in the module will stay in the plug to satisfy the minimum surface energy requirement. When flow is resumed, gas will pass out of the plug first since it has no surface tension. When sufficient gas has been vented from the plug, the downstream pressure becomes low enough for the poppet to open.

An important requirement for the poppet is that it must close with sufficient "tightness" to prevent the entire inside of the module from becoming filled with liquid in the no-flow condition. This will tend to happen because the cavity downstream of the plug will be wetted by hydrogen liquid and will fill up as soon as the porous plug is full.

The ratio between gas flow pressure drop and liquid flow pressure drop for a given mass flow and fixed porous plug configuration is too great to permit efficient use of the tank as the downstream pressure regulator. The gas-liquid ratio can be found by manipulating the relationships for gas and liquid flow through a porous plug as follows:

Gas flow (0.5 void fraction)

$$\Delta P_g = \frac{N_g \dot{M} T L}{(8.2)(10^{-10}) P_1 d^2 D^2 M_w} \qquad \text{(Eq. 10)}$$

(Reference 9)

Liquid flow (0.5 void fraction)

$$\Delta P_L = \frac{N_L \dot{M} L}{(5.98)(10^{-10}) d^2 D^2 \rho_1} \qquad \text{(Eq. 11)}$$

(Reference 10)

Where:

- ΔP = Pressure drop through plug (atm)
- N = Fluid viscosity (lb/ft-sec)
- T = Fluid temperature (°R)
- L = Plug length (in.)
- $\dot{M}$ = Fluid mass flow rate (lb/sec)
- P_1 = Tank pressure (atm)
- d = Average pore size (microns)
- D = Plug diameter (inches)
- M_w = Molecular weight
- ρ = Fluid density (lb/ft^3)

Subscripts

g = gas

L = Liquid

Dividing 10 by 11 we have

$$\frac{\Delta P_g}{\Delta P_L} = 0.73 \frac{N_g T \rho_I}{N_L P_1 M_w} \qquad \text{(Eq. 12)}$$

Since the gas and liquid are at approximately the same temperature and pressure, this reduces for hydrogen to

$$\frac{\Delta P_g}{\Delta P_L} = 2.42 \qquad \text{(Eq. 13)}$$

In order for the plug to be sized adequately, it must be able to pass gas at the required mass flow rate without excessive pressure drop. At the same time, it must be able to produce sufficient temperature and pressure drop to allow complete boiling of the liquid when liquid is flowing.

The following example illustrates the problem: A tank operates at a maximum pressure of 50 psia. A sonic metering orifice is fed with gas at constant temperature. For $\pm$ 10% variation in mass flow through the sonic orifice, the upstream pressure can be allowed to vary $\pm$ 10% (approximately 45.4 $\pm$ 4.54 psia). If the tank pressure can be maintained exactly constant, the allowable pressure variation (9.08 psi) can be taken across the fixed expansion plug. This condition will exist when gas is flowing. When liquid is flowing, the fixed restriction pressure drop would be

$$\Delta P_L = \frac{\Delta P_g}{2.42} = 3.75 \text{ psi} \quad \text{(From Equation 13)}$$

This ΔP would produce only 0.7 degrees of cooling from the tank when liquid is flowing. The heat exchanger needed to pass the required heat into the liquid would become large at this temperature differential. The required pressure drop is expected to be at least 10 psi for reasonable heat exchanger size.

A substantial increase in tank pressure would be required to provide 10 psi liquid pressure drop and still maintain + 10% downstream mass flow variation. This would result in increased system weight. There would still be no provision for tank pressure to vary under intermittent flow conditions.

By placing an adjustable poppet in front of a relatively large porous plug, the plug can be effectively resized to produce nearly constant pressure drop with widely varying inlet phase conditions. The allowable downstream pressure variation could be allowed to occur in the tank. This is desirable if high storage efficiency is to be maintained under intermittent flow conditions.

The heat exchanger must be sized to extract the required heat when saturated and surrounded by all of the liquid in the tank. This is the worst case because, when surrounded by gas, heat will flow much more easily under the condensing action of the cooled fins.

The check valve opens at a low differential (about 1 psi). This valve must prevent back-flow of hot gas from the downstream lines but not retard the downstream pressure excessively.

In order to make fullest use of the available refrigeration from the outflow gas, the gas feed line is wrapped around the module near the junction with the tank skin. The exit gas will be slightly cooler than the bulk fluid temperature when it leaves the porous plug and can still absorb a small amount of heat before passing through the insulation.

If a minimum surface energy liquid location system were practical, a liquid feed system could use a fixed restriction (porous plug, capillary or orifice) to provide pressure and temperature drop for vaporization. If liquid can always be guaranteed at the inlet of the gas delivery module, the self-adjusting poppet could be eliminated. Some positive close-off device at the inlet would still be required to prevent the hydrogen liquid from flowing slowly past the restriction and filling the downstream line under the no-demand condition.

Regenerative Gas Feed System Testing

A regenerative gas feed system was qualitatively tested. The schematic of the system is shown in Figure 15. Test runs were made in accordance with the test request in Appendix B. Table 6 is a summary of test results. The operations performed on the apparatus are described below.

1. With solenoid valve (1) in feed position, the feed valve (2) was adjusted for a flow of .07 lb./hr. when tank pressure reached 60 psi. (Cracking pressure of the feed expansion valve (3).)

FIGURE 15

HYDROGEN REGENERATIVE SYSTEM TEST SCHEMATIC

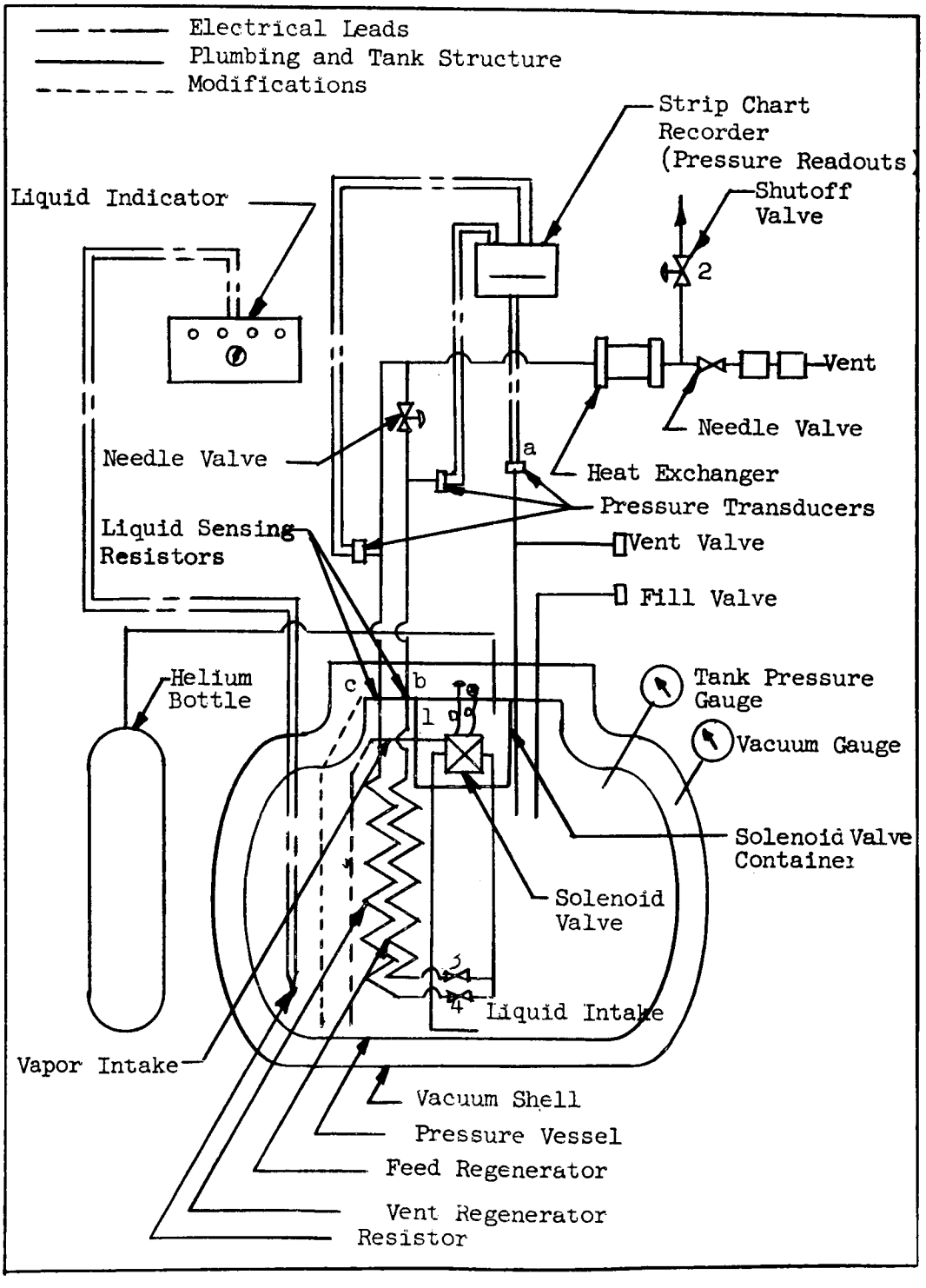

TABLE 6

HYDROGEN REGENERATIVE SYSTEM TEST RECORD

(Test Conducted 5-30-62)

Operation		Vacuum Reading Microns	Tank Pressure psig	Time Min.		Flow Rate lb/hr	Pressure Fluctuations psig	Ambient Temperature °F	Remarks
Begin Cooldown		. 280	0	7:55		0	0	58	Poor Batteries
Begin Fill			0	8:14					on Vacuum
Full Tank			0	8:22					Gauge
Pressurization		90	9	8:31					
			15	8:45					
			20	9:02					
			28.5	9:20					
			30.0	9:23					
			35.0	9:32					
			40.0	9:40					
			41.5	9:49					
		25	50.0	9:55					
			55.0	10:02					New Batteries
			60.0	10:09					on Vacuum
			65.5	10:15					Gauge
			71.5	10:22					
			75.0	10:26					
			80.0	10:32					
			86.5	10:40					
			90.0	10:42 1/2					
			95.0	10:47					
Pressurization			100.0	10:52		0	0	58	
Flow Thru Reg Feed System	Liquid Intake	25	60	10	Alternate	.07±005	0	62	Vapor Always Obtainable at Exit of Reg. Coils.
	Vapor Intake		60	10					
Flow Thru Reg. Vent System	Liquid Intake		80	10					Solenoid Could Be Heard to Actuate
	Vapor Intake		80	10		.07±005			
Max. Flow w/Vapor at Exit of Reg. Coils	Liquid Intake Flow Thru Reg Coils		80			.39			Light off
	Liquid Intake Flow By-Pass Reg. Coils		80			.27	0		Light off
Min. Flow w/liquid at Exit of Reg. Coils	Liquid Intake Flow Thru Reg.Coils		95			.47	.5 max		Light On
	Liquid Intake Flow-By-Pass Reg Coils	25	95			.40	.5 max	62	Light On

2. Tank and line pressure at points (a) and (b), respectively, were monitored on tape with no indication of pressure fluctuations or liquid at the exit of the regenerative feed coils.

3. Solenoid valve (1) was actuated to liquid feed position with no pressure or flow fluctuations nor indication of liquid at the exit of the regenerative coils.

4. Changing from gas feed to liquid feed was done at a rate of approximately 10 cycles/minute. No condition could be induced which would show any pressure or flow fluctuations or liquid indication at the exit of the regenerative coils.

5. The above procedures were repeated on the vent system at 80 psi (cracking pressure of vent expansion valve (4) with the same result as that obtained from the feed system.)

6. The flow rate was then increased to .7 lb/hr (limit of the wet meters) to determine whether or not liquid could be obtained at the exit of the regenerative coils. The result was no indication of liquid, and maximum pressure fluctuations were .5 psi.

The results of the tests seem to indicate that a regenerative system using simple check valves as expansion valves will act as an effective liquid-vapor separator. It is the opinion of the writers, however, that the test results and observations of the operating equipment should be evaluated with caution. There are several questionable points:

1. Referring to Figure 15, note the location of the liquid sensing resistors b. and c. In the actual set-up, these resistors were placed next to a heavy aluminum cover plate. It can be argued that heat input through the insulation and metal cover are boiling the liquid before it can be sensed. The resistors, therefore, would not necessarily indicate complete vaporization at the end of the regenerative coils as a result of the reduced pressure downstream of the expansion valves 3 and 4.

2. Small entrained droplets of liquid would not necessarily be sensed by the resistors. The thermal capacity of these elements could easily overcome the cooling effect of the droplets at low flow rates and sufficient resistance charge for measurement would not be created.

3. The entire tank insulation scheme, thermodynamic flow system, and system dynamics are radically different from an actual flight-weight system. Any conclusions regarding pressure fluctuations or system surges in the test setup do not necessarily indicate the action of a flight-weight system.

The value of the testing is that it served to point out the need for a highly refined testing technique.

The testing also served to point out many of the pitfalls which could be encountered in the design of a similar flight system.

Many of the observations of the operating test system carry over to the fully modulated system proposed in the preceding section. Theoretical system logic and calculations will be relied upon for future designs until refined test information becomes available.

Thixotropic Liquid Location

Thixotropes (gel < > sol) have several properties which can be used to advantage in zero gravity gas feed systems. Gels are prepared by adding a small quantity of a certain finely divided powder to a liquid. The stiffness of the gel depends on the quantity of powder added and the chemical properties of the gelling agent and liquid. Practically any liquid can be gelled by adding the proper agent.

The chemical phenomenon of thixotropy of isothermal gel-sol transformation is very complex and is not well understood. The subject needs to undergo extensive basic research and development before it can be stated that the true mechanics have been determined.

Certain observed properties and theory, however, give possible explanation for a part of this phenomenon.

Numerous gels are rendered fluid by mechanical agitation or by ultrasonic energy. These same gels, after a rest period, again assume their gelatinous properties. This characteristic of being reversible (sol < > gel) is unique to a certain class of gel and is termed thixotropy. The theoretical explanation of this phenomenon, as well as gelation and stability, necessitates the assumption that the forces of attraction and repulsion that exist as electrical potentials between ions, atoms, and molecules also exist between colloidal particles. These forces are very apparent in the energy required to alter the density of all orderly discontinuous matter.

Liquid hydrogen was gelled in a simple qualitative test at Beech. The test was performed to prove that hydrogen could be gelled. No attempt was made to determine the physical properties of the substance. Providing that further study and tests prove that hydrogen gels are satisfactory from a chemical and physical standpoint, the following system could be constructed. Figure 16 shows such a system. The tank is initially filled

FIGURE 16

THIXOTROPIC LIQUID LOCATION TANK

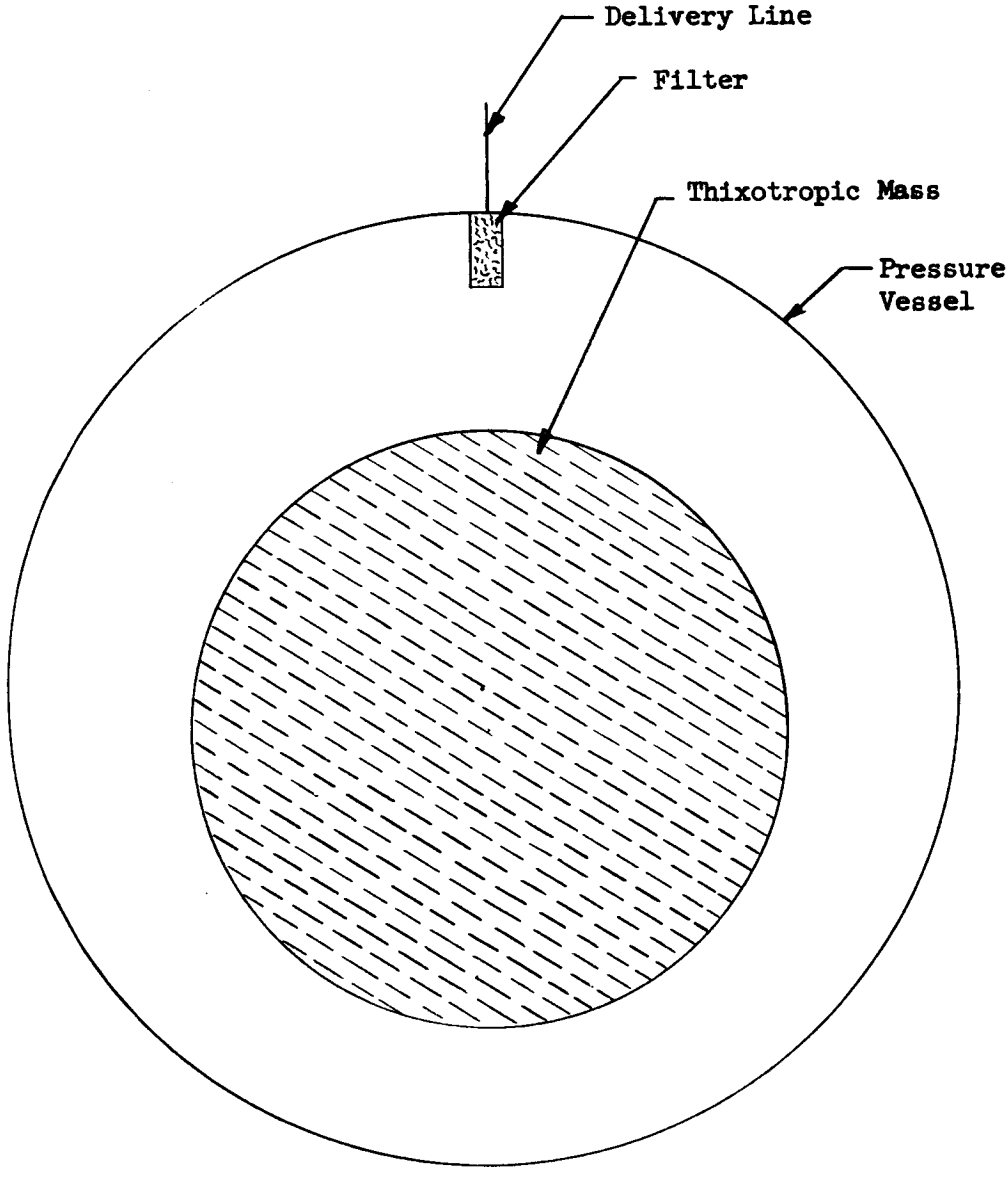

with thixotropic hydrogen. As heat leaks into the tank, gas is evolved from the gelled mass. The gelling agent floats about in the gas under zero gravity conditions. A filter placed in the outlet will not allow the agent to pass out of the tank. The resultant pure gas stream is fed to the engine.

The filter inlet is made large so that a build-up of powder at this location will not restrict the outlet gas flow excessively. The gel is made stiff enough so that it cannot be extruded through the filter. The stiffness of the gel also overcomes surface tension and minimum surface energy forces cannot control liquid location. Loose chunks of this substance can float about in the tank at random and not disturb the outflow or pressure control.

A treatment of the testing of this type of tank is presented under ammonia systems. (See Section 2.2).

2.1.1.3 Flow Control and Metering

The gaseous hydrogen propellant must be delivered to the engine under specific thermodynamic conditions. The required flow control system depends on these conditions. Basically, the engine requires 2 (10^{-5}) pounds per second of the gas within certain temperature and pressure limits. The system will take two different forms depending on the mode of flow. The two systems supply flow in:

1. Long-duration pulses or continuous flow. Starting and stopping transients for this system are unimportant.

2. Short-duration pulses. Starting and stopping transients for this system must be carefully controlled.

Long Pulse Control System

This type of system is the easiest to construct. The proposed system requires no electrical power or electronic controls. Valves and temperature controls may be allowed to readjust slowly because start-up and shut-down flow transients are not critical. Precise attainment of mass flow is not required immediately.

Tank pressure is maintained within certain limits by adding heat as fluid is withdrawn. Ideally, it is desirable to design a tank so that the boil-off rate due to heat leak exactly matches the desired use rate when highly efficient insulation is available. In this method of operation, the tank pressure would remain exactly constant. There are two reasons, however, why this condition is not practical.

1. The environmental (tank skin) temperature may change.

2. Flow occurs in pulses requiring instantaneous changes in heat input.

The practical way to operate a tank is to allow the pressure to cycle within certain limits. The "pressure band", or allowable pressure variation, should be as wide as possible and still fall within the allowable downstream variation. The upper limit on tank pressure is controlled by a relief valve, and the lower limit by a heat input device. Figure 17 shows how the pressure band would be controlled.

The heater cut-out point is located as close as possible to the lower pressure limit. This location will allow maximum use of the available refrigeration in the tank contents. Should the outlet flow be stopped at the heater cut-out point, considerable heat input can be absorbed as the pressure rises to the relief pressure.

The amount of heat leak energy which can be absorbed in the liquid when no flow is present can be calculated by the basic thermodynamic relationship written for the constant volume process:

$$dQ = dU = C_v \Delta T \qquad \text{(Eq. 14)}$$

Where dQ = Heat absorbed by stored fluid $(\frac{B}{lb})$

U = Bulk internal energy of stored fluid $(\frac{B}{lb})$

C_v = Specific heat at constant volume of bulk fluid $(\frac{B}{lb\text{-}^{\circ}R})$

ΔT = Temperature change from heater cut-out point to pressure relief point. $(^{\circ}R)$

Either C_v can be taken as an approximate constant or dU can be determined from appropriate charts, and tables.

The time required for the pressure to build from low pressure to the relief valve setting can be calculated by:

$$d\Theta = \frac{M\,(d\,Q)}{\dot{Q}_1} = \frac{M\,(d\,U)}{\dot{Q}_1} = \frac{MC_v\Delta T}{\dot{Q}_1} \qquad \text{(Eq. 15)}$$

FIGURE 17

TANK PRESSURE CONTROL BAND

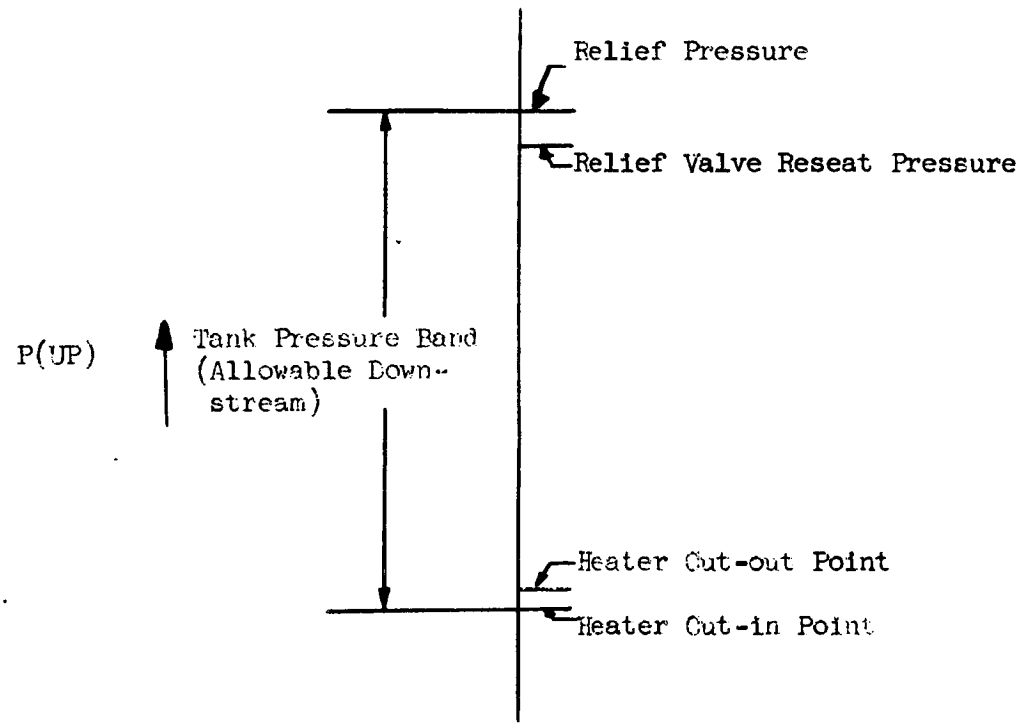

Where $d\theta$ = Time to pressurize (hr.)

M = Mass of fluid in tank (lb)

$\dot{Q}_1$ = Insulation heat leak rate $(\frac{B}{hr.})$

The time required for the pressure to decay from the relief valve reseat pressure to the heater cut-in point can be determined by the method given below. It is assumed here that the heat input due to heat leak is zero during this time. The expansion process in the tank is isentropic. Referring to the temperature entropy diagram in Figure 18, the change in bulk fluid density can be determined between any two pressures.

The change in mass is:

$$dM = (d\rho)_s V = (\rho_1 - \rho_2) V \qquad \text{(Eq. 16)}$$

Where V = Volume of tank (ft^3)

ρ_1 = Initial fluid density $(\frac{lb.}{ft^3})$

ρ_2 = Final fluid density $(\frac{lb}{ft^3})$

dM = Change in mass (lb)

$(\ )_s$ = At constant entropy

The time required for pressure decay between ρ_1 and ρ_2 is

$$d\theta = \frac{dM}{\dot{M}(3600)} = \frac{(\rho_1 - \rho_2)V}{\dot{M}(3600)} \qquad \text{(Eq. 17)}$$

Where $d\theta$ = Time to decay (hr.)

$\dot{M}$ = Outflow gas flow rate $(\frac{lb.}{sec.})$

By examining the variables in Equations 15 and 17, it can be seen that both the build-up and decay time will vary as the mass in the tank is depleted.

FIGURE 18

TEMPERATURE ENTROPY DIAGRAM

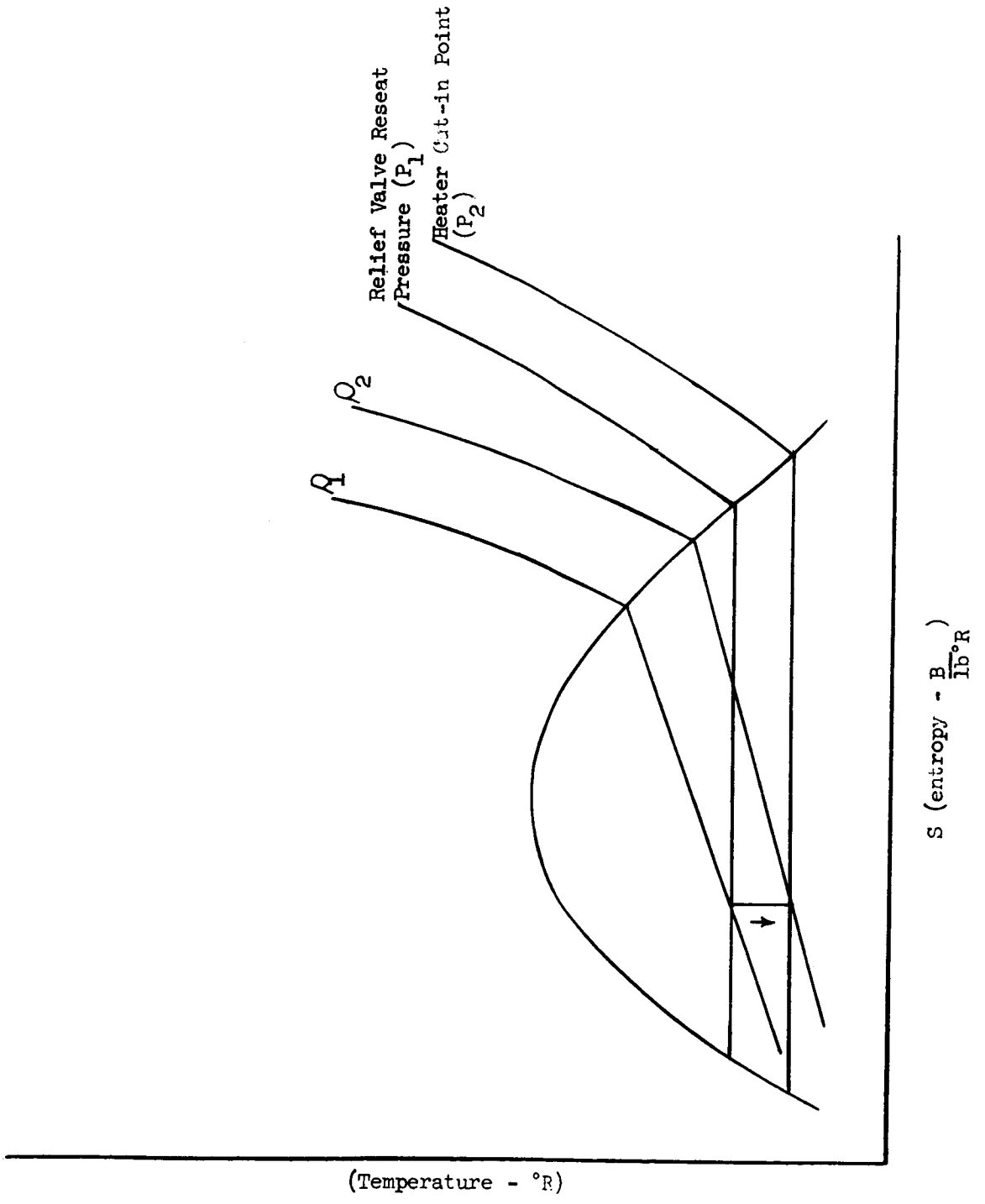

When the tank pressure drops to the heater cut-in point, heat is required to maintain pressure in the amounts shown in Figure 13. Figure 19 shows a proposed device for adding heat in small quantities to a liquid-hydrogen tank. The heater contains pressure sensing elements almost identical to those used in snap-action pressure switches. Instead of making electrical contact, though, the unit provides a thermal short between the outer tank covering and the pressure vessel. If properly designed, the elements should be sensitive to pressure variations of $\pm$ 1% of the absolute tank pressure.

Two pressure elements are included in the heater. The inner element disconnects the pressure vessel from the vacuum shell during ground stand-by and part of the launch period. As the vehicle rises from the ground, the atmospheric pressure begins to decrease. At some predetermined pressure altitude, the element snaps into the closed position providing a permanent thermal short between the pressure vessel and vacuum shell.

The outer element acts only on tank absolute pressure. This thermal switch controls heat input when tank pressure becomes too low.

The approximate size of the thermal shorting rod can be calculated by the Fourier equation.

$$A = \frac{QL}{k\Delta T} \qquad \text{(Eq. 18)}$$

Where
- A = Cross-sectional area of rod (ft^2)
- Q = Heat input requirement ($\frac{B}{hr.}$)
- L = Length of rod (ft)
- k = Thermal conductivity of rod ($\frac{B\ ft}{hr.ft^2 \cdot R}$)
- ΔT = Temperature differential across rod (°R)

Example: Calculate the diameter of the thermal shorting rod required for the following conditions.

LH_2 tank pressure	= 50 psia
Mass flow rate	= 2×10^{-5} lb/sec
Rod length	= 1.5 in.
Thermal conductivity of rod	= (28) $\frac{B\ ft.}{hr.ft^2 \cdot R}$ (aluminum)
Heat Input Required	= 12.5 BTU (from Figure 13)

FIGURE 19

TANK HEATER

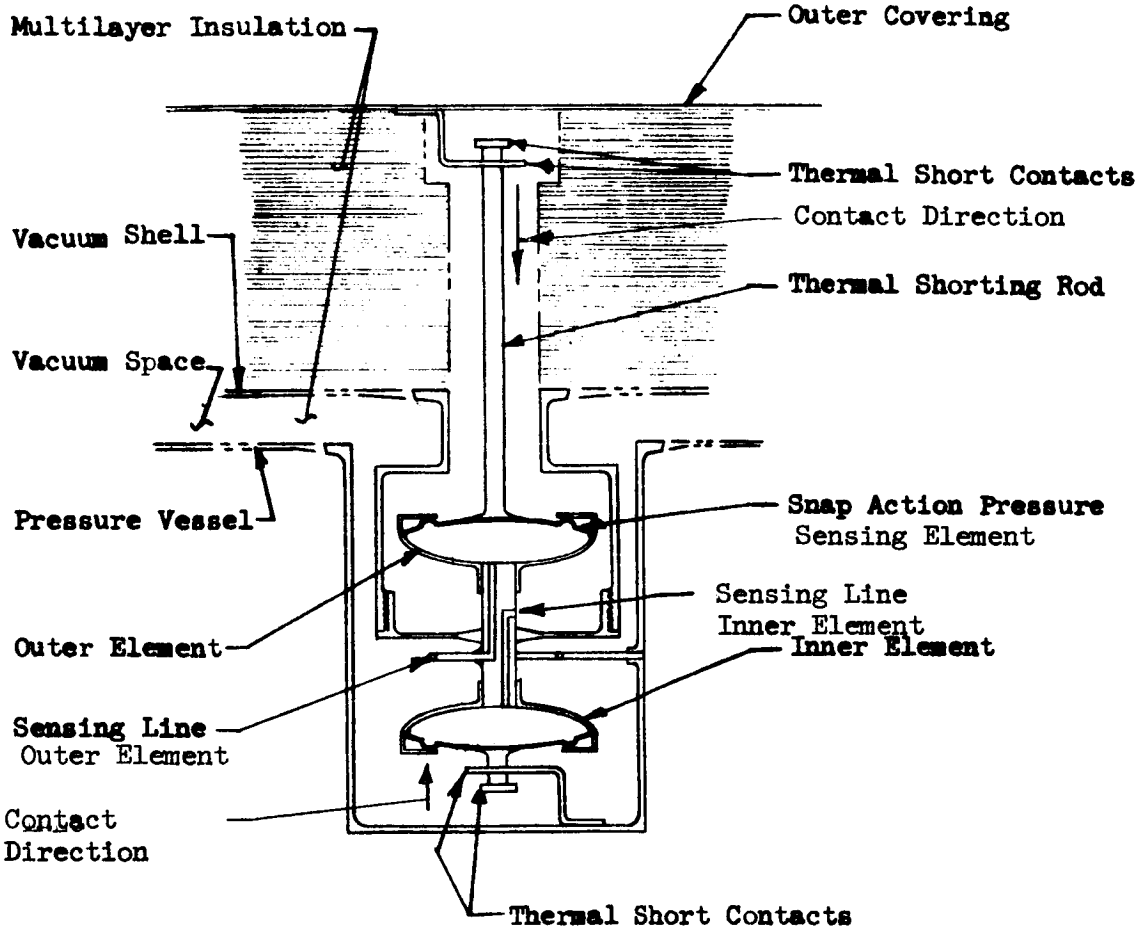

Fluid temperature = 36.5°R

Outer covering temperature = 300°R

$$A = 0.0305 \text{ in.}^2$$

$$D = \frac{4A}{\pi} = 0.197 \text{ in.}$$

which is well within the limits of practicality.

Note that the drain of heat from the outer tank covering will not significantly reduce Teq calculated from Equation 1, Section 2.1.1.1.

An increase in contact area at the connection must be provided in order to make up for reduced conductivity at this point. The contact coefficient will depend on the cleanliness and contact pressure. The contact coefficient of the switch will be improved and the problem of high vacuum cold welding will be minimized by application of a silicone oil or grease.

When disconnected, the heat leak at the thermal short will be negligible. Heat flows on the order of those shown in the section on Insulation Discontinuity Protection in Section 2.1.1.1 will be present.

Mass flow is easily controlled by maintaining constant temperature and pressure at the inlet of a fixed sonic-flow device. The useful characteristic of any sonic-flow device is that mass flow across the restriction is independent of the downstream pressure providing the proper pressure ratio is present. The pressure ratio is defined as the ratio between the downstream and upstream total pressures. For a flat-plate orifice passing a diatomic gas such as hydrogen in the perfect gas region, this ratio must not exceed 0.53 if the orifice is to remain sonic. The pressure ratio is determined by standard thermodynamic means (see Reference 11).

The sonic-flow relationships for capillary tubes and porous plugs are complicated by the frictional effects upstream of the outlet, but the same general thinking applies. As long as the device remains sonic, fluctuations in pressure downstream will not effect mass flow.

Single flat-plate orifices providing mass flows under the conditions specified for this study are generally less than 0.010 inch in diameter. These small restrictions are easily plugged by tiny pieces of foreign matter. In addition, it is difficult to produce such an orifice with the required dimensional consistency. These problems can be relaxed by using capillaries or porous plugs. A bundle of capillaries or a porous plug cut to proper length in a calibration procedure is more satisfactory. If these devices are of sufficient length, it is not necessary to maintain extremely precise tolerances on the length of the part. Porous plugs and capillary bundles are not easily plugged, there being many redundant paths through which the gas can flow.

The mass flow through a sonic restriction is proportional to the upstream total pressure and inversely proportional to the square root of the upstream total temperature. Therefore, it is necessary to maintain these conditions constant within the limits required for adequate mass flow regulation.

As described in the preceding section, upstream pressure is maintained within the allowable band by the limits set by the tank heater and the pressure relief valve. This type of pressure regulation is adequate providing that high-storage efficiency (low-weight system) can be maintained. If large variations in demand cycles or large ambient temperature fluctuations occur frequently, it may be necessary to allow wide tolerances on tank pressure to maintain reasonable storage efficiency. In such cases, tank pressures must be higher; and secondary regulation for the pressure at the inlet to the metering device would be necessary. A typical design for a pressure regulator is shown in Figure 20.

Temperature regulation can be obtained by the use of a simple temperature mixing valve. Figure 21 shows such a valve. Temperature regulated gas is passed over a stack-up of bimetallic wafers which are connected to an orifice control poppet. The wafers assume different contours depending on the temperature of the regulated gas. The large stack of wafers is very sensitive to outlet temperature variations. The resultant movement of the poppet changes the ratio of hot and cold gas entering the valve to control outlet temperature within approximately $\pm$ 10°R. The valve can be supplied with sufficient hot and cold gas for regulation to approximately 450°R by splitting the gas flow from the tank into two streams. The cold stream is protected by insulation and passes directly to the mixing valve. The other stream passes through a warm place in the vehicle where heat is absorbed at constant pressure. The hot stream is directed to the mixing valve where the proper outlet gas temperature is obtained without the expense of significant pressure drop. Heat requirements are low because the mass flow rate of gas is low. Less than 36 B/Hr would be required for a flow rate of $2(10^{-5})$ pounds/second hydrogen flow rate if the normal line temperature fluctuation does not exceed 150°R.

Engine chamber pressure will not be controlled by the flow system described above. This statement is reasoned as follows: Two fixed sonic devices are in series - engine nozzle and metering restriction - the metering restriction will control mass flow. If mass flow is constant and the engine outlet size is not variable, the chamber pressure must assume a value depending on the temperature of the fluid exhausted through the engine.

FIGURE 20

PRESSURE REGULATOR

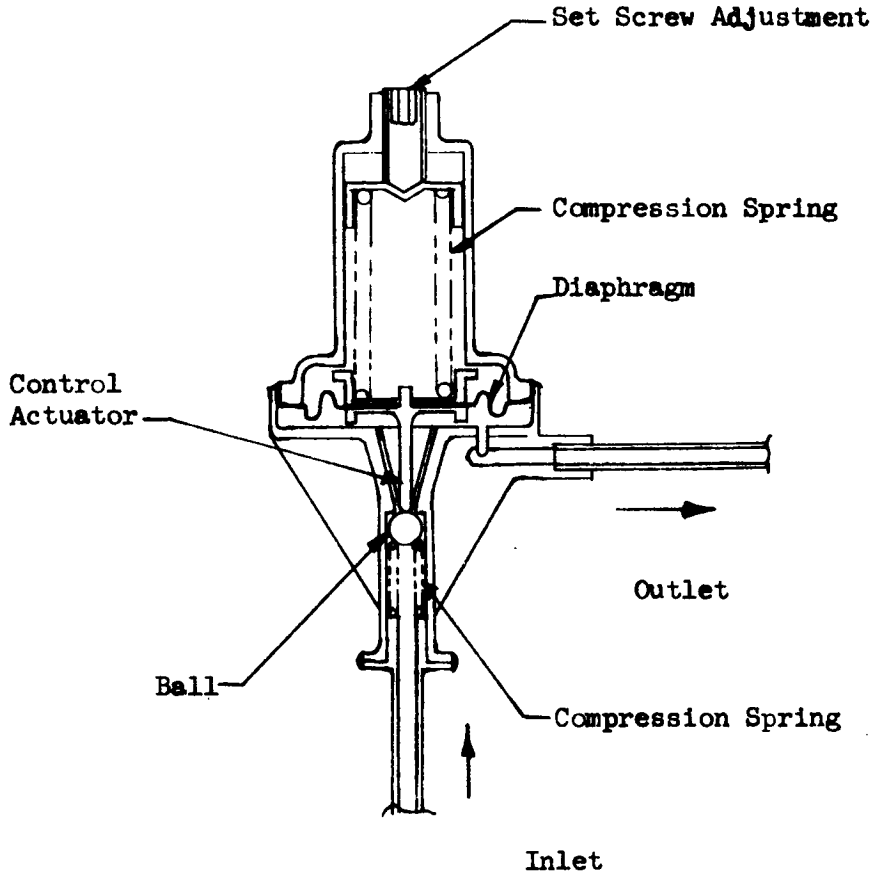

FIGURE 21

TEMPERATURE MIXING VALVE

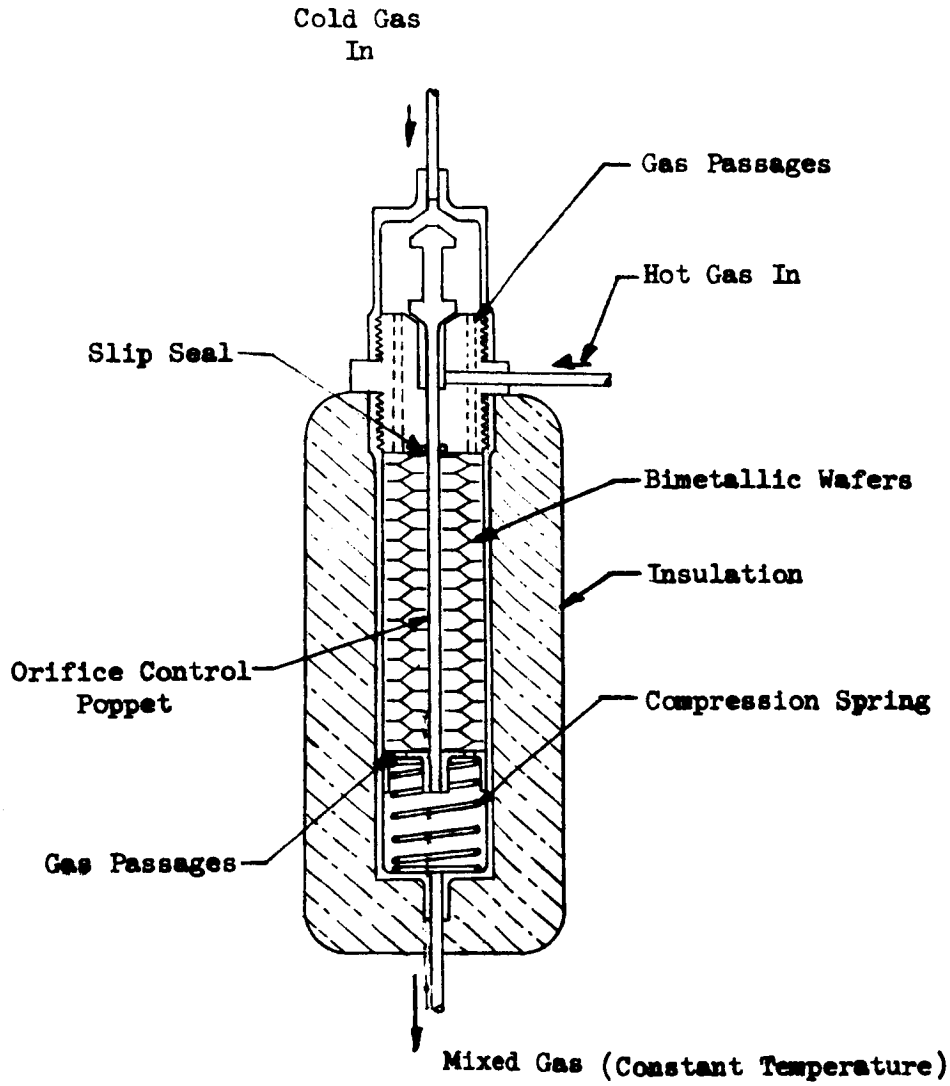

A shutoff valve is required upstream of the engine. Figure 22 shows an electric solenoid valve designed for this purpose. Placement of the valve in relation to the sonic metering device will depend on engine requirements. Figure 23 illustrates the action of the mass flow under the two possible combinations. When the metering restriction is placed upstream of the shutoff valve, a volume of unregulated gas lies between these points. When flow is initiated, this gas tends to rush into the engine at increased mass flow. Depending on the line length and diameter, this temporary overshoot could represent a loss of engine efficiency. If the shutoff valve is placed upstream of the metering restriction, mass flow will not overshoot.

Short Pulse Control System

There are several special considerations in the design of a system which will accurately control mass flow in extremely short pulses. As described in the foregoing section, relatively constant temperature and pressure must be obtained before the sonic metering device will control mass flow. There is a limit, however, to the speed at which this condition can be attained.

This limit is set by the following factors:

1. The amount of required gas temperature and pressure change
2. Gas mass flow rate
3. Gas thermodynamic properties
4. Environmental conditions of temperature and gravity
5. Component and line mass
6. Component and line thermodynamic properties
7. Spring rates and mechanical resistances of component parts
8. In general, all of the physical dimensions of the system parts.

The dynamic system can be designed to minimize the time required to reach a steady-state condition, but some definite limit will always exist.

A device which would permit extremely fast mass-flow regulation is shown in Figure 24. The system would work providing that the tank pressure is maintained within the limits required for mass flow regulation at the sonic restriction. As stated before, this is possible when environmental temperature and demand cycles are constant enough to permit lightweight design.

FIGURE 22

SOLENOID VALVE

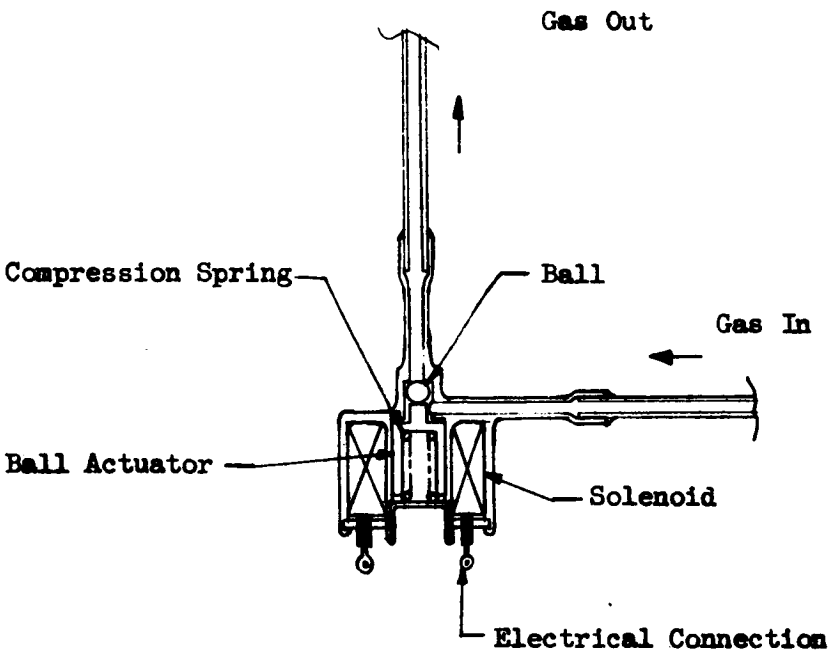

FIGURE 23
ARRANGEMENT OF SHUTOFF VALVE AND METERING RESTRICTION

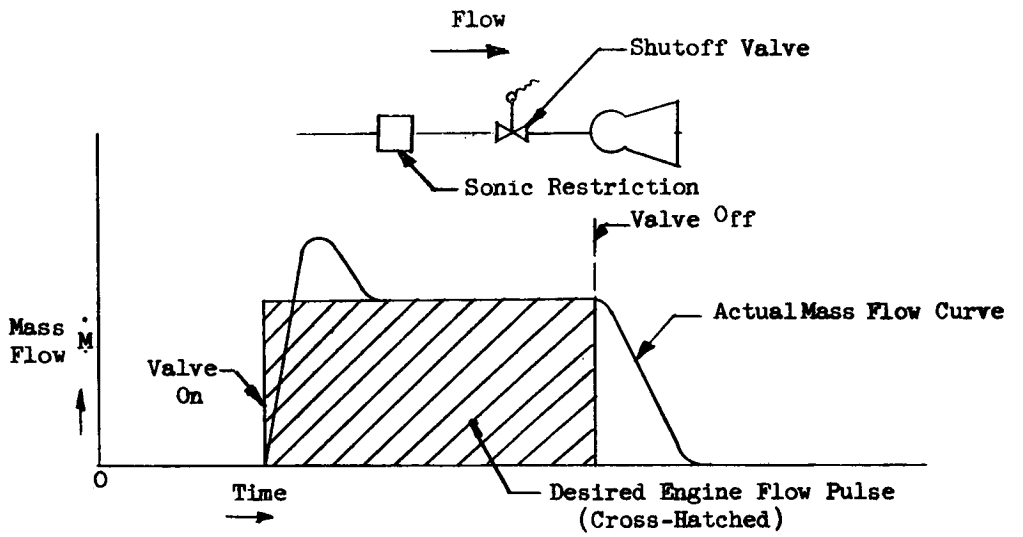

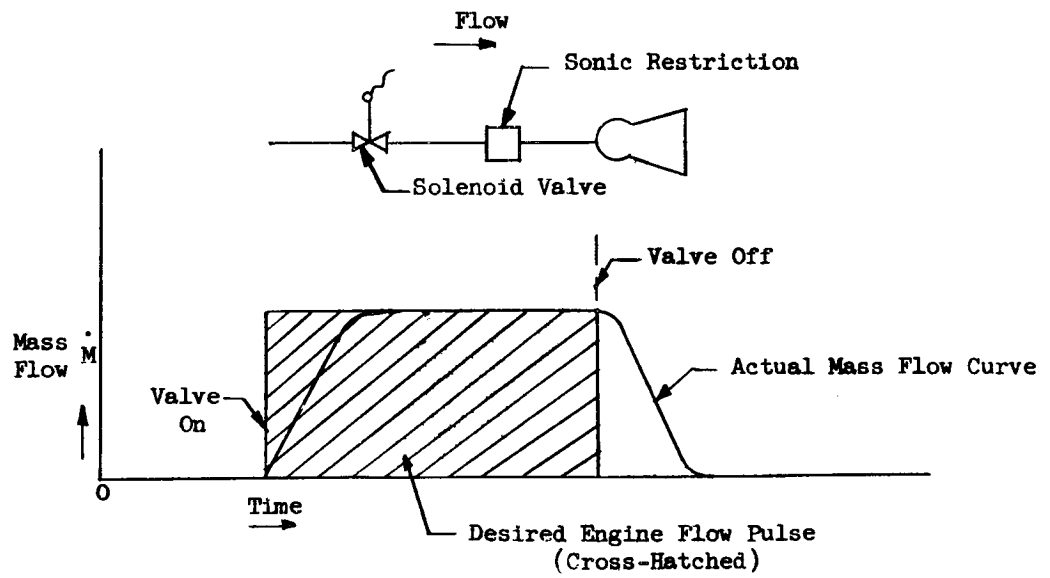

FIGURE 24

TEMPERATURE CONTROLLED PLENUM

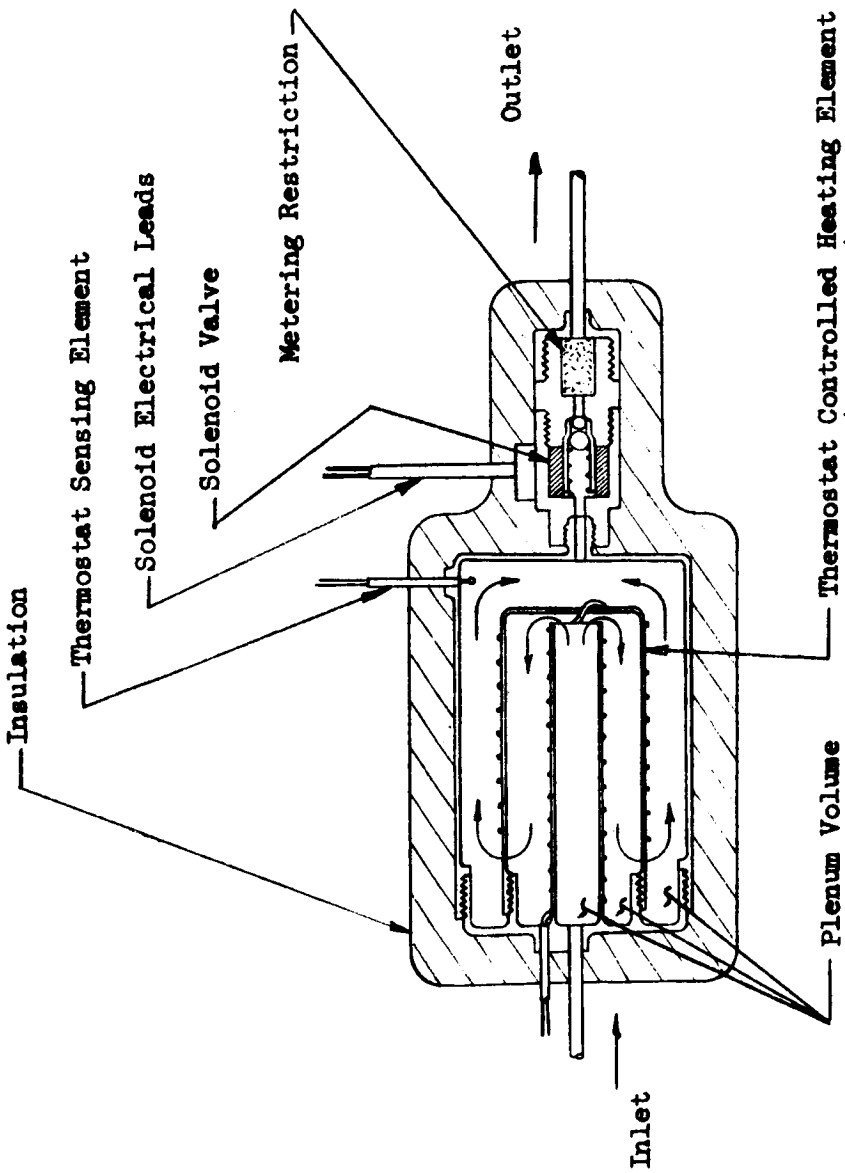

A temperature-controlled plenum is installed in the system and closely coupled to the metering restriction and engine. This plenum includes protective insulation, thermostat, and electrical resistance heater. The plenum is of sufficient size that initiation of flow can occur without significant change in metering restriction inlet conditions. Temperature is controlled within close limits of the heater and thermostat. The metering restriction is soaked at the temperature of the gas in the plenum. With this arrangement, there is no lag in time for the fluid or components to reach proper metering conditions.

In the no-flow condition, the cold gas in the lines upstream of the plenum is expanded by heat leak. To prevent significant changes in plenum pressure as a result of this action, the plenum is sized to have a volume much greater than the upstream line volume between the check valve and plenum. The plenum will then absorb the expanded gas at relatively constant pressure.

For extremely low flow applications the return of hot gas to the tank is undesirable. For higher flow applications where the return of hot gas to the tank is not objectionable, the check valve would not be required. In this case, the size of the plenum is not critical.

2.1.2 Complete Storage and Feed System

From the concepts described in Section 2.1.1, it is now possible to assemble complete storage and feed systems for liquid hydrogen.

2.1.2.1 Structural Plan

For a complete description of the component parts of the regenerative gas feed tank, refer to applicable paragraphs in Section 2.1.1. The unit can be easily converted to a minimum surface energy, or thixotropic liquid-location tank. Structural equations used for the basic tankage are given in Appendix C.

Loading

The tankage is subjected to the following loads:

1. Internal pressure
2. Atmospheric pressure
3. Inertial loads

Failure

The maximum principal stress theory of failure was used in all equations to size components. This is the most conservative of the theories of failure, but it is felt that this theory should be used in cryogenic applications until sufficient low temperature testing has been performed to prove the accuracy of another theory.

Pressure Shell

The pressure shell is subjected primarily to the static pressure of the contained fluid. Fluid pressures resulting from inertial effects are relatively small. The use of load-bearing insulation between the inner and support shells eliminates any point loading on the shell which would result if the shell were rigidly connected to other structures.

Under this condition of loading, the shell is for the most part in the pure membrane condition. Discontinuities exist at one pole where the thermal standoff and vent line are attached to the shell. The standoff has been designed so that the shell is free to expand in the radial direction. The items attached to the shell are relatively rigid and are assumed to cause total restraint against expansion in the circumferential direction and allow no edge rotation at the juncture with the shell. The added stresses resulting from the discontinuities have been analyzed by the methods of Reference 12.

Support Shell

The support shell must carry the inertial load of the pressure vessel, load-bearing insulation, and fluid. In addition, it is subjected to a differential pressure due to atmospheric pressure on the outer surface and a vacuum on the inner surface. Material thickness must be sized to withstand both of these loads. The main portion of the shell will be stressed in a uniform biaxial compression, but additional stresses will be produced in the area of the support ring. Inertial loads will introduce bending moments resulting from rotation of the support ring. Tensile loads will result around the support lugs when the support ring deflects. Discontinuity stresses, which are produced in the area of the ring, must be added to the compressing stresses produced by external pressure. The support shell must withstand atmospheric pressure without buckling. This condition is imposed by thermal rather than strength requirements, since buckling could result in decreased insulation thickness which would be accompanied by increased heat transfer through the insulation.

Support Ring

The support ring is subjected to various combinations of direct and torsional moments. A circular cross section was chosen for the ring because of its ability to resist torsional loads. Deformations of the ring must be minimized to produce minimum uniform loads in the support shell. In addition, changes from the pure spherical form of the support shell, which would be introduced by ring deflections, could result in buckling of the shell by external pressure.

The ring was analyzed by an energy method as described in Reference 13. Equations for maximum moment, torque, deflection, and rotation were derived for any number of ring supports. Both a uniform direct load and a uniform couple were considered.

2.1.2.2 Complete Flow Systems

Figures 25 and 26 are the schematic diagrams showing all valves and controls on a regenerative gas feed system. A minimum surface energy gas feed system would not require the gas delivery module (Figure 14). A thixotropic liquid location tank would require replacement of the gas delivery module with a filter. Check valves are required in all systems.

Figure 25 shows the required system for supplying long duration pulses or continuous flow. A brief description of the operation follows. For a complete description of control components see applicable paragraphs in Sections 2.1.1.2 and 2.1.1.3.

On demand from an electrical signal, the solenoid valve opens and allows gas to pass to the sonic restriction. After a short period of time, temperature at the inlet of the sonic restriction stabilizes to a point where constant mass flow is delivered to the engine within certain tolerance limits. Gas is obtained from the tank on demand by the action of the gas delivery module. Tank pressure is maintained within the limits required for mass flow control at the sonic restriction by the pressure relief valve and the tank heater. In systems where the flow demand or environment changes in a very irregular pattern, it may be necessary to add a pressure regulator and allow wide tolerances on tank pressure to meet the mass flow tolerance and still achieve minimum weight.

Figure 26 shows the required system for supplying short duration pulses. A brief description of the operation follows. For a complete description of control components see applicable paragraphs in Sections 2.1.1.2 and 2.1.1.3.

On demand from an electrical signal, the solenoid valve opens and allows gas to pass to the sonic restriction. Gas is fed from the constant temperature plenum. The temperature in the plenum is maintained within the limits required for mass flow control at the sonic restriction by the thermostat and heater. The tank pressure is maintained within the limits required for mass flow control at the sonic restriction by the pressure relief valve and the tank heater.

FIGURE 25
LONG PULSE SUPPLY SYSTEM
REGENERATIVE GAS FEED TANK - HYDROGEN TANK

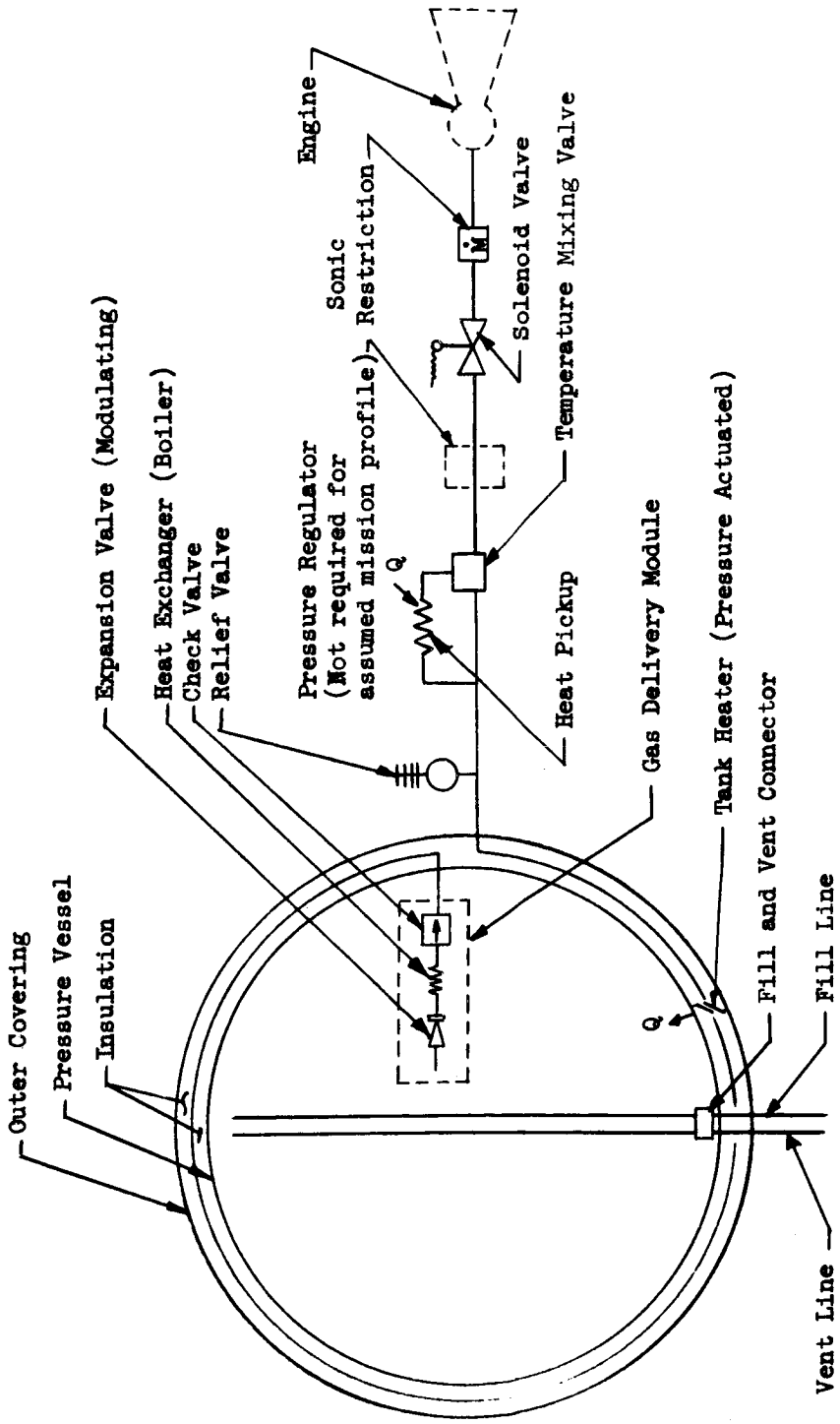

FIGURE 26
SHORT PULSE SUPPLY SYSTEM
REGENERATIVE GAS FEED TANK - HYDROGEN TANK

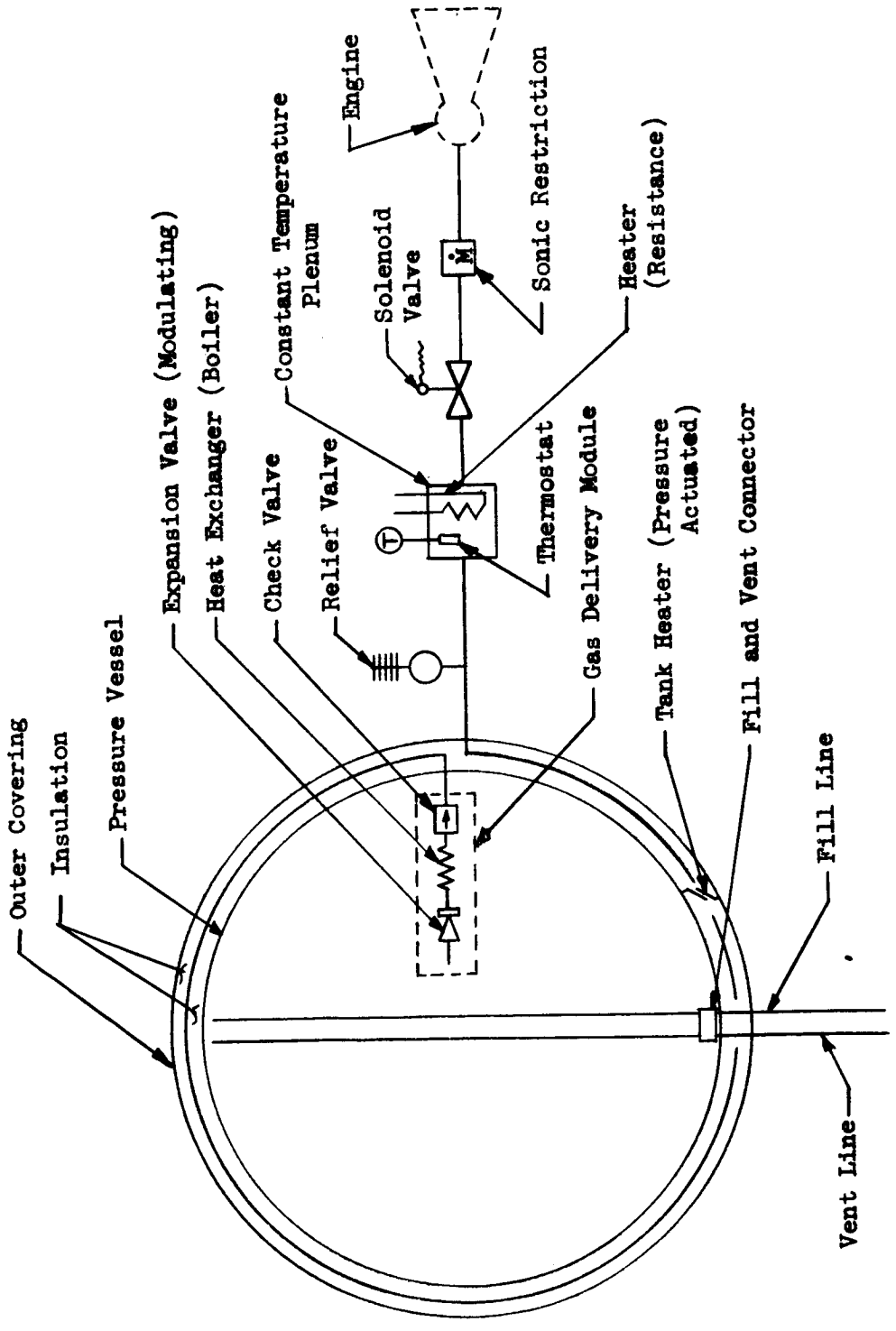

2.1.3 Tank System Weight Studies

Tank Sizing and Weight Optimization

In a subcritical cryogenic storage system, if the stored fluid is not used continuously, various related factors may be adjusted to produce the minimum weight system. This may be demonstrated by considering a period of time during a mission when no fluid is used. During this time heat continues to enter the tank; and if pressure is to remain constant within the tank, the entering heat must be allowed to convert a portion of the stored liquid into a vapor form which is vented. Assuming constant thermal conductivity of the insulation, the thickness of the insulating material determines the rate at which gas is expelled from the tank. If a thick insulation is used, a small amount of gas will be vented; and if a thin insulation is used, a large quantity of gas will be expelled. It is now evident that the proper balance between insulation thickness and; therefore, insulation weight and vented gas will produce a minimum weight system.

Figure 27 shows the result of this method of optimization. The figure shows that the optimum system is not that which vents a minimum amount of fluid. It also shows that the optimum vented weight for a particular system with constant insulation thickness is a function of insulation density.

Figure 28 gives weight comparisons for various flow conditions in the hydrogen system. For each tank the weight of the usable fluid is 20 lbs. and the tank may or may not contain fluid to be vented. Where it is applicable, the weights have been optimized as shown in Figure 27. For each flow condition, weights are shown for two insulation densities. The weights consist of inner shell, insulation, outer shell, and all fluid.

The most basic system is that where the fluid is used continuously at a constant rate for the three-year period. These curves are those labeled $\dot{M} = \dot{M}u$ in Figure 28. If pressure is allowed to cycle within limits, and no fluid is vented, this condition will represent the actual design.

The remaining curves of Figure 28 represent the two extremes of the actual operation. For the curves labeled $\dot{M} = \dot{M}_v$, the tank initially contains 20 lbs. of usable fluid and, in addition, it contains a quantity of fluid to be vented. The expression, $\dot{M} = \dot{M}_v$, means that only the vented fluid is used for cooling of the shield. The phase change of the used fluid is completely ignored. This system may be thought of as containing the

FIGURE 27

HYDROGEN TANK WEIGHT OPTIMIZATION CURVE

T_o = 275°R (Outer Covering Temperature)

P_i = 50 psia (Tank Pressure)

Tank Material = 6Al-4V Titanium ρ = 0.161 $\frac{lb}{in^3}$

Allowable Stress = 65,000 psi

Poisson's Ratio = 0.35

Modulus of Plasticity = 15,500,000 psi

Outer Shell is Rigid

ρ = Insulation Density (lb/ft^3)

Usable Fluid = 59.12 pounds

Mission Time = 3 years

k = .0003 $\frac{B-Btu}{hr-ft^2-°R}$

Safety Factor = 2 off Ultimate

Boil-off Reduction Factor = 2.0

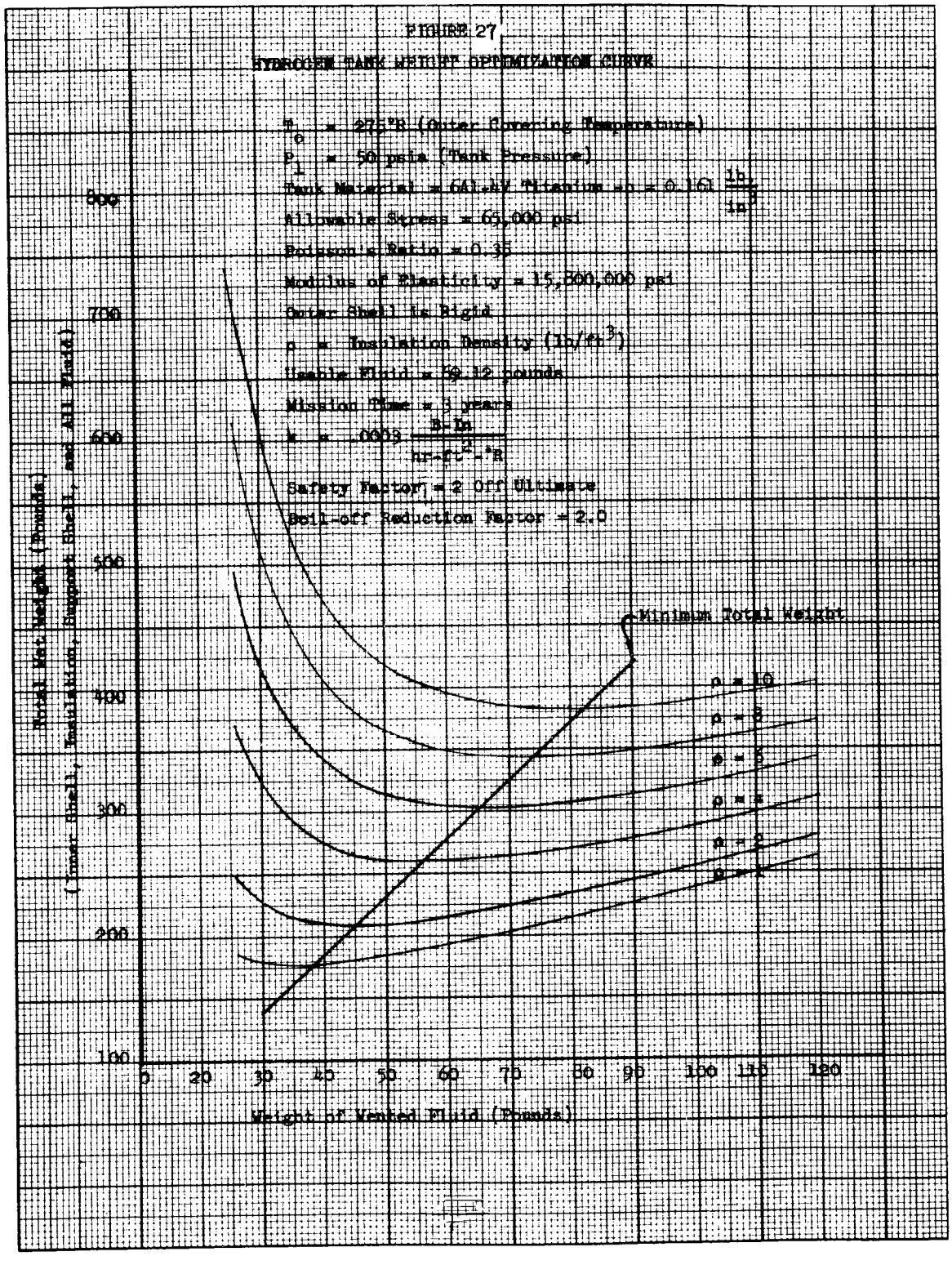

FIGURE 28

HYDROGEN TANK WEIGHT OPTIMIZATION CURVE

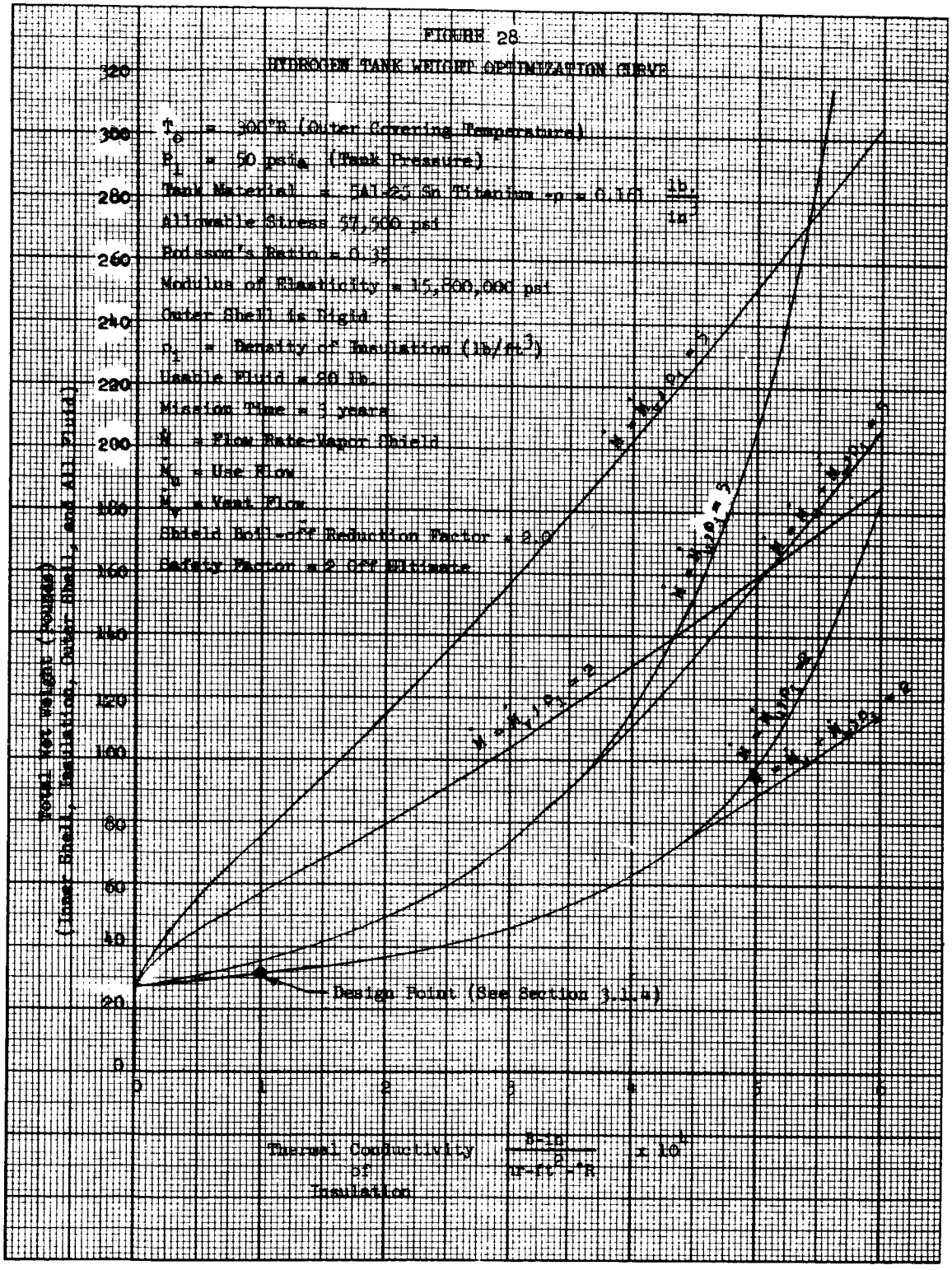

20 lbs. of usable fluid throughout the three-year mission. During the three years, all entering heat is absorbed by the vented gas. At the end of the three years, the total quantity of usable fluid is removed in some manner. This is the worst extreme condition of operation in that no cooling or heat absorption is furnished by the used fluid. This usable fluid penalizes the system by increasing the surface area of the insulation.

The third condition, shown by the curve labeled $\dot{M} = \dot{M}_u + \dot{M}_v$, is the best possible condition of operation. In this system, both the usable and vented fluid are used at a constant rate through the cooling coils for the three-year period. This is considered the optimum system, since maximum use is made of the usable fluid. Note that there is no advantage to carrying additional vented fluid if the insulation is highly efficient (low thermal conductivity).

The actual optimum system weight will lie somewhere between the curves where $\dot{M} = \dot{M}_v$ and $\dot{M} = \dot{M}_u + \dot{M}_v$. Before this weight (and basic tank dimensions) can be finally optimized, it is necessary to know the demand cycle within reasonable limits.

Pressure vessel weight is directly proportional to tank pressure. A change in hydrogen system weight caused by changed design pressure also depends on the latent heat of vaporization (L_v) of the hydrogen. In general, an increase in tank pressure will cause a decrease in (L_v) which will require more insulation for maintenance of storage efficiency. Figure 29 can be used to estimate pressure vessel weights based on pressure. Figure 30 can be used to estimate pressure vessel weights based on shell thickness. There is a practical limit to the minimum thickness of any vessel. This thickness is often greater than the thickness required to theoretically contain the pressure. When this occurs, the weights shown on Figure 30 will be higher than those shown on Figure 29 for a given fluid mass or tank size.

2.2 Ammonia Storage and Feed System

The supply of ammonia is stored in the liquid phase in this study. The fluid is in equilibrium with the environment; that is, its temperature and vapor pressure are determined by the temperature of the tank covering when no flow is present. The storage concept is equivalent to a household aerosol bomb.

2.2.1 Technical Studies of Practical Design Concepts

The storage and feed concepts studied in Section 2.1.1 apply to ammonia feed systems in a general way. The special considerations given to the design of ammonia systems are discussed in the following sections.

FIGURE 29

SPHERICAL PRESSURE VESSEL WEIGHTS
FOR HYDROGEN-BASED ON PRESSURE

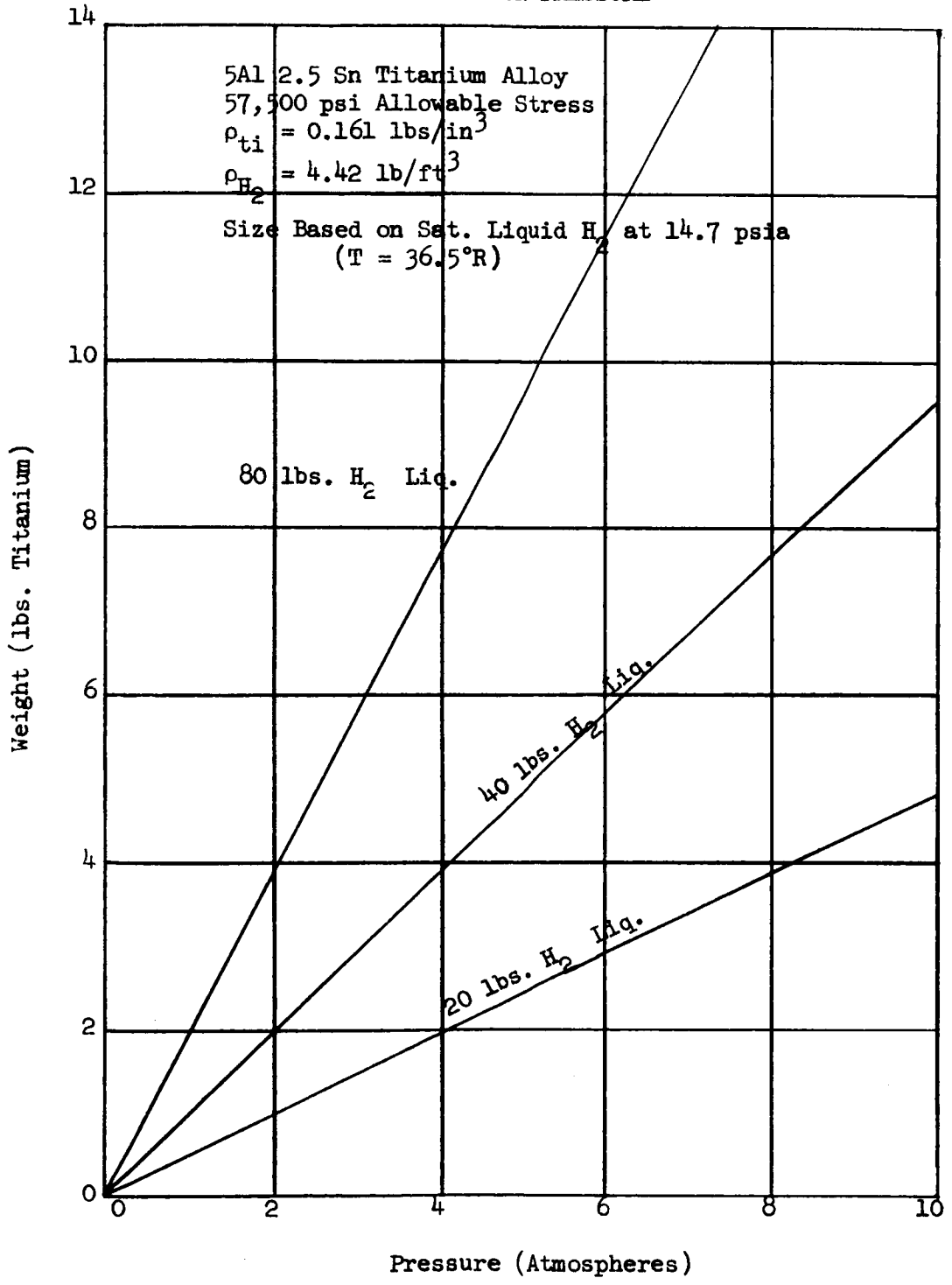

FIGURE 30
SPHERICAL PRESSURE VESSEL WEIGHTS
FOR HYDROGEN-BASED ON THICKNESS

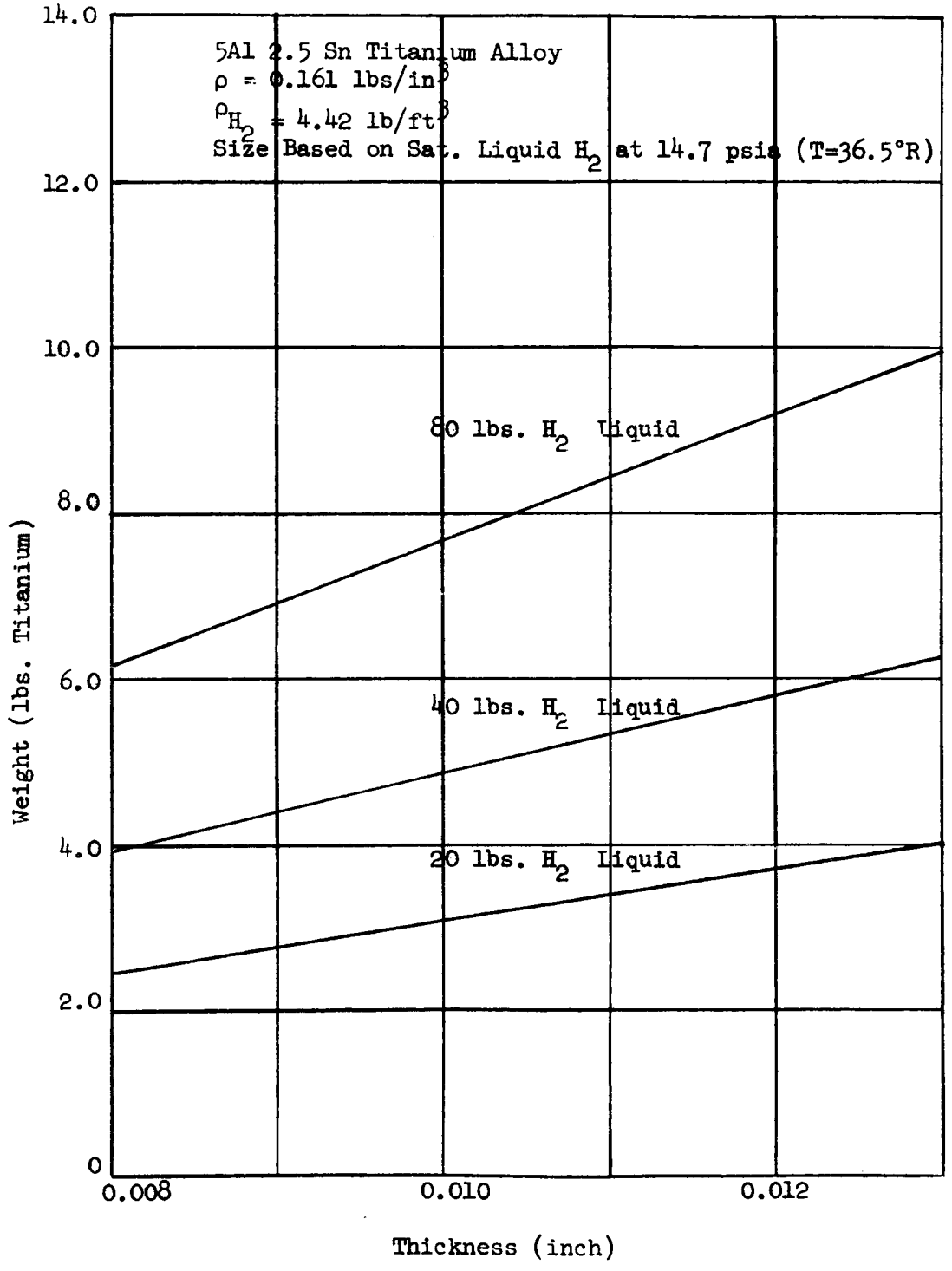

2.2.1.1 Insulation Scheme

If the environmental sources of thermal radiation are relatively constant, it is possible to design an ammonia storage system without insulation. This statement can be visualized by studying the vapor pressure curve shown on Figure 31. The pressure in the tank will be determined by the temperature of the fluid.

Equilibrium Skin Temperature Control

The analysis of equilibrium skin temperature given in Section 2.1.1.1 applies. In the case of ammonia systems, however, it is not desirable to obtain the lowest possible skin temperature. Referring to Figure 1, note that the desirable temperatures are in the region of the black body case. Coatings and finishes which will produce the desired temperatures are easily obtainable. The effect of the required heat input to the liquid (Q_{10}, Eq. 1) on skin temperature is very small for the low flow rate systems studied.

Insulation for the Transient Condition

In most earth satellite applications there will be times when this vehicle will be hidden from the sun. For high altitude satellites, the period of eclipse is short. Without the benefit of the sun's rays, however, the equilibrium temperature of lightweight space-exposed surfaces will drop rapidly during the period of eclipse. Uninsulated ammonia tanks would feel sharp reductions in tank pressure resulting from the reduced skin temperature. The pressure reduction will be especially noticeable when the stored mass is low. The rate of pressure reduction can be retarded by adding thermal insulation to the exterior of the tank. The proper amount of insulation will retard the pressure drop within tolerable limits until the satellite again comes into view of the sun.

Once viewing the sun, the loss of heat from the system will be restored and the initial equilibrium will be approached. The amount of insulation must not be too great to prevent maintenance of pressure in the feed condition when small quantities of heat are required. A transient analysis of tank system heat inputs has not been attempted for this study.

2.2.1.2 Zero Gravity Feed Concepts

Little or no work has been done on the behavior of ammonia in a zero gravity environment. Except for differences in surface tension, density, and wetting characteristics, the zero "g" action of ammonia is not expected to differ

FIGURE 31
VAPOR PRESSURE CURVE FOR AMMONIA

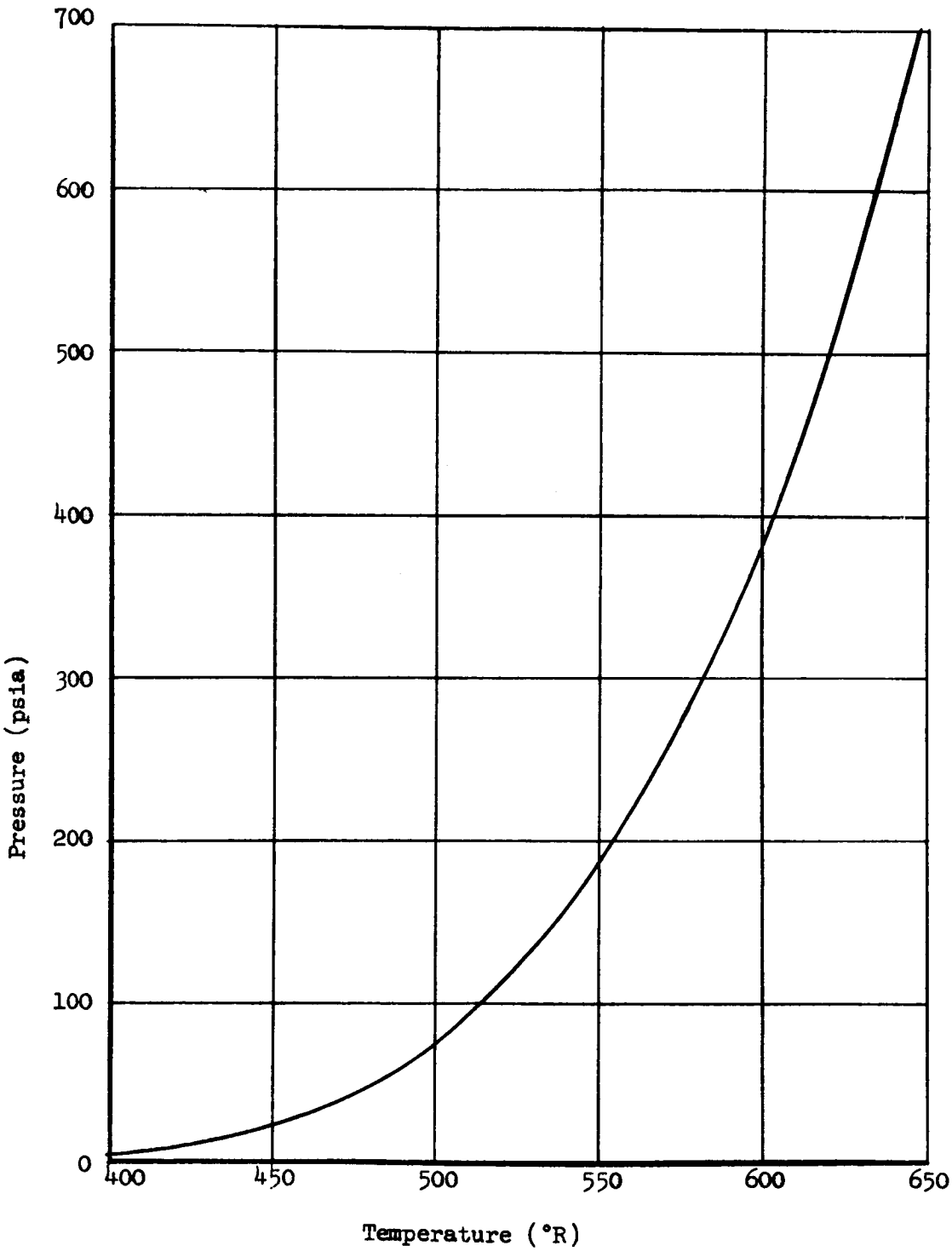

significantly from hydrogen. The engine feed requirement is for gas; however, in low flow rate systems there is no storage requirement which dictates that gas must always be present at the tank exit. As in hydrogen systems, downstream pressures are low enough to preclude the need for efficient liquid pumping. Two systems are proposed.

1. External gas generation.
2. Thixotropic liquid location.

The system principles, component design, advantages, and disadvantages are discussed in the following sections.

External Gas Generation

In this system it is assumed that either gas or liquid will be fed from the storage tank at any time. If liquid is fed from the tank at 2 (10^{-5}) lb/sec instead of gas, the tank pressure will be slightly higher due to the lack of a small amount of refrigeration.

Before the fluid can be allowed to pass to the metering controls, it must be converted to the gaseous phase. Figure 32 shows how this is done. A heated, porous plug is installed in the feed line. If liquid flows out of the tank, it becomes trapped by surface tension forces in the plug. As long as the plug is not full, only gas can escape to the metering controls. Figure 33 indicates the amount of heat necessary to convert a steady stream of liquid ammonia to gas at various system pressures. This heat must be available at a temperature level above the boiling temperature of the liquid. In order to prevent the escape of liquid to the downstream line in the no demand condition, the exit face of the porous plug is always maintained at a temperature above the saturation temperature of the ammonia. Heat is obtained from an electrical resistance heater which is controlled by the thermostat on the plug exit face.

The disadvantage of such a system is that it requires heat at the rates shown in Figure 33 to be added at constant pressure. There is also a reliability penalty associated with the thermostat and heater. In a system which would supply only gas from the tank, the tank pressure can be allowed to cycle between limits. The exit gas can obtain a large fraction of the required heat from the remaining stored fluid and the tank mass.

Thixotropic Liquid Location

The general nature of thixotropes is described in Section 2.1.1.2 under zero "g" feed concepts. A schematic (Figure 16) of this type of gas feed

FIGURE 32

GAS GENERATOR

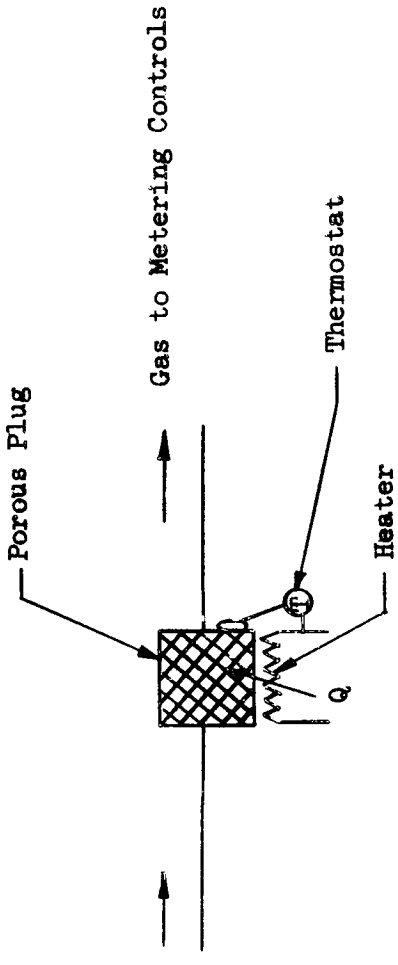

FIGURE 33
AMMONIA VAPORIZATION HEAT INPUT
REQUIREMENT ACROSS POROUS PLUG

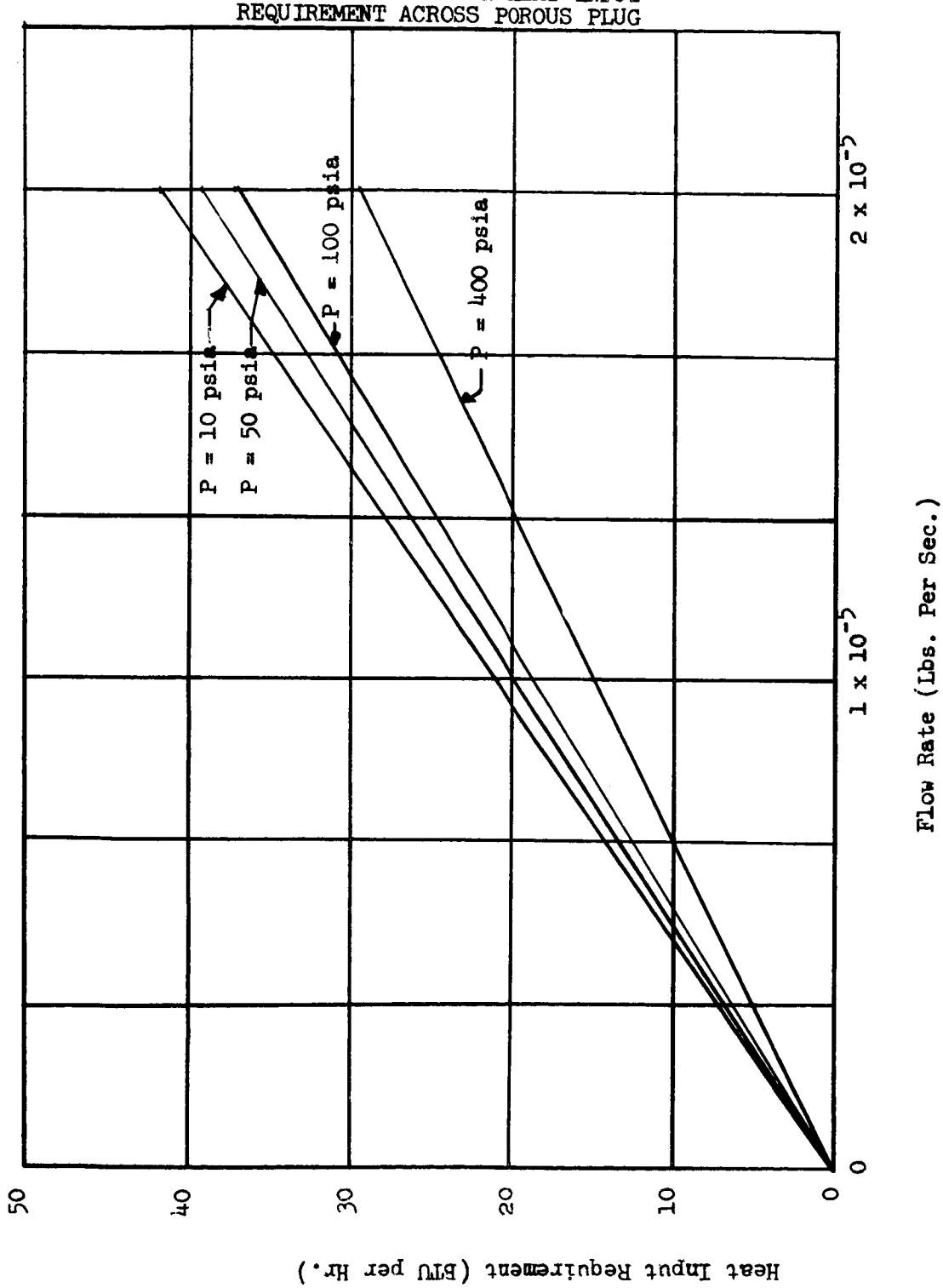

tank and a description are also given in that section. An ammonia tank of this type was built and tested at Beech. The following section describes the testing.

Thixotropic Ammonia Tank Testing

A thixotropic ammonia tank was constructed and tested. The purpose of the experiment was to obtain preliminary information as to the feasibility of this kind of zero "g" phase separation. A description of the testing follows:

The gaseous ammonia was supplied from an ammonia pressure cylinder. The ammonia gas was liquefied by passing it through a heat exchanger immersed in liquid nitrogen. The liquid was caught in a container suspended in an open mouth dewar filled with liquid nitrogen. Temperature of the liquid ammonia was controlled by the depth of immersion of the container in the liquid nitrogen. Temperature of the liquid ammonia was maintained so that its vapor pressure was less than one atmosphere.

Various thixotropic agents were used as the gelling agent to make the thixotropic mixture. Approximately 5%, by weight, of this powder was used to make a mixture of the consistency shown by the photograph in Figure 34. The consistency was stiff enough so that the mixture would stand without slumping or pulling away from the spatula under 1 "g" acceleration.

The test setup is shown by the photograph in Figure 35. The setup consisted of a supply tank for the thixotropic mix, thermocouple probe, filter, pressure gauge, pressure regulator, flow meter, tubing and valves.

The supply tank was made from a 1" stainless steel tube with fittings on both ends. A thermocouple probe was inserted through the fitting on one end into the thixotropic mix. During filling, the supply tube was immersed in liquid nitrogen while the thixotropic mix was spooned into the tube. This procedure kept the vapor pressure of the thixotropic ammonia below the atmospheric pressure. From the supply tube a 1/4" stainless steel tube led to the filter. The filter was made from a 1" stainless steel tee packed with fiberglass wool. This made a very effective filter as later tests proved. A 200-lb. precision laboratory pressure gage was used to measure the vapor pressure of the ammonia gas. A tube filled with light oil was used as a protective barrier between the brass parts of the pressure gage and the corrosive effect of the ammonia gas. A pressure regulator was used to control flow from the supply tube to the flow meter. A precision wet test meter of stainless steel construction was used to measure the ammonia gas flow rate. The meter was filled with diesel engine fuel

FIGURE 34

SAMPLE OF BOILING THIXOTROPIC AMMONIA

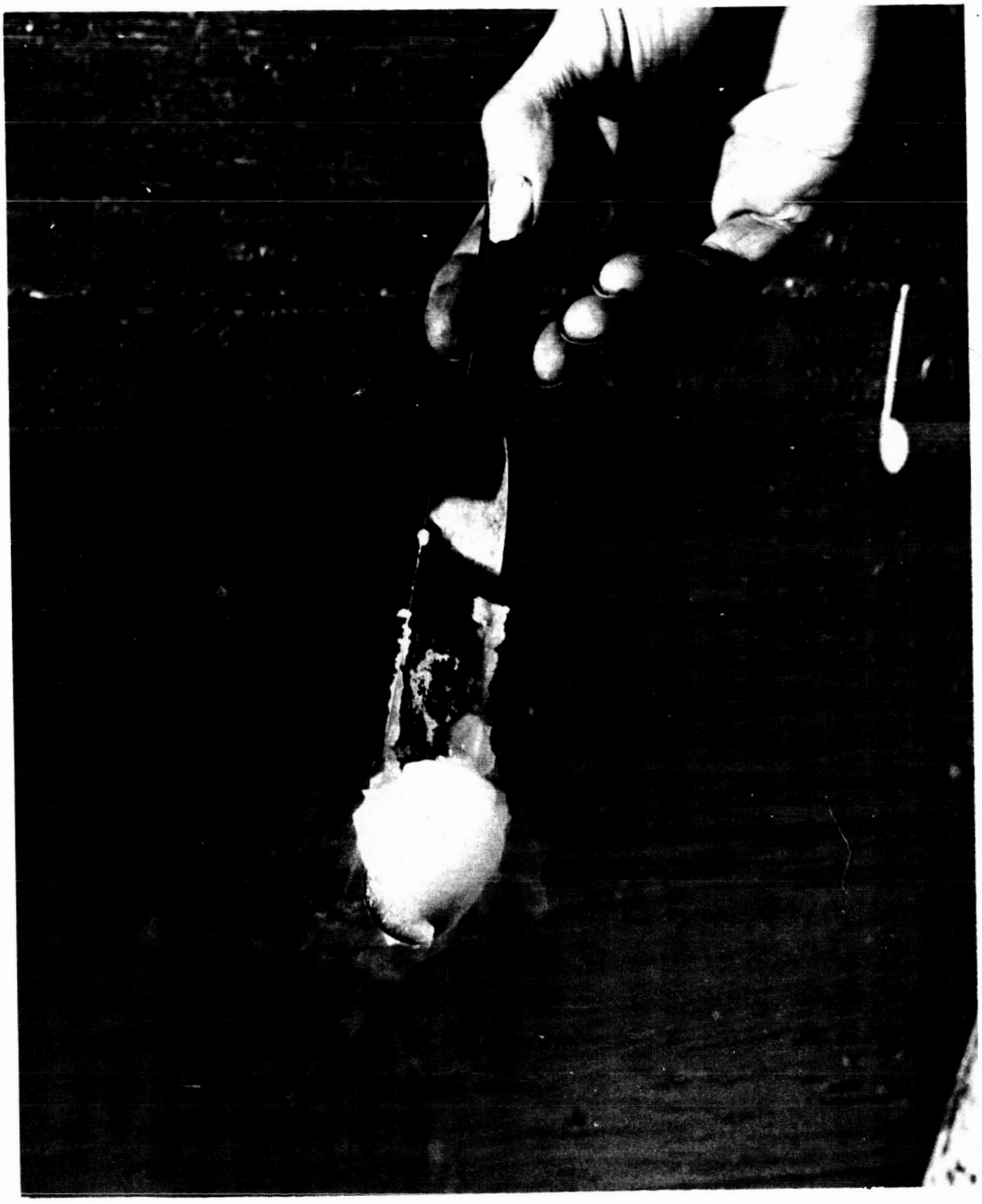

FIGURE 35

SETUP FOR THIXOTROPIC AMMONIA TESTS

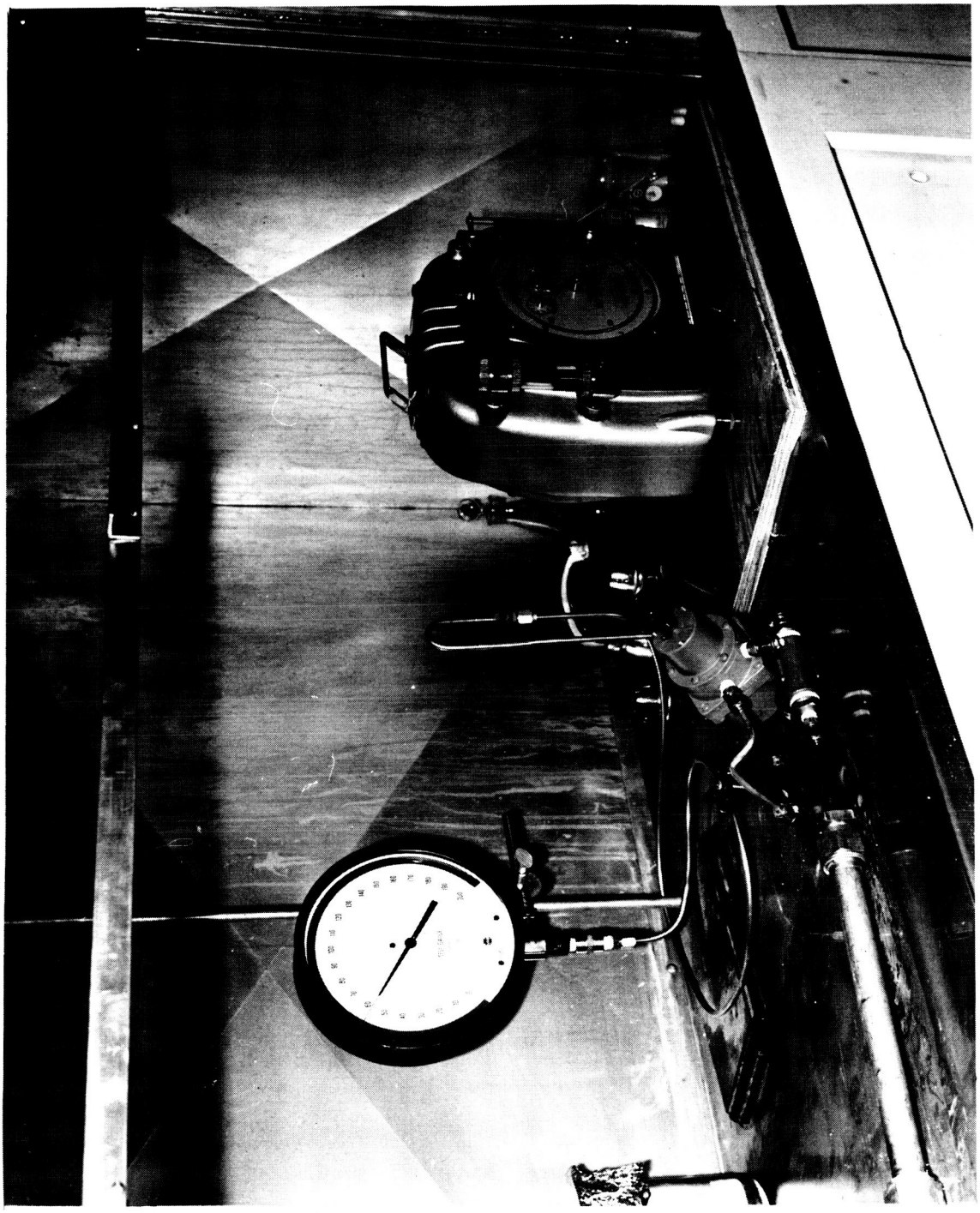

The flow through the regulator was adjusted so that a drop in the pressure occurred in the system. Pressure vs. temperature readings were recorded and a plot of these readings is shown in Figure 36. A plot of ammonia vapor pressure vs. temperature from National Bureau of Standards data is also shown for comparison. No significant differences in the vapor pressure curves of the thixotropic ammonia and saturated ammonia were found.

Visual observations were made of the thixotropic mixture under pressure. The stainless steel supply tube was replaced with a pyrex glass tube for these observations. The glass tube was filled with the thixotropic mix of liquid ammonia. After equilibrium pressure and temperature were reached, the regulator was opened so that a small gas flow was maintained. No liquid could be observed in the glass tube. The thixotropic mixture appears moist at first, but as the gas is drawn off, the thixotropic mixture shrinks away from the walls of the tube and turns white in color. The thixotropic mix shrinks to about 1/4 of its original volume and leaves a compact hard residue. The mixture acts as its own filter letting the gas buried within the mixture escape to the surface. There was no tendency for the mix to be extruded through the simple fiberglass filter. No traces of the colloidal silica were found downstream of the filter after the tests. It was concluded that separation in zero gravity using this phenomenon appears to be feasible for low flow rate ammonia supply systems.

2.2.1.3 Flow Control and Metering

The gaseous ammonia propellant must be delivered to the engine under specific thermodynamic conditions. The discussion of long pulse and short pulse control systems in Section 2.1.1.3 also applies to ammonia systems. Special considerations for ammonia systems are given below.

Unlike a hydrogen tank, it will probably not be necessary to employ a tank heater. As fluid is withdrawn and tank pressure starts to decrease, a temperature differential is created and heat flows to the stored fluid. At any given flow rate a new tank pressure and temperature will be established. At flow rates not exceeding 2 (10^{-5}) lb/sec, these conditions will be only slightly lower than those for the no-flow case.

A heater would be required only if the environmental temperature fluctuations caused the tank pressure to fall outside the allowable flow metering range. Since no positive temperature differential between the tank covering and the fluid would exist, heat must be added by means of a controlled electrical resistance heater. If wide pressure variations in the tank are more desirable under the known environmental changes, secondary regulation for metering purposes can be accomplished by a pressure regulator similar to the one shown in Figure 20.

FIGURE 36

COMPARISON OF VAPOR PRESSURE VS. TEMPERATURE CURVES FOR THIXOTROPIC AMMONIA TEST DATA AND AMMONIA DATA FROM N.B.S.

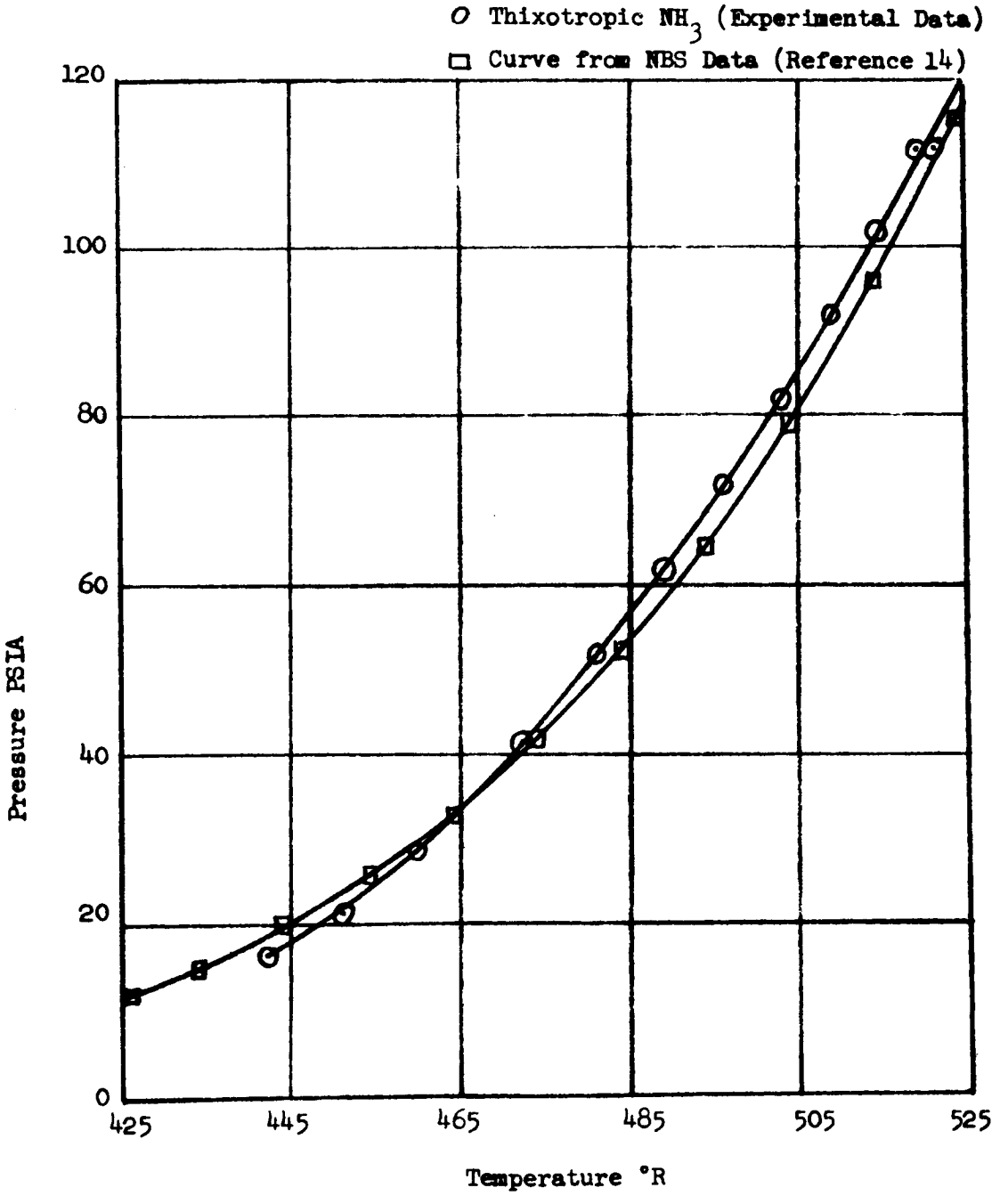

2.2.2 Complete Storage and Feed Systems

Complete ammonia storage and feed systems are assembled using the concepts given in the preceding sections.

2.2.2.1 Structural Plan

The thixotropic liquid location tank unit can be easily converted to an external gas generation system by omitting the filter. Structural equations used for the basic tankage are given in Appendix C. Structural considerations are given in Section 2.1.2.1. The basic structural difference between the ammonia and hydrogen tanks is that the ammonia tank does not require a vacuum supporting outer shell.

2.2.2.2 Complete Flow Systems

Figures 37 and 38 are the schematic diagrams showing all valves and controls on a thixotropic liquid location tank. An external gas generation system would require the filter to be replaced by a heated porous plug.

Figure 37 shows the required system for supplying long duration pulses or continuous flow. A brief description of the operation follows.

On demand from an electrical signal, the solenoid valve opens and allows gas to pass to the sonic restriction. After a short period of time, temperature at the inlet of the sonic restriction stabilizes to a point where constant mass flow is delivered to the engine within certain tolerance limits. Gas is obtained from the tank by the action of the filter. Tank pressure is maintained within the limits required for mass flow control at the sonic restriction by the pressure relief valve and the equilibrium skin temperature. In systems where the flow demand or environment changes in a very irregular pattern, it may be necessary to add a pressure regulator and allow wide tolerances on tank pressure to meet the mass flow tolerance and still achieve minimum weight.

Figure 38 shows the required system for supplying short duration pulses. On demand from an electrical signal, the solenoid valve opens and allows gas to pass to the sonic restriction. Gas is fed from the constant temperature plenum. The temperature in the plenum is maintained within the limits required for mass flow control by the thermostat and heater. The tank pressure is maintained within the limits required for mass flow control at the sonic restriction by the pressure relief valve and the equilibrium skin temperature.

FIGURE 37
LONG PULSE SUPPLY SYSTEM
REGENERATIVE GAS FEED TANK - AMMONIA TANK

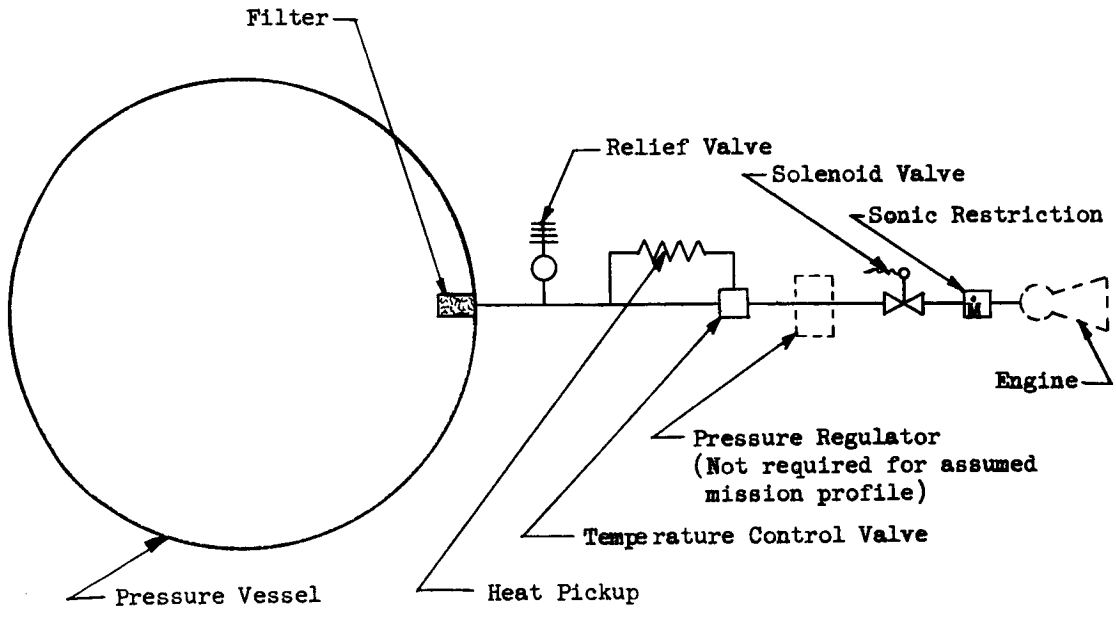

FIGURE 38
SHORT PULSE SUPPLY SYSTEM
REGENERATIVE GAS FEED TANK - AMMONIA TANK

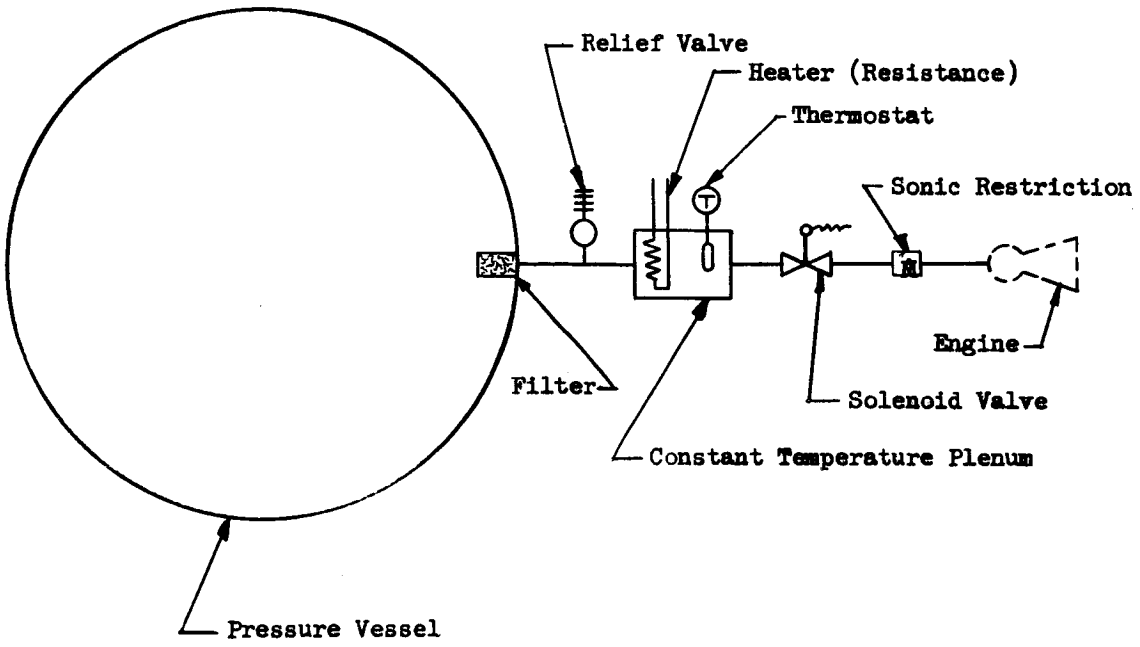

2.2.3 Pressure Vessel Weights

Figure 39 can be used to estimate pressure vessel weights based on pressure. Figure 40 can be used to estimate pressure vessel weights based on thickness.

FIGURE 39

SPHERICAL PRESSURE VESSEL WEIGHTS
FOR AMMONIA-BASED ON PRESSURE

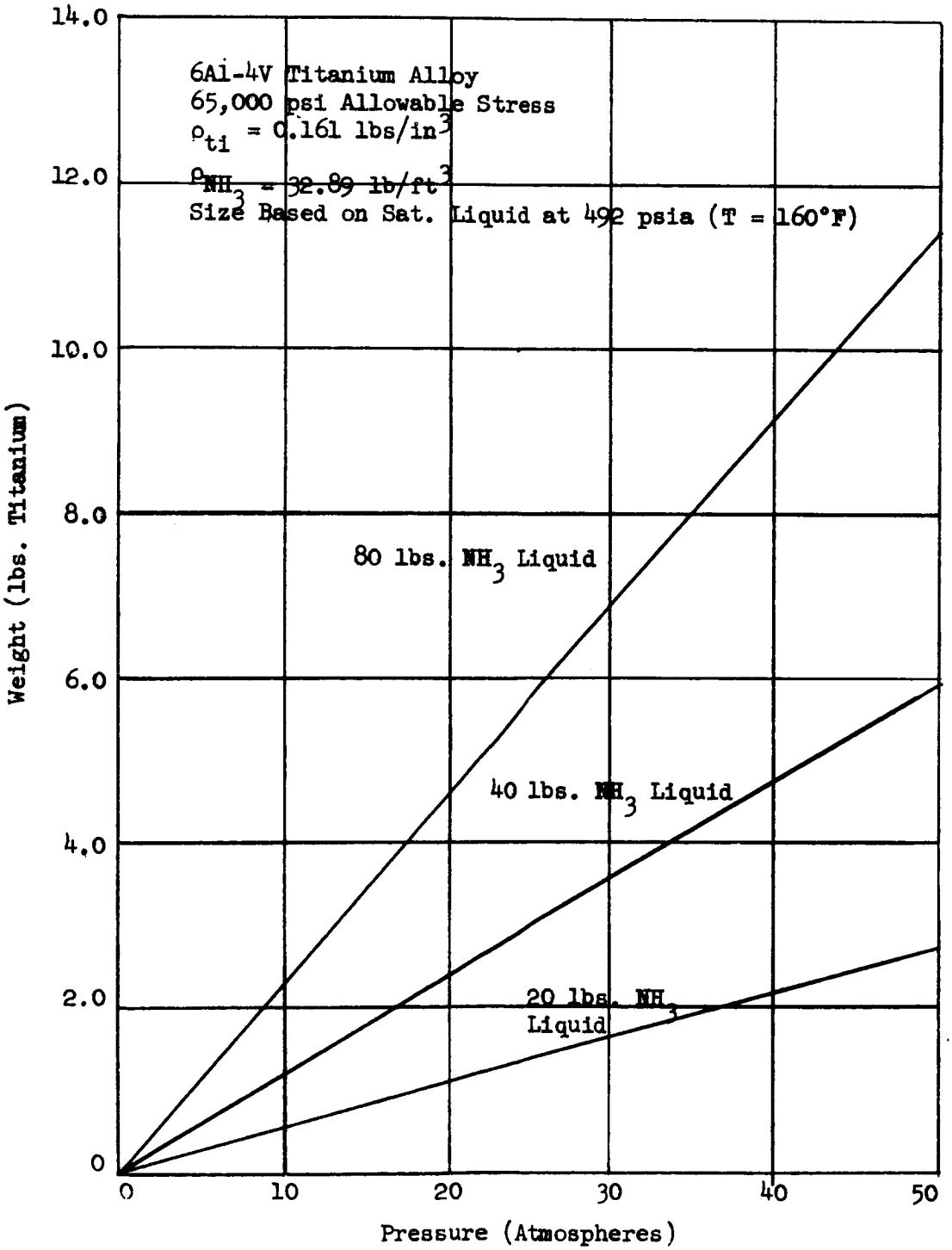

FIGURE 40

SPHERICAL PRESSURE VESSEL WEIGHT
FOR AMMONIA-BASED ON THICKNESS

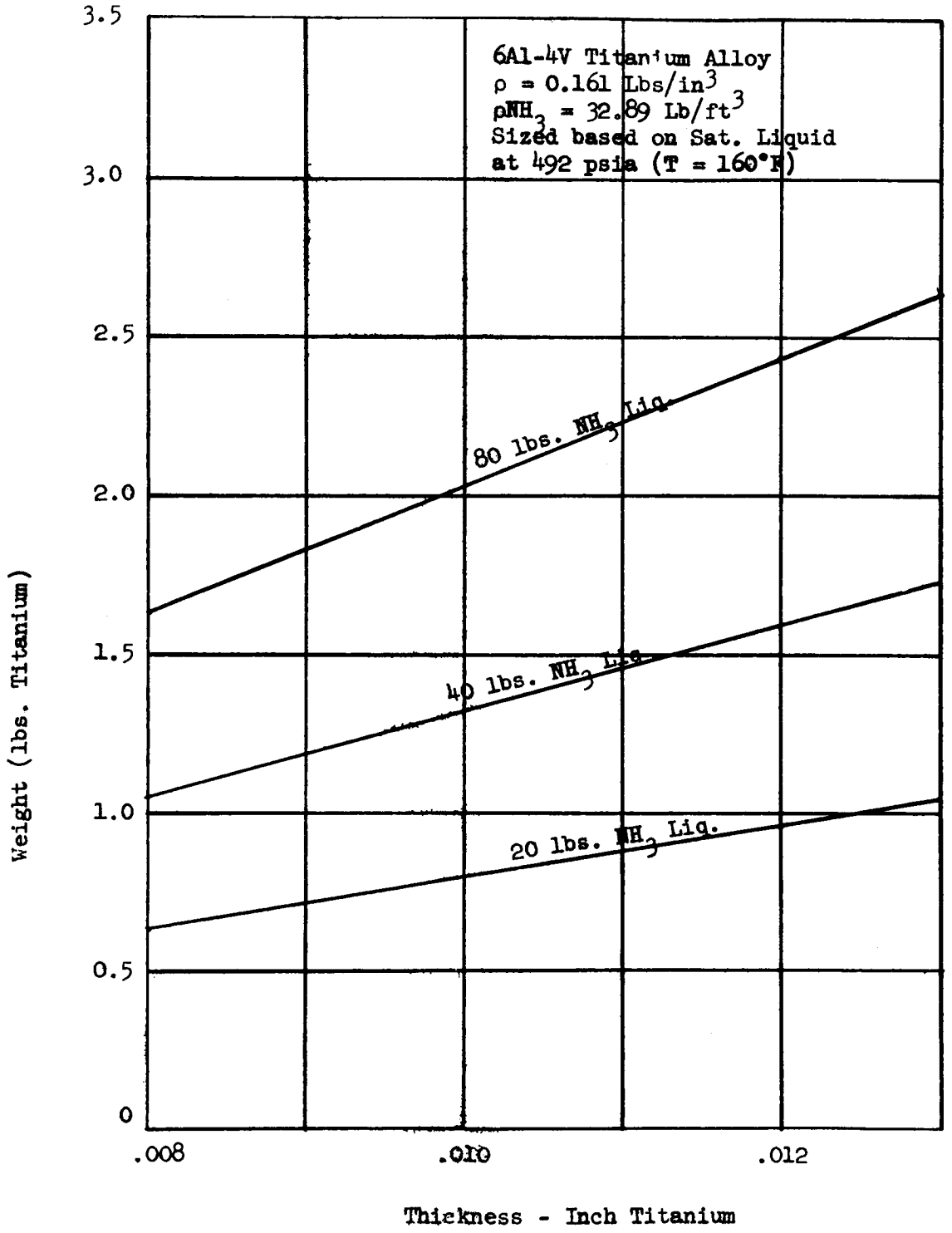

3.0 SPECIFIC MISSION DESIGN PROGRAM

The objective of this program is to establish designs for a hydrogen and an ammonia propellant storage and feed system. Requirements for the system and operating environments are given in Table 7.

The specified altitude can place the satellite in a stationary orbit over the equator. In this position, the vehicle sees the sun almost all of the time. There is a short period of time in the spring and fall when the vehicle is in the shadow of the earth. The maximum period of time in the shadow is 1.16 hours per day. It is assumed that this is the design condition to be met. It is also assumed that the gravitational environment during system operation can approach zero gravity.

3.1 Hydrogen Storage and Feed System

The regenerative gas feed system was chosen for the design. Since the flow is supplied in extremely short pulses, the system shown in Figure 26 applies. This concept was chosen for the following reasons:

1. The system can be proven by ground tests
2. Gas delivery is maintained under a large variation of acceleration forces
3. System weight is low

3.1.1 Performance Specifications

Table 8 lists the system performance specifications.

3.1.2 Material Specifications

Basic qualities of the construction materials are given in Table 9.

3.1.3 Tank System Dimensions

Dimensions of the component structural parts are given in Table 10.

3.1.4 Weight Breakdown

Weight breakdown of the system is given in Table 11. Structural components are optimized by the method given in Section 2.1.3. The design point is marked in Figure 38.

TABLE 7

SPECIFIC MISSION STORAGE AND FEED SYSTEM REQUIREMENTS

	Propellant	
	Hydrogen	Ammonia
Propellant Mass Flow (lbs/sec)	$1(10^{-5})$	$1.428\ (10^{-5})$
Pressure to Arc Chamber (atm)	1 to 3	1 to 3
Mass Flow and Pressure Tolerance	$\pm$ 10%	$\pm$ 10%
Total Propellant Used, 3 Years (lbs)	18.39	26.26
Total Propellant Stored (lbs)	20.0	27.5
Propulsion Cycles Per Year	$3.15(10^{5})$	
Stay Time (Years)	3	
Minimum Thrusters (one used at a time)	6	
Maximum Acceleration During Launch	8 g s	
Hold Time on Ground (hrs)	6	
Orbital Altitude (miles)	22,400	
Maximum Tank Diameter (ft)	4.5	
Available Voltage	400	
Shortest Flow Burst (milliseconds)	20	
Engine Specific Impulse (sec)	1000	
Vehicle Weight (lbs)	550	

TABLE 8

PERFORMANCE SPECIFICATIONS-SPECIFIC MISSION
HYDROGEN TANK

Storage	Liquid Phase
Space Equilibrium Skin Temperature	300°R
Gas Delivery "g" Range	0 to 8
Vacuum Shell External Design Pressure	1 atmosphere
Vacuum Level of Load-Bearing Insulation	10^{-6} Torr
k Factor of Load-Bearing Insulation (540-37°R)	$1\ (10^{-3})\ \frac{\text{B-In}}{\text{Hr-Ft}^2\text{-°R}}$
Vacuum Level of Non-Load-Bearing Insulation	Open to Space
k Factor of Non-Load-Bearing Insulation (300-37°R)	$1(10^{-4})\ \frac{\text{B-In}}{\text{Hr-Ft}^2\text{-°R}}$ (2 year projection)
Average Heat Leak in Space (300-37°R)	$0.458\ \frac{\text{B}}{\text{Hr}}$
Design Maximum Tank Pressure	50 psia
Operating Pressure Band	9.08 psi
No Flow Pressure Band Build-up Time	266 hr (beginning of mission)
No Flow Pressure Band Build-up Time	70.2 hr (end of mission)
Pressure Band Decay Time with Flow	155 hr. (beginning of mission)
Pressure Band Decay Time with Flow	4.8 hr. (end of mission)

Ground and launch supports retracting in zero "g".
Non-load-bearing insulation free venting for rapid ascent.
External fill and fill-vent lines removed before launch.
Insulation discontinuities automatically capped.

TABLE 9

MATERIAL SPECIFICATIONS-SPECIFIC MISSION
HYDROGEN TANK

Part	Material	Specification
Pressure Vessel	5 Al 2.5 Sn Titanium(annealed)	Ultimate Stress = 115,000 psi
Vacuum Shell	5 Al 2.5 Sn Titanium(annealed)	Ultimate Stress = 115,000 psi
Support Ring	5 Al 2.5 Sn Titanium(annealed)	Ultimate Stress = 115,000 psi
Vapor Shield	6061-0 Aluminum	Annealed
Cooling Coils	Commercially Pure Titanium	
Outer Covering	6061-0 Aluminum	Annealed
Retracting Support	2024-T4 Aluminum	Hard Anodized
Support Lug	5 Al 2.5 Sn Titanium(annealed)	Ultimate Stress = 115,000 psi
Thermal Standoff	Commercially Pure Titanium	
Fill Line	Commercially Pure Titanium	
Vent Line	Commercially Pure Titanium	
Fill Head	Commercially Pure Titanium	
Fillers	Fiberglass	5 lb/ft^3
Load-Bearing Insulation	Fiberglass and Al Foil	5 lb/ft^3
Non-Load-Bearing Insulation	Aluminized Mylar Layers	2.0 lb/ft^3
Fill Vent Connector	Commercially Pure Titanium	
Fill Vent Cap	Commercially Pure Titanium	
Relief Valve	Stainless Steel	
Tank Heater	Commercially Pure Titanium, Beryllium Copper,	
Plenum	Stainless Steel	
Solenoid Valve	Stainless Steel	
Sonic Restriction	Bronze	

TABLE 10

DIMENSIONS-SPECIFIC MISSION
HYDROGEN TANK

Part	Dimension (In)
Pressure Vessel Inner Diameter	24.62
Pressure Vessel Thickness	0.008
Non-Load-Bearing Insulation Thickness	1.43
Vacuum Shell Thickness	0.015
Support Ring Diameter	1.00
Support Ring Thickness	0.020
Load-Bearing Insulation Thickness	0.19
Vapor-Cooled Shield Thickness	0.008
Distance Between Vacuum Shell and Shield	0.60
Outer Covering Thickness	0.005

TABLE 11

SYSTEM WEIGHT BREAKDOWN-SPECIFIC MISSION
HYDROGEN TANK

Part	Wt. (lb)
Usable Liquid Hydrogen	20.00
Pressure Vessel	2.45
Vacuum Shell	4.94
Support Ring	0.79
Vapor-Cooled Shield and Cooling Coils	2.46
Outer Covering	1.27
Retractable Supports	0.90
Support Lug	0.06
Thermal Standoff	0.13
Fill and Vent Line	0.24
Insulation Fillers	0.76
Load-Bearing Insulation	1.07
Non-Load-Bearing Insulation	3.51
Fill Vent Connector	0.35
Gas Delivery Module	0.30
Fill Vent Cap and Miscellaneous Hardware	0.79
Relief Valve	0.25
Tank Heater	0.25
Plenum	0.25
Solenoid Valve (6)	1.20
Sonic Restriction	0.10
System Dry Weight Total	22.07
System Wet Weight Total (Includes H_2)	42.07

3.1.5 Ground Handling and Prelaunch Considerations

As required, the liquid hydrogen is placed in the tank six hours before launch. During this time, the high vacuum load-bearing insulation protects the tank. The non-load-bearing insulation is not evacuated during this time and will tend to remain at the environmental temperature. After launch, it will be a long time before this insulation can stabilize at the low operational temperature. The resultant loss of storage efficiency will reduce the usable fluid quantity. This effect can be eliminated by a simple nitrogen cooling system which works as follows: A 1/4" diameter aluminum tube extends from ground support equipment into the compartment where the tank is housed. The tube ends in a shower-head arrangement above the vessel. During the standby period, liquid nitrogen is sprayed over the tank maintaining the non-load-bearing insulation at about 140°R. Shortly before launch, the supply of nitrogen is removed. The thermal inertia of the non-load-bearing insulation will maintain high storage efficiency during the launch and stabilization period. Flight vehicle weight penalty for the system described above should not exceed 0.50 pound.

3.1.6 Design Information Required for Further Optimization

There are several factors which must be established before final system optimization can be performed.

3.1.6.1 Vehicle Heat Inputs

No vehicle heat inputs were used in the given design. Figure 1 shows that an equilibrium temperature of about 280°R can be obtained for this condition. The design equilibrium temperature was taken as 300°R assuming a small amount of outer coating deterioration. An accurate evaluation of all vehicle heat inputs is necessary to establish the actual skin temperature.

In the study, it was assumed that the tank is exposed to direct sunlight 100% of the time. In an actual vehicle, the tank may "hide" behind solar cells or other exposed parts of the satellite. Shape, size, and vehicle orientation factors should be known.

3.1.6.2 Duty Cycle

In the study, all 20 lbs. of stored fluid is usable. If the thrusters are used in a very irregular manner, it may be necessary to vent some of the usable fluid to maintain acceptable pressure. To prove that weight optimization as shown in Section 2.1.3, Figure 28 is correct,

the following must be known:

1. Usable propellant reserve requirement versus time in orbit.
2. Expected frequency of, and duration of, flow pulses.
3. Time in transit from initial orbit to final orbit.

This information will also establish or eliminate the need for secondary pressure regulation downstream of the tank because the optimum pressure control band can be determined.

3.1.6.3 Arc Chamber Pressure

The given system weights are based on 50 psia tank pressure to avoid a lengthy parametric study. If other tank pressures are more desirable, the pressure vessel weight can be adjusted by using the curves shown in Figures 29 and 30. The error in system weight will be negligible for corrected pressures below 90 psia.

3.1.6.4 Arrangement of Multiple Thrusters

For satisfactory short pulse operation, the metering controls must be closely coupled with the thrusters. The locations of the thrusters must be known before the need for multiple metering controls can be determined.

3.2 Ammonia Storage and Feed System

The thixotropic liquid location system was chosen for the design. Since the flow is supplied in extremely short pulses, the system shown in Figure 38 applies. This concept was chosen for the following reasons:

1. The system can be proven by ground tests.
2. Gas delivery can be maintained under a large variation of acceleration forces.
3. A minimum of external power is required.

3.2.1 Performance Specifications

Table 12 lists the system performance specifications.

3.2.2 Material Specifications

Basic qualities of the construction materials are given in Table 13.

TABLE 12

PERFORMANCE SPECIFICATIONS-SPECIFIC MISSION
AMMONIA TANK

Storage	Liquid Phase
Space Equilibrium Skin Temperature (Fluid Temperature)	482°R
Ground Storage Allowable Temperature	160°F
Gas Delivery "g" Range	0 to 1
Vacuum Level of Load-Bearing Insulation	Open to Space
k Factor of Load-Bearing Insulation	$5\ (10^{-3})\ \frac{\text{B-In}}{\text{Hr-Ft}^2\text{-°R}}$
Design Maximum Tank Pressure (160°F)	480 psig
Nominal Tank Space Operating Pressure	50 psia
Operating Pressure Band	9.08 psi

Load-Bearing Insulation Free Venting for Rapid Ascent.
Tank is closed by manual valve when in storage.

TABLE 13

MATERIAL SPECIFICATIONS-SPECIFIC MISSION
AMMONIA TANK

Part	Material	Specification
Pressure Vessel	6 Al 4V Titanium Heat Treated	Ultimate Stress=161,400 psi
Load-Bearing Insulation	Fiberglass	5 lb/ft^3
Support Ring	6 Al 4V Titanium Annealed	Ultimate Stress=130,000 psi
Outer Covering	6 Al 4V Titanium Annealed	Ultimate Stress=130,000 psi
Support Lug	6 Al 4V Titanium Annealed	Ultimate Stress=130,000 psi
Filter Case	Stainless Steel	
Filter	Fiberglass	
Feed Line	Stainless Steel	
Manual Valve	Stainless Steel	
Plenum	Stainless Steel	
Relief Valve	Stainless Steel	
Solenoid Valve	Stainless Steel	
Sonic Restriction	Bronze	

3.2.3 Tank System Dimensions

Dimensions of the component structural parts are given in Table 14.

3.2.4 Weight Breakdown

Weight breakdown of the system is given in Table 15.

3.2.5 Ground Handling and Prelaunch Considerations

It is intended that the ammonia tank be filled before installation in the vehicle. This eliminates the need for clumsy filling equipment on the launch pad. A number of systems can be held in reserve storage on the ground. The pressure vessel is constructed to contain the vapor pressure of the ammonia at the hottest expected ground temperature (160°F).

3.2.6 Design Information Required for Further Optimization

Some additional information is needed to further optimize the ammonia storage system. The following data would be useful:

1. Evaluation of vehicle heat inputs for accurate estimation of equilibrium skin temperature and its variation.
2. Desired arc chamber pressure.
3. Arrangement of multiple thrusters for metering and control purposes.

TABLE 14

DIMENSIONS-SPECIFIC MISSION
AMMONIA TANK

Part	Dimension (1N)
Pressure Vessel Inner Diameter	14.02
Pressure Vessel Thickness	0.020
Load-Bearing Insulation Thickness	0.19
Outer Covering (Shell) Thickness	0.008
Support Ring (Tube) Diameter	0.750
Support Ring Thickness	0.016

TABLE 15

SYSTEM WEIGHT BREAKDOWN-SPECIFIC MISSION
AMMONIA TANK

Part	Wt (lb)
Usable Liquid Ammonia	27.50
Pressure Vessel	2.00
Load-Bearing Insulation	0.35
Outer Covering (Shell)	0.85
Support Ring (Tube) and Lugs	0.28
Gelling Agent	1.40
Filter and Manual Valve	0.24
Cap, Tubing and Miscellaneous Insulation	0.20
Relief Valve	0.25
Plenum	0.25
Solenoid Valves (6)	1.20
Sonic Restriction	0.10
System Dry Weight Total	7.12
System Wet Weight Total (Includes NH_3)	34.62

LIST OF REFERENCES

1. Smith, W. and Spieth, C. Preliminary Design of Spacecraft Liquid Propulsion Systems. Vought Engineering Report AST/EOR13157 or Beech Engineering Report 9227, September 1960, pp. 4.17.

2. a. Establishing Proven Design Criteria for Cryogenic Boost Tanks Beech Engineering Report 7602, pp. 106-120.

   b. Beech Insulation Group Progress Report, July, 1962.

3. a. M. M. Fulk, Evacuated Powder Insulation for Low Temperatures, "Progress in Cryogenics", London, Heywood and Co., Ltd., 1959.

   b. M. P. Hnilicka, Engineering Aspects of Heat Transfer in Multilayer Reflective Insulation and Performance of NRC Insulation, "Advances in Cryogenic Engineering", Vol. 5, Plenum Press, 1960.

   c. P. M. Riede and D. I-J. Wang, Characteristics and Applications of Some Superinsulations, "Advances in Cryogenic Engineering", Vol. 5 Plenum Press, 1960.

4. Bell, J., Pike, J., Sutton, H. Electrothermal Engine Propellant Storage and Feed System Study. Beech Engineering Report 12606, September 1961, Appendix A.

5. Shaffer, A. Analytical Methods for Space Vehicle Atmospheric Control Process-Part 1 ASD Technical Report 61-162. AiResearch Manufacturing Company, Dec. 1961, pp. 115.

6. Scott, R. B. Cryogenic Engineering. D. Van Nostrand Company, Inc. Princeton, New Jersey, 1959. pp. 148.

7. Satterlee, H. M. Propellant Control at Zero G. Space/Aeronautics Magazine, July 1962, pp. 72.

8. Li, T. Liquid Behavior in a Zero G Field, Convair (Astronautics) Division, General Dynamics Corporation. Sept. 1960.

9. Love, C. C. Liquid Hydrogen Transport Time Limits in Space. Conference on Design of Space Vehicle Structures, Santa Barbara, Calif. April 1960.

10. Mann, D. B. and Stewart, R. B. Thermodynamic Properties of Helium at Low Temperatures and High Pressures. Journal of Heat Transfer, p. 81, 1959.

LIST OF REFERENCES

11. **Binder, R. C. Fluid Mechanics. Prentice-Hall, Inc., New York, 1949, p. 167.**

12. NASA TR R-102. "Theoretical Elastic Stress Distributions Arising from Discontinuities and Edge Loads in Several Shell-Type Structures" Robert H. Johns and Thomas W. Orange, 1961. (See also Appendix C, Section 2.)

13. "Advanced Mechanics of Materials". Fred B. Seely and James O. Smith. John Wiley and Sons, Inc., New York, 1952. (See also Appendix C, Section 2.)

14. National Bureau of Standards Circular 142.

    "Theory of Elastic Stability" S. Timoshenko, McGraw-Hill Book Co., Inc., New York, 1936. See Appendix C, Section 2.

15. "Studies of Liquid-Vapor Interface Configuration in Weightlessness" Donald A. Petrash and Edward W. Otto prepared for ARS Bulletin No. 2514-62.

APPENDIX A

Analysis of Vapor-Cooled Shields as Applied to Liquid Hydrogen Storage Vessels

This appendix includes the theoretical analyses of single and dual vapor-cooled shields. The results of the calculations are plotted in Figures A2 through A27.

1.0 Single Vapor-Cooled Shield

The heat balance for the single shield is shown schematically in Figure A1. The analysis is based on the following assumptions:

1. Outer covering temperature is constant and uniform over the entire shell. This assumption is approximately correct for a covering which is a good conductor.

2. Heat leak to the stored liquid and the effect of the vapor-cooled shield do not control the equilibrium skin temperature. This is very nearly true for the highly insulated tanks studied in this report.

3. Shield temperature is uniform. This is true if the fluid passages are arranged correctly and are in contact with a good conductor.

4. The gas entering the shield is 100% saturated vapor.

5. The temperature of the gas leaving the shield is equal to the temperature of the shield.

6. No liquid enters the shield.

7. Insulation has a constant thickness and the shield is placed at a constant distance from either edge.

8. Pressure drop through the shield is zero.

1.1 Single Vapor-Cooled Shield Analysis Based on Fourier Equation

Equations and derivations are given below. The results are plotted in Figure A2 through A7. The curves should be read as follows:

1. If the tank pressure and ambient temperature (equilibrium skin temperature) are known, the boil-off is found on the ordinate in terms of tank inner radius and insulation thermal conductivity for any shield location.

FIGURE A1

SCHEMATIC-SINGLE VAPOR-COOLED SHIELD

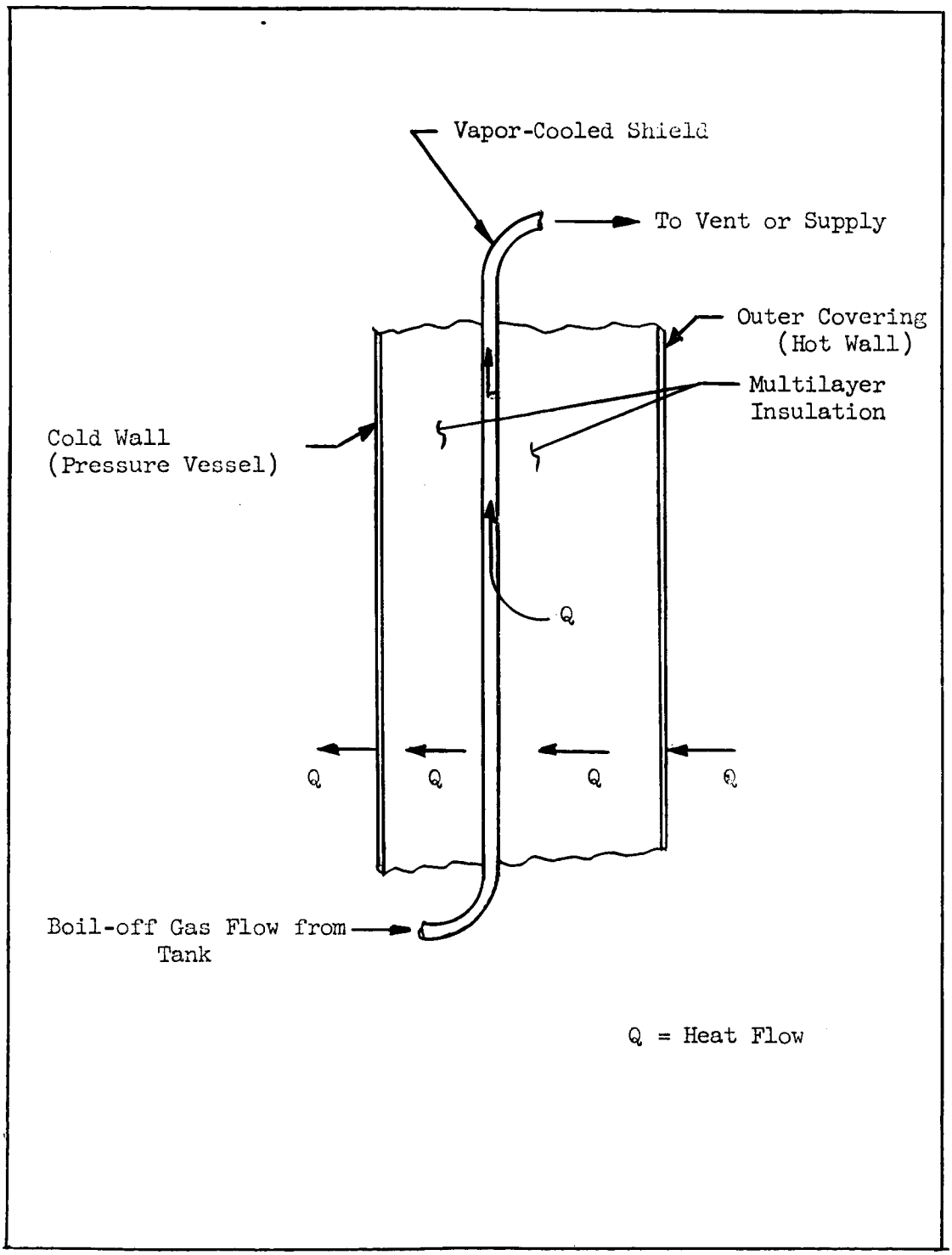

If the ratio of outer insulation radius to inner insulation radius $(\frac{r_3}{r_1})$ does not exceed 1.1, the answer is valid.

2. The temperature of the shield when placed at any location is found on the temperature curves for the given ambient temperature and tank pressure. Note that the temperature curves do not represent temperature distributions through the insulation, but only indicate the temperatures that shields would attain at particular locations.

The heat reaching the liquid is expressed by:

$$Q_1 = \frac{4\pi K r_1 r_2 (T_2 - T_1)}{(r_2 - r_1)} = \dot{M} L_v \qquad (A1)$$

The heat reaching the shield is:

$$Q_2 = \frac{4\pi K r_2 r_3 (T_3 - T_2)}{(r_3 - r_2)} = \dot{M} L_v + \dot{M} \Delta h \qquad (A2)$$

Where:

Q_1 = Heat flow to liquid

Q_2 = Heat flow to shield

K = Thermal conductivity of insulation

r_1 = Inner tank radius

r_2 = Shield radius

r_3 = Outer radius of insulation

T_1 = Liquid temperature

T_2 = Shield temperature

*T_3 = Temperature of outer surface of insulation

$\dot{M}$ = Boil-off rate

L_v = Latent heat of vaporization

Δh = Heat absorbed in shield from T_1 to T_2

* For highly insulated tanks, T_3 is very close to the ambient temperature or equilibrium skin temperature.

Simultaneous equations (A1) and (A2) can be solved to find the temperature of the vapor-cooled shield and the resulting boil-off for a given tank design and environment. By suitably rearranging these equations and plotting the results, a clear picture of effects on the vapor-cooled shield can be presented.

Dividing (A1) by (A2)

$$\frac{\dot{M} L_v}{\dot{M} L_v + \dot{M} \Delta h} = \frac{4\pi K r_1 r_2 (T_2 - T_1)(r_3 - r_2)}{4\pi K r_2 r_3 (T_3 - T_2)(r_2 - r_1)} \tag{A3}$$

or

$$\frac{L_v}{L_v + \Delta h} = \frac{r_1 (T_2 - T_1)(r_3 - r_2)}{r_3 (T_3 - T_2)(r_2 - r_1)} \tag{A4}$$

Let $r_3 = a\, r_1$ (A5)

Let $r_2 = b\, r_1$ (A6)

Then

$$\frac{L_v}{L_v + \Delta h} = \frac{r_1 (T_2 - T_1)(a\, r_1 - b\, r_1)}{a\, r_1 (T_3 - T_2)(b\, r_1 - r_1)} \tag{A7}$$

or

$$\frac{L_v}{L_v + \Delta h} = \frac{(T_2 - T_1)(a - b)}{(T_3 - T_2) a (b - 1)} \tag{A8}$$

which reduces to

$$\frac{a\,(b-1)}{(a-b)} = \frac{(T_2 - T_1)(L_v + \Delta h)}{(T_3 - T_2)\;L_v} = g \qquad (A9)$$

The quantity g is convenient because it depends only on thermodynamic properties and environments.

From the left number of (A9) solving for b,

$$a\,b - a = a\,g - b\,g \qquad (A10)$$

or

$$a\,b + b\,g = a\,g + a$$

or

$$b = \frac{a\,g + a}{a + g} = \frac{a\,(g+1)}{a+g}$$

To plot boil-off rates in general terms solve (A1) for $\frac{\dot{M}}{r_1 K}$.

$$\frac{\dot{M}}{r_1 K} = \frac{4\pi\, r_2\,(T_2 - T_1)}{(r_2 - r_1)\,L_v} \qquad (A11)$$

or

$$\frac{\dot{M}}{r_1 K} = \frac{4\pi\, b\, r_1\,(T_2 - T_1)}{(b\, r_1 - r_1)\,L_v} \qquad (A12)$$

or

$$\frac{\dot{M}}{r_1 K} = \frac{4\pi\,(T_2 - T_1)}{L_v}\left(\frac{b}{b-1}\right) \tag{A13}$$

Solving the last factor on the right side of (A13) in terms of a and g:

$$\frac{b}{b-1} = \frac{\frac{a(g+1)}{a+g}}{\frac{a(g+1)}{a+g} - 1} = \frac{\frac{a(g+1)}{a+g}}{\frac{a(g+1) - a - g}{a+g}} \tag{A14}$$

or

$$\frac{b}{b-1} = \frac{a(g+1)}{g(a-1)} \tag{A15}$$

Substituting (A15) into (A13) we have

$$\frac{\dot{M}}{r_1 K} = \frac{4\pi(T_2 - T_1)}{L_v}\,\frac{a(g+1)}{g(a-1)} \tag{A16}$$

which is plotted on the ordinate in Figures A2, A4, and A6.

On the abscissa $(r_2 - r_1)/(r_3 - r_1)$ represents the fraction of the way from inner to outer shell at which the vapor-cooled shield is placed.

$$\frac{r_2 - r_1}{r_3 - r_1} = \frac{b\,r_1 - r_1}{a\,r_1 - r_1} = \frac{b-1}{a-1} \tag{A17}$$

or

$$\frac{r_2 - r_1}{r_3 - r_1} = \frac{\frac{a(g+1)}{a+g} - 1}{a-1} = \frac{\frac{ag + a - a - g}{a+g}}{a-1} \tag{A18}$$

which reduces to:

$$\frac{r_2 - r_1}{r_3 - r_1} = \frac{\frac{g(a-1)}{a+g}}{a-1} = \frac{g}{a+g} \qquad \text{(A19)}$$

where: $\Delta h = H_2 - H_1$

H_2 = From T_2 and P

H_1 = From T_1 and P

P = Tank Pressure

The method of calculation is to solve (A16) and (A19) for a range of T_2 at a particular T_1, T_3, and a. A value of 1.1 was used for a. The results approach flat wall conditions. Shield temperature (T_2) is plotted versus shield location $(\frac{r_2 - r_1}{r_3 - r_1})$ in Figures A3, A5, and A7.

1.2 Single Vapor-Cooled Shield Analysis Based on Stefan-Boltzmann Equation

Equations and derivations are given below. The results are plotted in Figures A8 through A16. The curves should be read as follows:

1. If the tank pressure and ambient temperature (equilibrium skin temperature) are known, the boil-off is found on the ordinate in terms of the total number of radiation reflectors, reflector area, and over-all shield emissivity for any shield location.

2. The temperature of the shield when placed at any location is found on the temperature curves for the given ambient temperature and tank pressure.

The heat reaching the liquid is expressed by:

$$Q_1 = \sigma A (T_2^4 - T_1^4)\left(\frac{E_s}{N_{12} + 1}\right) = \dot{M} L_v \qquad \text{(A20)}$$

The heat reaching the vapor-cooled shield is:

$$Q_2 = \sigma A (T_3^4 - T_2^4)\left(\frac{E_s}{N_{23} + 1}\right) = \dot{M} L_v + \dot{M} \Delta h \qquad \text{(A21)}$$

FIGURE A2
BOIL-OFF FOR VAPOR-SHIELDED SPHERICAL HYDROGEN TANKS
BASED ON FOURIER EQUATION

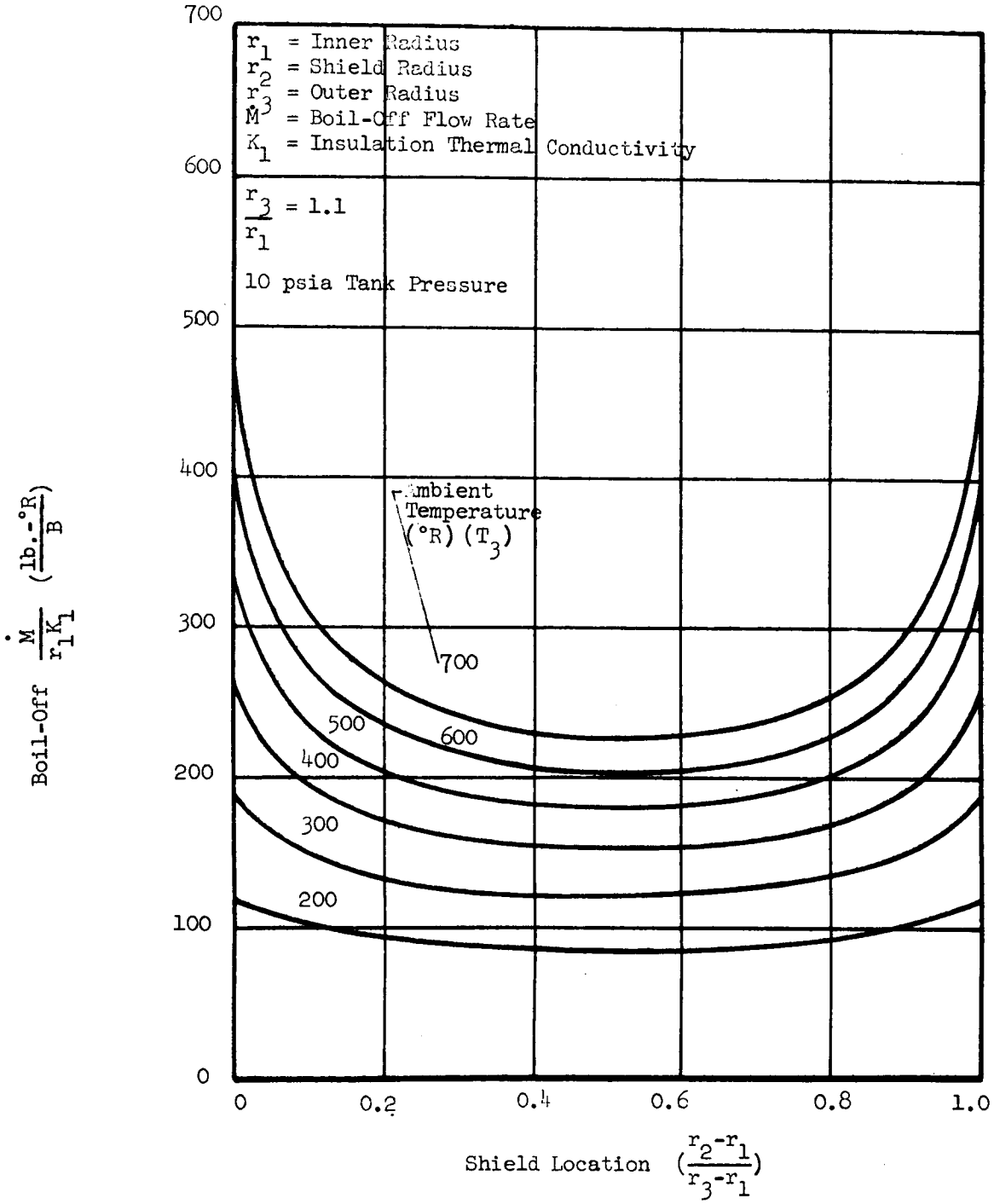

FIGURE A3
TEMPERATURE OF VAPOR-COOLED SHIELDS ON SPHERICAL HYDROGEN TANKS
BASED ON FOURIER EQUATION

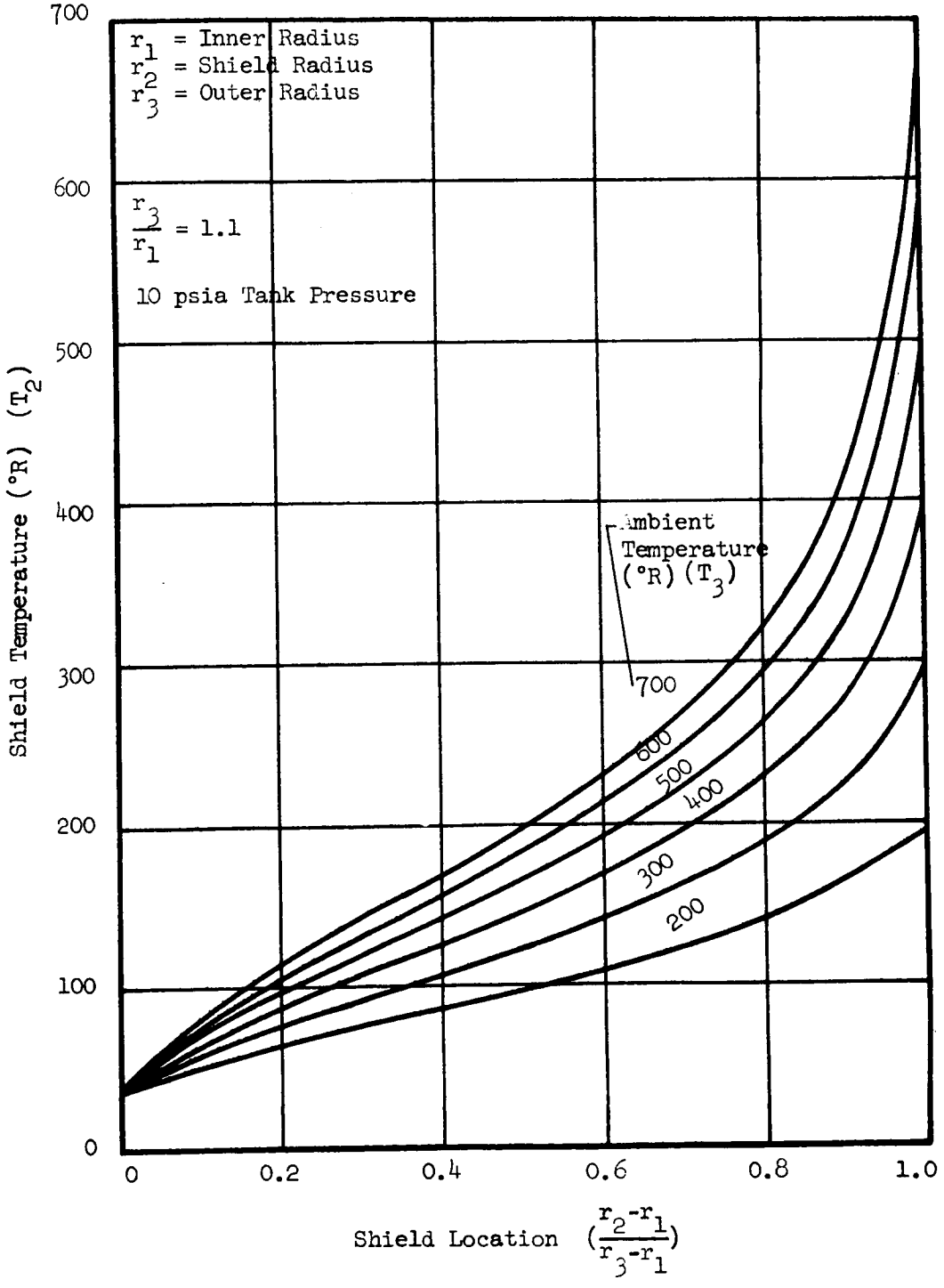

FIGURE A4
BOIL-OFF FOR VAPOR-SHIELDED SPHERICAL HYDROGEN TANKS
BASED ON FOURIER EQUATION

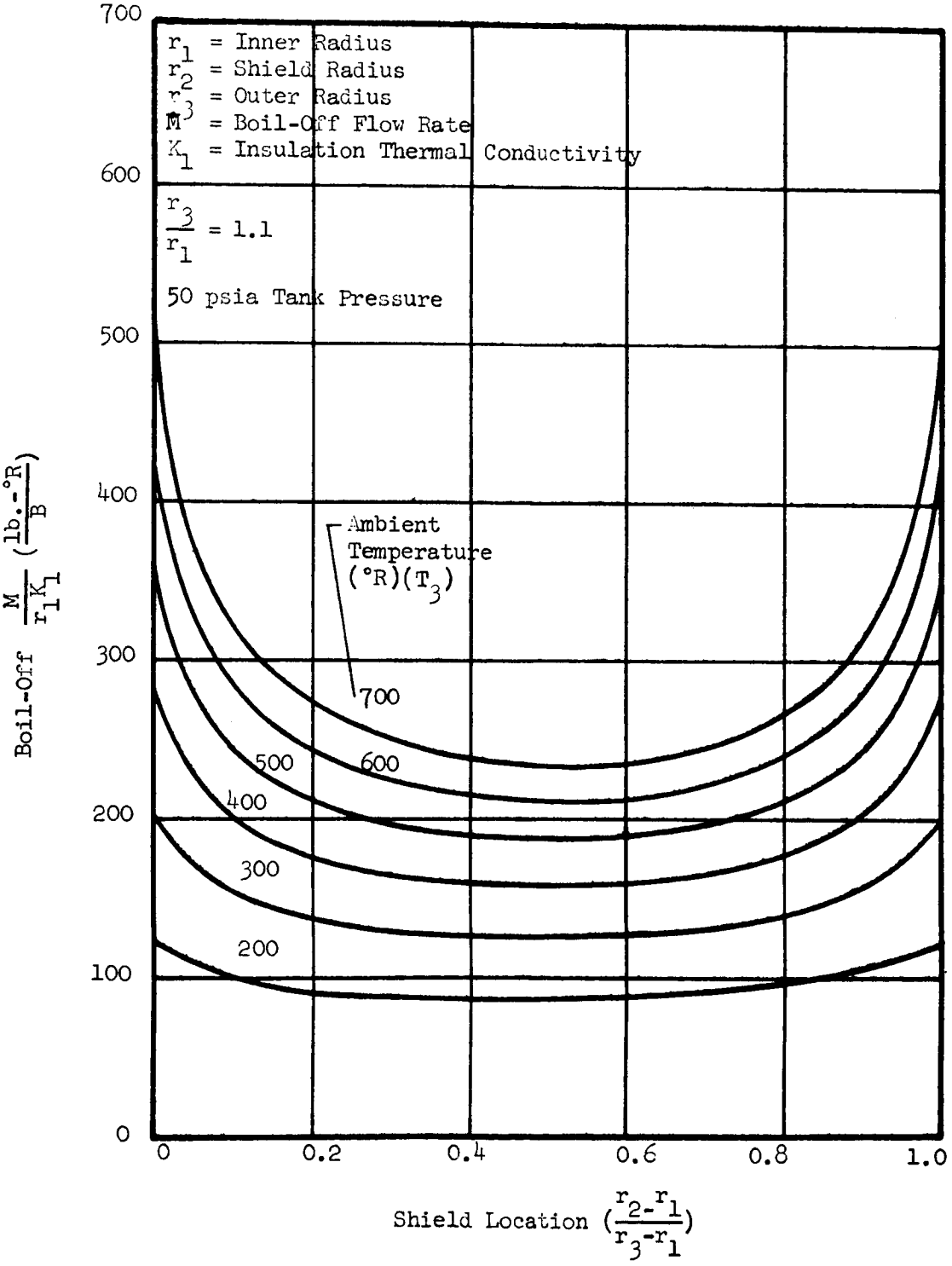

FIGURE A5

TEMPERATURE OF VAPOR-COOLED SHIELDS ON SPHERICAL HYDROGEN TANKS BASED ON FOURIER EQUATION

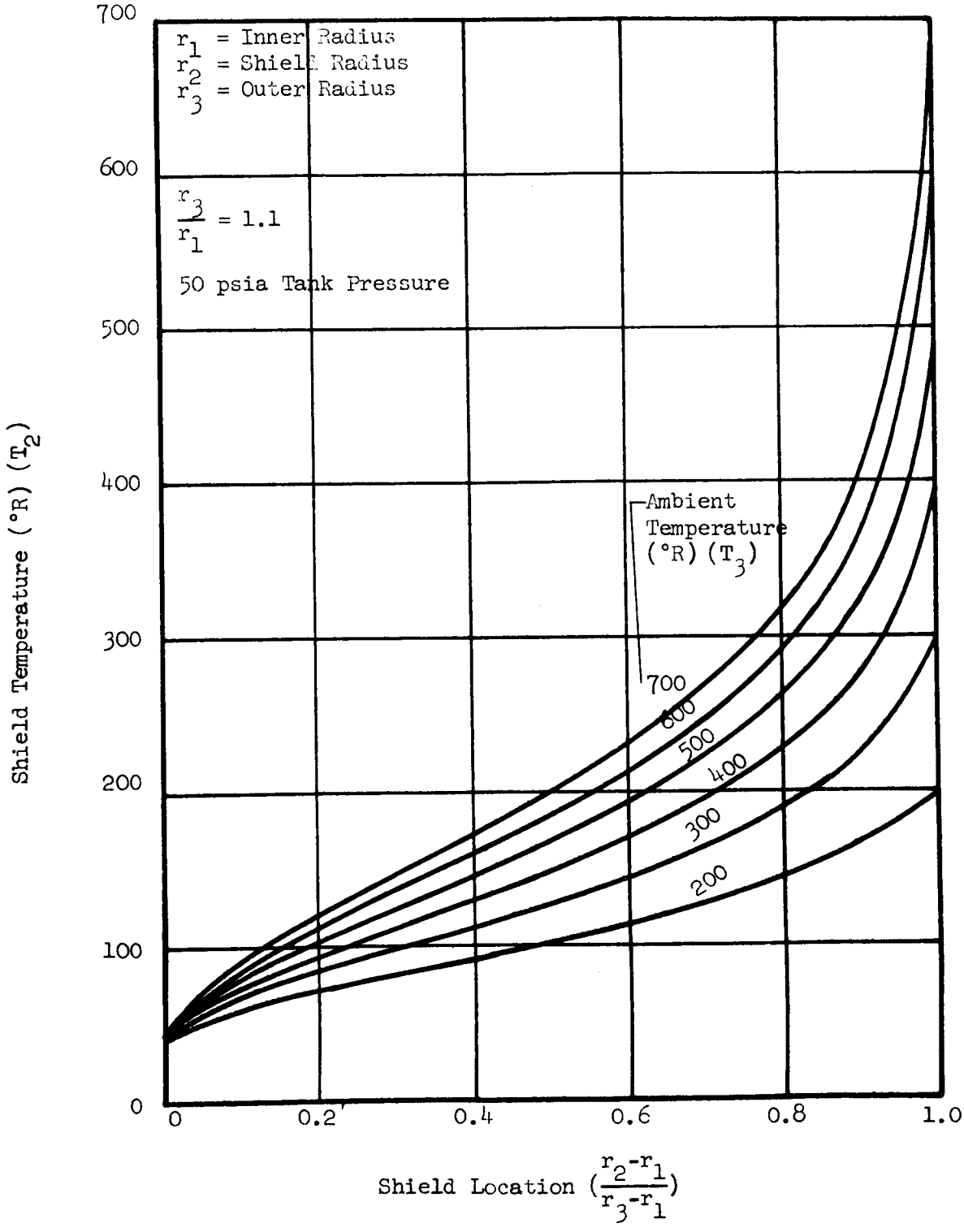

FIGURE A6
BOIL-OFF VAPOR-SHIELDED SPHERICAL HYDROGEN TANKS
BASED ON FOURIER EQUATION

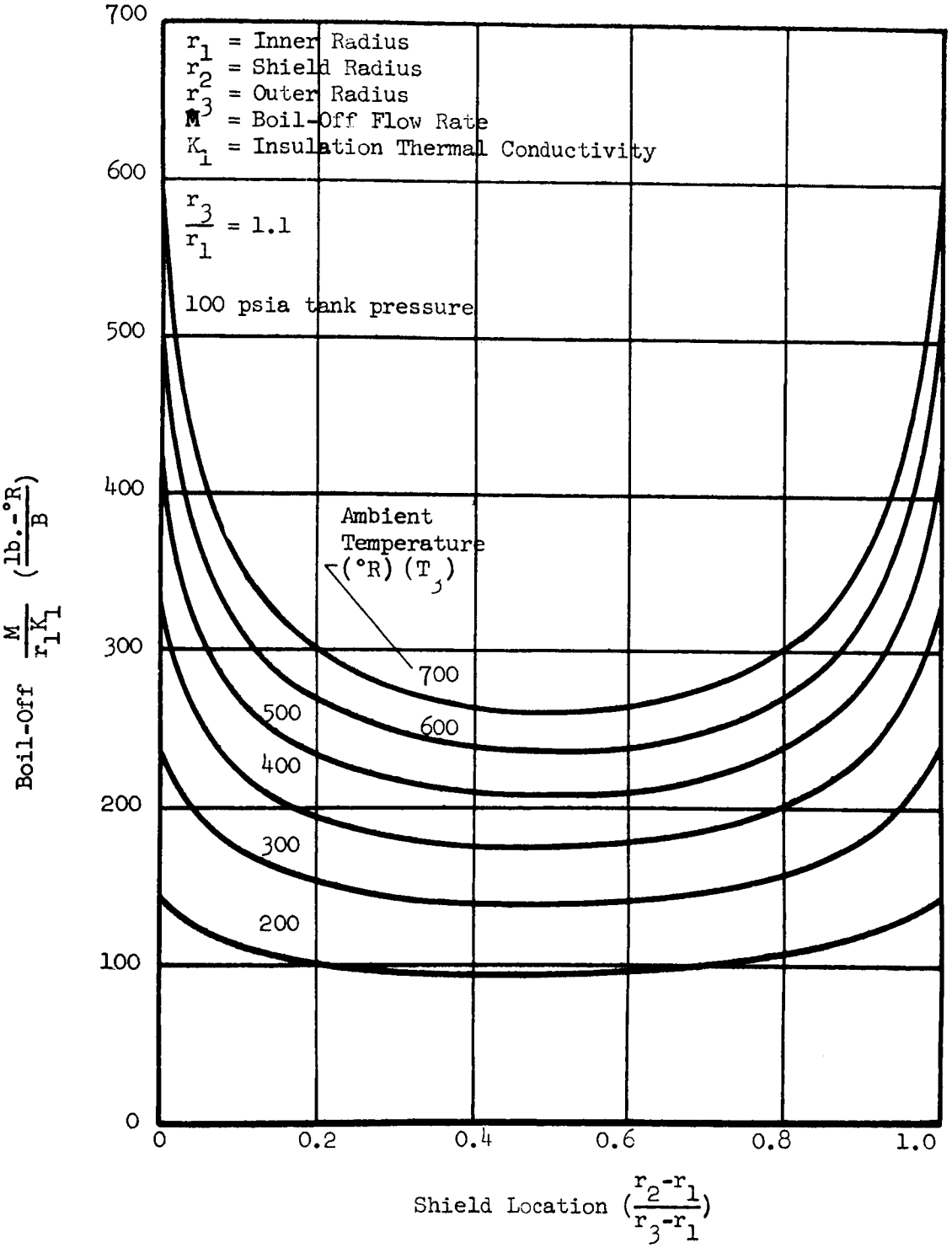

FIGURE A7
TEMPERATURE OF VAPOR-COOLED SHIELDS ON SPHERICAL HYDROGEN TANKS
BASED ON FOURIER EQUATION

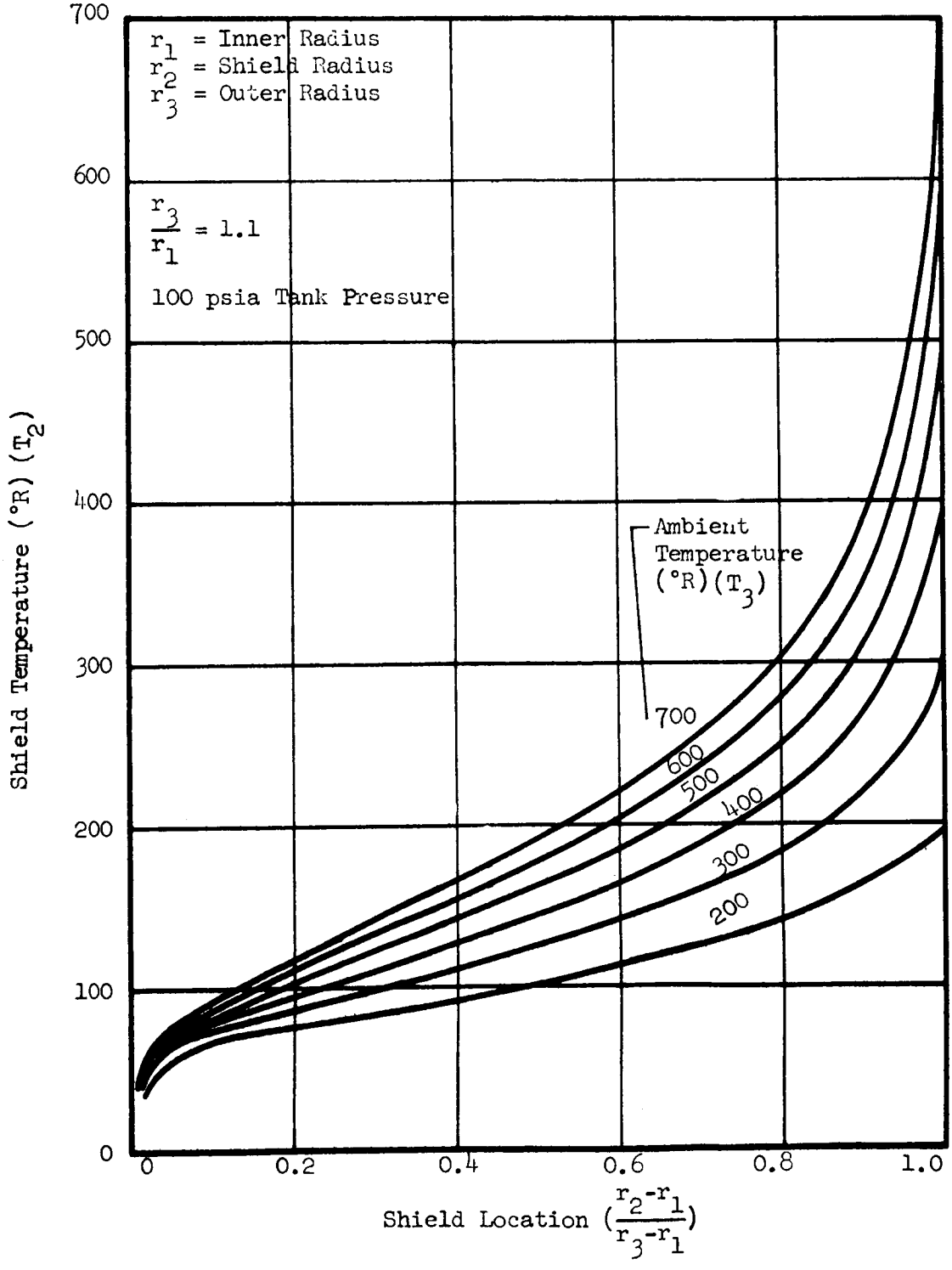

Where

Q_1 = Heat flow to liquid

Q_2 = Heat flow to shield

σ = Stefan-Boltzman constant

A = Area of radiation barriers

T_1 = Liquid temperature

T_2 = Vapor-cooled shield temperature

$*T_3$ = Temperature of outer covering

E_s = Emissivity of radiation barriers, vapor-cooled shield, inner tank and outer covering

N_{13} = Number of radiation barriers between inner shell and outer covering

N_{12} = Number of radiation barriers between inner shell and vapor-cooled shield

N_{23} = Number of radiation barriers between vapor-cooled shield and outer covering

$\dot{M}$ = Boil-off rate

L_v = Latent heat of vaporization of liquid

Δh = Heat absorbed in shield from T_1 to T_2

* = For highly insulated tanks, T_3 is very close to the ambient or equilibrium skin temperature.

Simultaneous equations (A20) and (A21) can be solved to find the temperature of the vapor-cooled shield and the resulting boil-off for a given tank design and environment.

By suitably rearranging these equations and plotting the results, the effects of the vapor-cooled shield placed between radiation barriers can be seen.

Dividing (A20) by (A21):

$$\frac{L_v}{L_v + \Delta h_{12}} = \frac{(T_2^4 - T_1^4)}{(T_3^4 - T_2^4)} \frac{(N_{23} + 1)}{(N_{12} + 1)} \qquad \text{(A22)}$$

or

$$\frac{(N_{12} + 1)}{(N_{23} + 1)} = \frac{(L_v + \Delta h)}{(L_v)} \frac{(T_2^4 - T_1^4)}{(T_3^4 - T_2^4)} = g \tag{A23}$$

g depends only on thermodynamic properties and environments.

Rearranging equation (A20):

$$\frac{\dot{M}\,(N_{12} + 1)}{\sigma A E_s} = \frac{(T_2^4 - T_1^4)}{L_v} \tag{A24}$$

Dividing both sides of (A24) by (A23):

$$\frac{\dot{M}}{\sigma A E_s} = \frac{(T_2^4 - T_1^4)}{L_v (g)(N_{23} + 1)} \tag{A25}$$

Multiplying both sides by $(N_{13} + 1)$

$$\frac{\dot{M}\,(N_{13} + 1)}{A \sigma E_s} = \frac{(T_2^4 - T_1^4)}{L_v} \frac{(N_{13} + 1)}{g\,(N_{23} + 1)} \tag{A26}$$

Now

$$N_{13} = N_{12} + N_{23} \tag{A27}$$

and from (A23)

$$N_{12} + 1 = (N_{23} + 1)\, g \tag{A28}$$

Solving (A27) and (A28) for N_{12}

$$N_{12} + 1 = (N_{13} - N_{12} + 1)\, g \tag{A29}$$

$$N_{12} + 1 = N_{13}\, g - N_{12}\, g + g \tag{A30}$$

$$N_{12}\,(1 + g) = N_{13}\,g + g - 1 \tag{A31}$$

$$N_{12} = \frac{g\,(N_{13} + 1) - 1}{1 + g} \tag{A32}$$

Substituting (A27) into (A26)

$$\frac{\dot{M}\,(N_{13} + 1)}{A\sigma E_s} = \frac{(T_2^{\,4} - T_1^{\,4})}{L_v}\;\frac{(N_{13} + 1)}{g\,(N_{13} - N_{12} + 1)} \tag{A33}$$

Substituting (A32) into (A33)

$$\frac{\dot{M}\,(N_{13} + 1)}{A\sigma E_s} = \frac{(T_2^{\,4} - T_1^{\,4})\,(N_{13} + 1)}{(L_v)\,g\left[N_{13} - \left(\dfrac{g\,(N_{13} + 1) - 1}{1 + g}\right) + 1\right]} \tag{A34}$$

If N_{13} is large, $N_{13} + 1 \cong N_{13}$

$$\frac{\dot{M}\,(N_{13} + 1)}{A\sigma E_s} = \frac{(T_2^{\,4} - T_1^{\,4})}{L_v}\;\frac{(N_{13} + 1)}{g\left[N_{13} - \left(\dfrac{g\,N_{13} + g - 1}{1 + g}\right) + 1\right]} \tag{A35}$$

$$\frac{\dot{M}\,(N_{13} + 1)}{A\sigma E_s} = \frac{(T_2^{\,4} - T_1^{\,4})}{L_v}\;\frac{(N_{13} + 1)\,(1 + g)}{g\left[N_{13} + gN_{13} - gN_{13} - g + 1 + 1 + g\right]} \tag{A36}$$

$$\frac{\dot{M}\,(N_{13} + 1)}{A\sigma E_s} = \frac{(T_2^{\,4} - T_1^{\,4})}{L_v}\;\frac{(N_{13} + 1)(1 + g)}{g\,(N_{13} + 2)} \tag{A37}$$

Equation A37 reduces to

$$\frac{\dot{M}\,(N_{13}+2)}{A\sigma E_s} = \frac{(T_2^4 - T_1^4)}{L_v}\,\frac{1+g}{g} \qquad (A38)$$

which is plotted on the ordinate in Figures A8, A9, A11, A12, A14, and A15.

This is plotted against the abscissa

$$\frac{N_{12}}{N_{13}} = \frac{\dfrac{g(N_{13}+1)-1}{1+g}}{N_{13}} \text{ for large N } = \frac{\dfrac{gN_{13}-1}{1+g}}{N_{13}} \qquad (A39)$$

$$\frac{N_{12}}{N_{13}} = \frac{gN_{13}-1}{N_{13}(1+g)} \qquad (A40)$$

Where $\Delta h = H_2 - H_1$

H_2 = From T_2 and P

H_1 = From T_1 and P

P = Tank Pressure

The method of calculation is to solve (A38) and (A40) for a range of T_2 at a particulat T_1, T_3, and N_{13}. Shield temperature (T_2) is plotted versus shield location (N_{12}/N_{13}) in Figures A10, A13, and A16. The curves were calculated using a value of 10^6 shields for N_{13}. Values are accurate for $N_{13} > 100$, but percent error increases as number of shields decrease below 100.

1.3 Summarized Results of Fourier and Stefan-Boltzmann Shield Analyses

Figure A17 is a plot of the maximum boil-off reduction factors obtained for liquid hydrogen tanks at various pressures and ambient temperatures. The curves should be read as follows: If the tank pressure and ambient temperature are known, addition of an optimum vapor-cooled shield to an existing design will reduce the boil-off by a factor shown on the abscissa. The factor for real insulations can be expected to lie between the Fourier and Stefan-Boltzmann curves.

FIGURE A8
BOIL-OFF FOR VAPOR SHIELDED HYDROGEN TANKS
BASED ON STEFAN-BOLTZMANN EQUATION

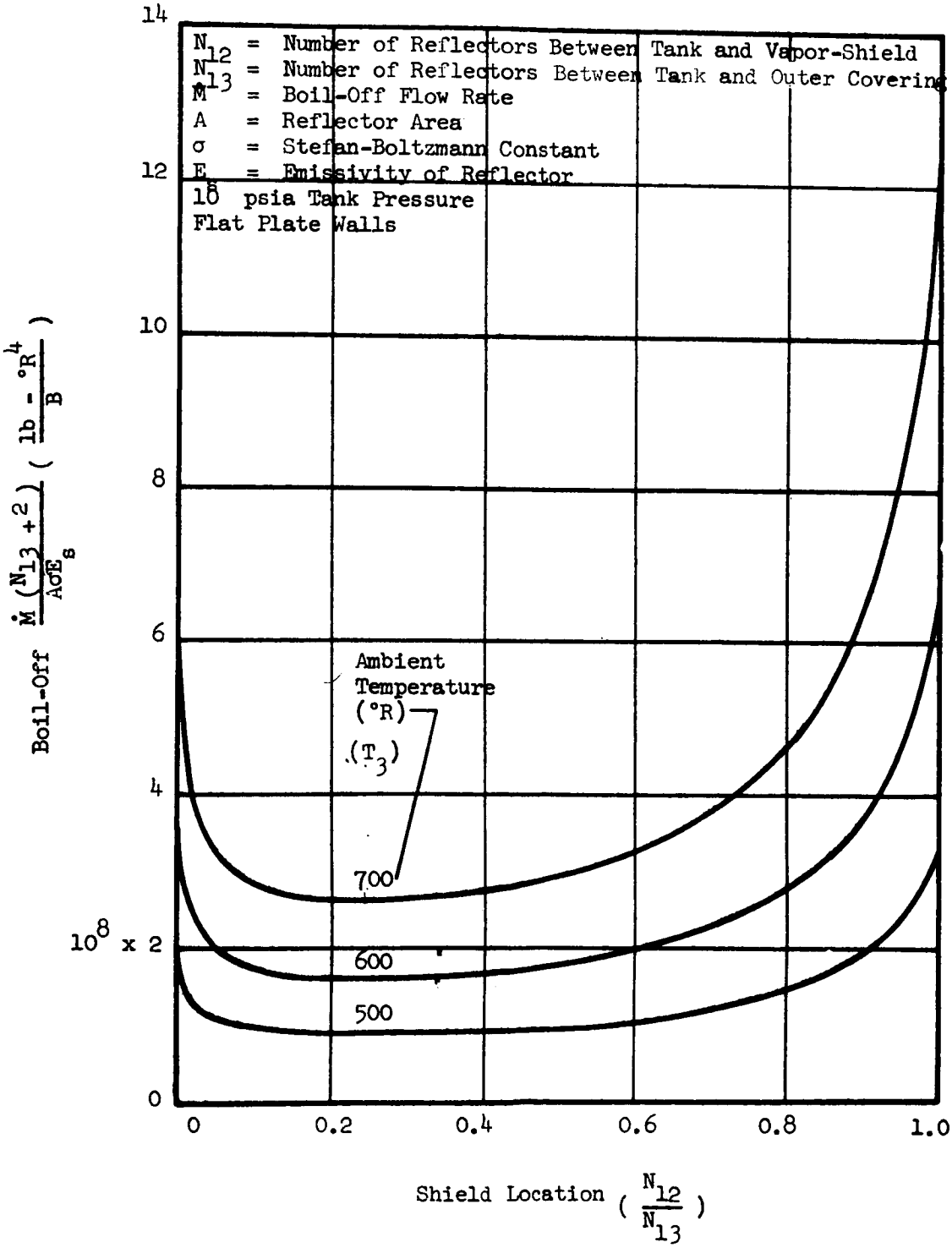

FIGURE A9
BOIL-OFF FOR VAPOR SHIELDED HYDROGEN TANKS
BASED ON STEFAN-BOLTZMANN EQUATION

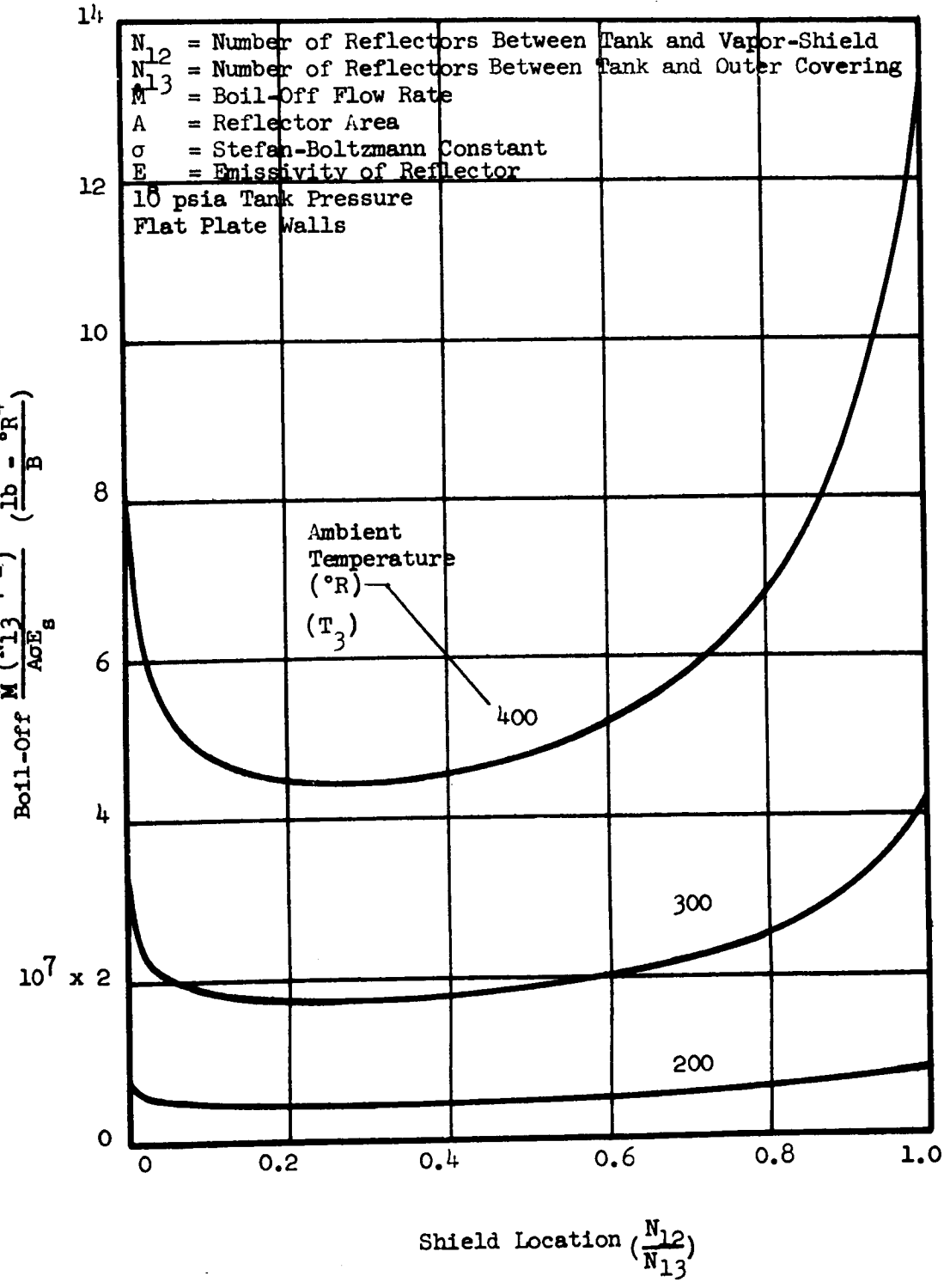

FIGURE A10
TEMPERATURE OF VAPOR-COOLED SHIELDS ON HYDROGEN TANKS
BASED ON STEFAN-BOLTZMANN EQUATION

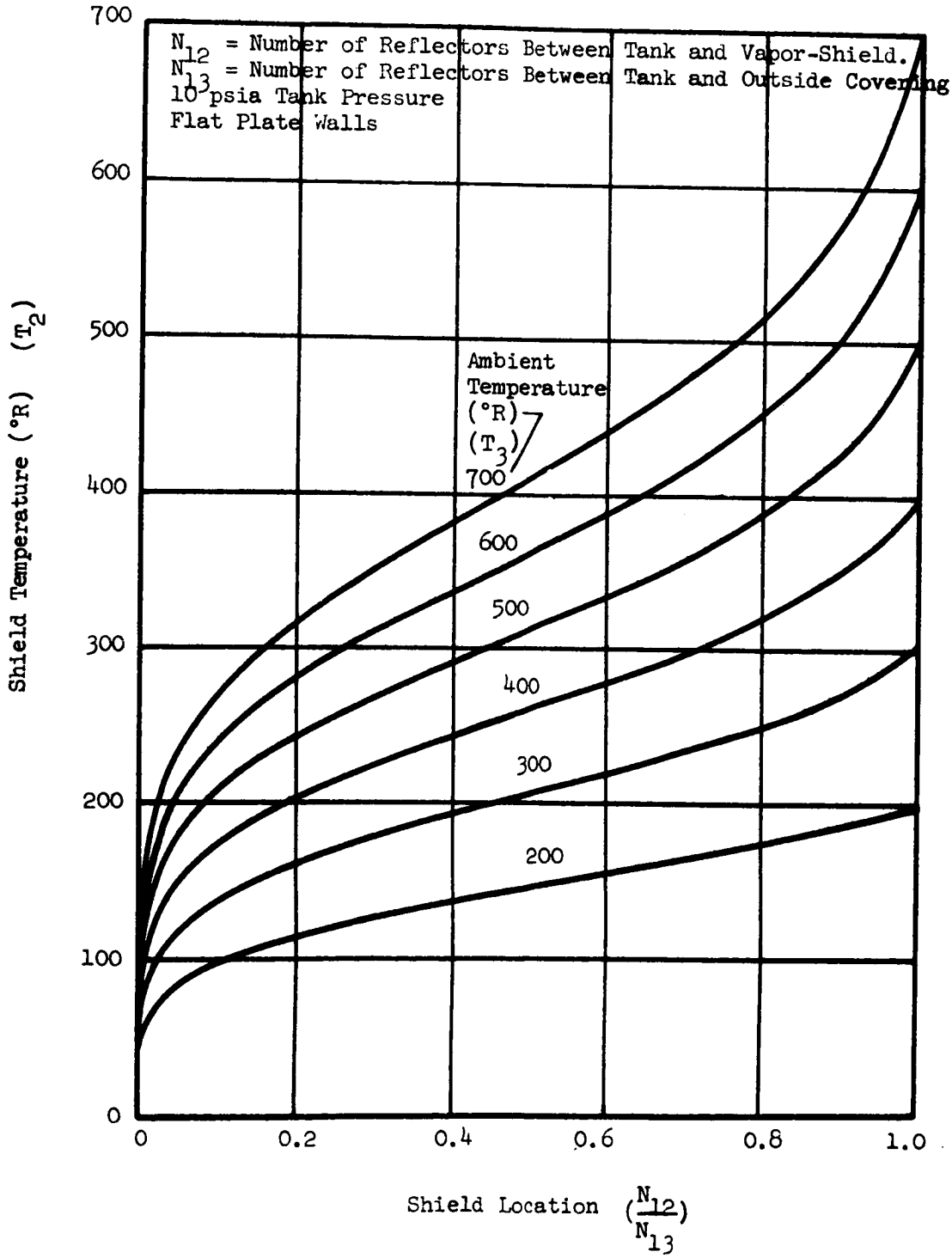

FIGURE A11
BOIL-OFF FOR VAPOR SHIELDED HYDROGEN TANKS
BASED ON STEFAN-BOLTZMANN EQUATION

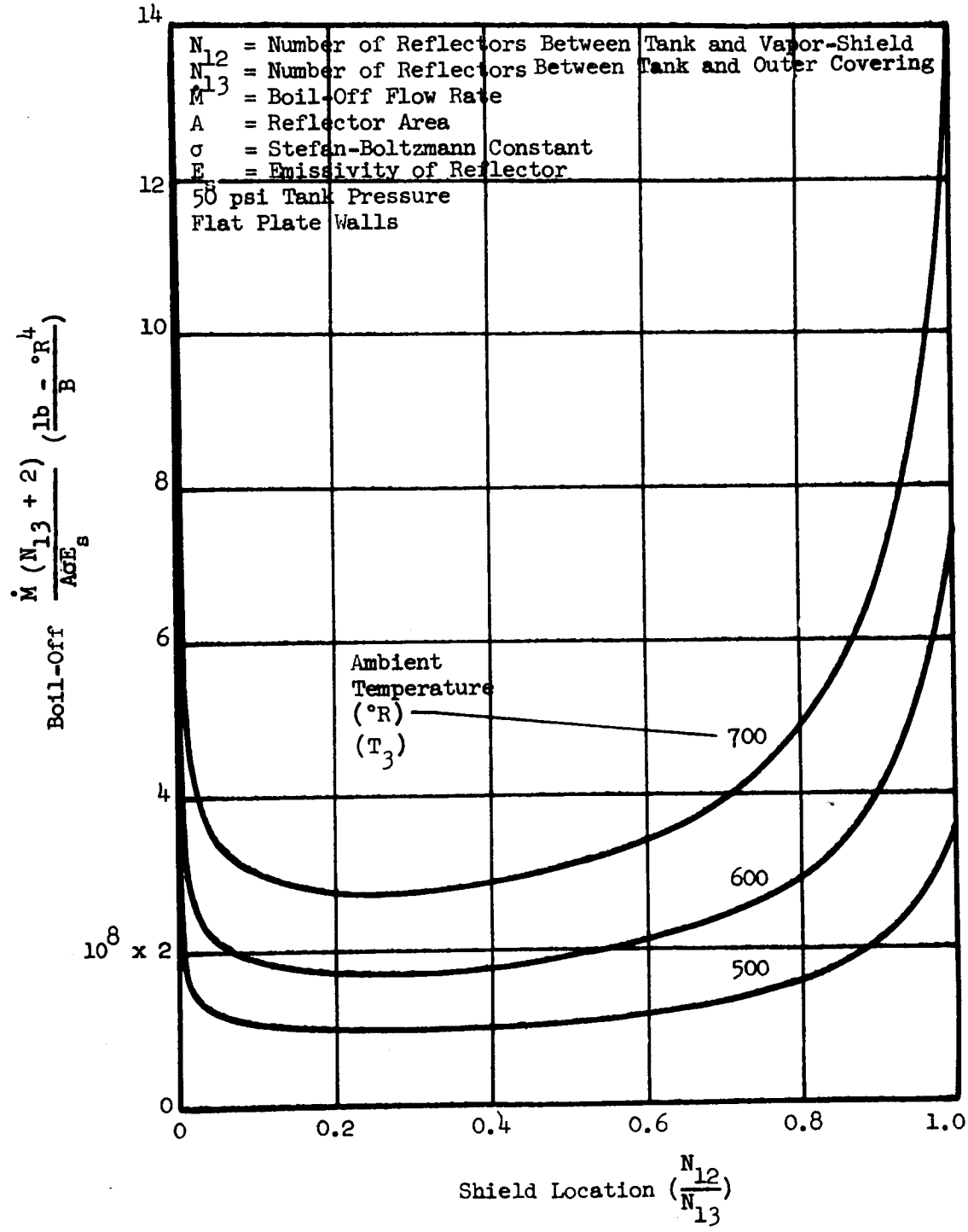

FIGURE A12
BOIL-OFF FOR VAPOR SHIELDED HYDROGEN TANKS
BASED ON STEFAN-BOLTZMANN EQUATION

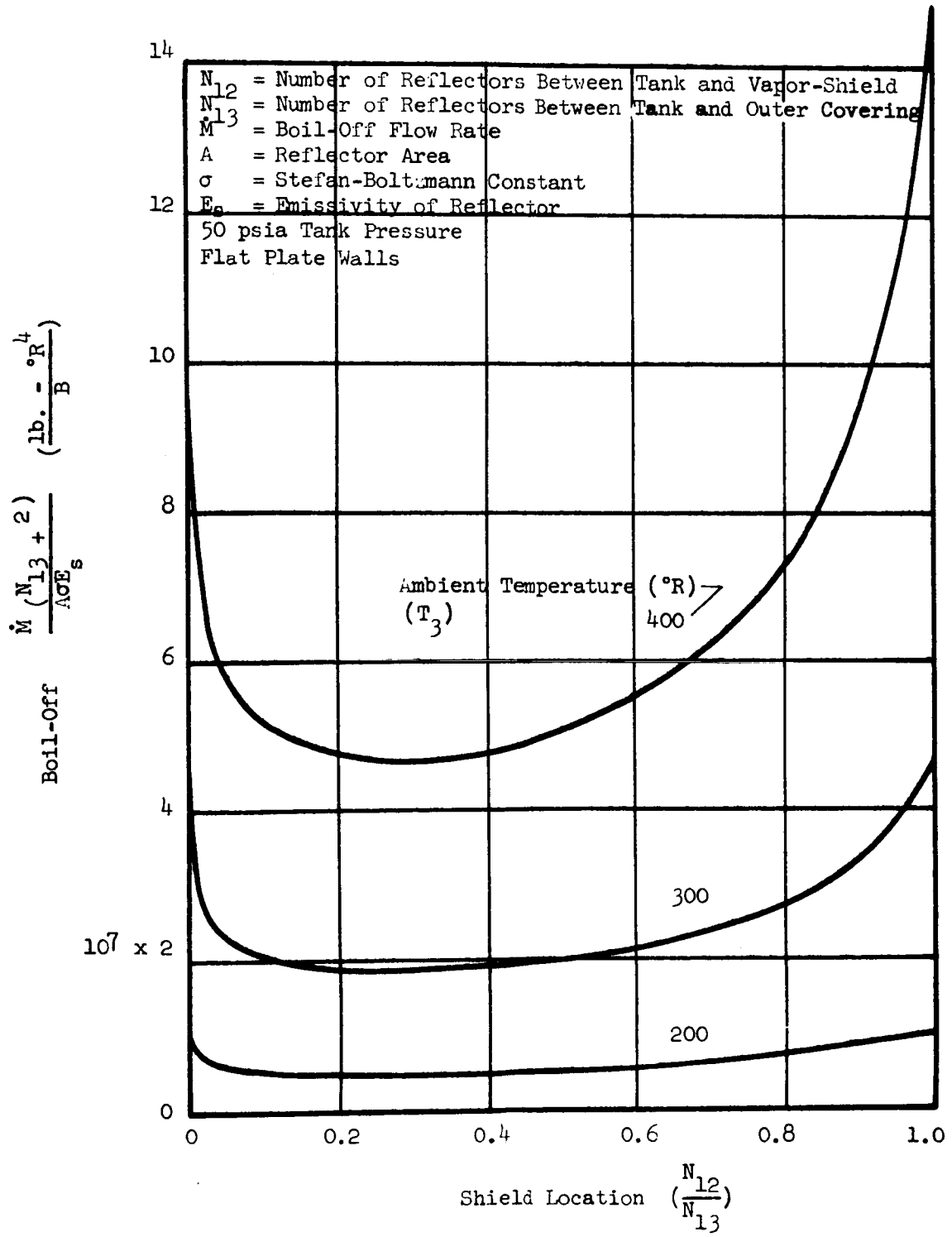

FIGURE A13
TEMPERATURE OF VAPOR-COOLED SHIELDS ON HYDROGEN TANKS
BASED ON STEFAN-BOLTZMANN EQUATION

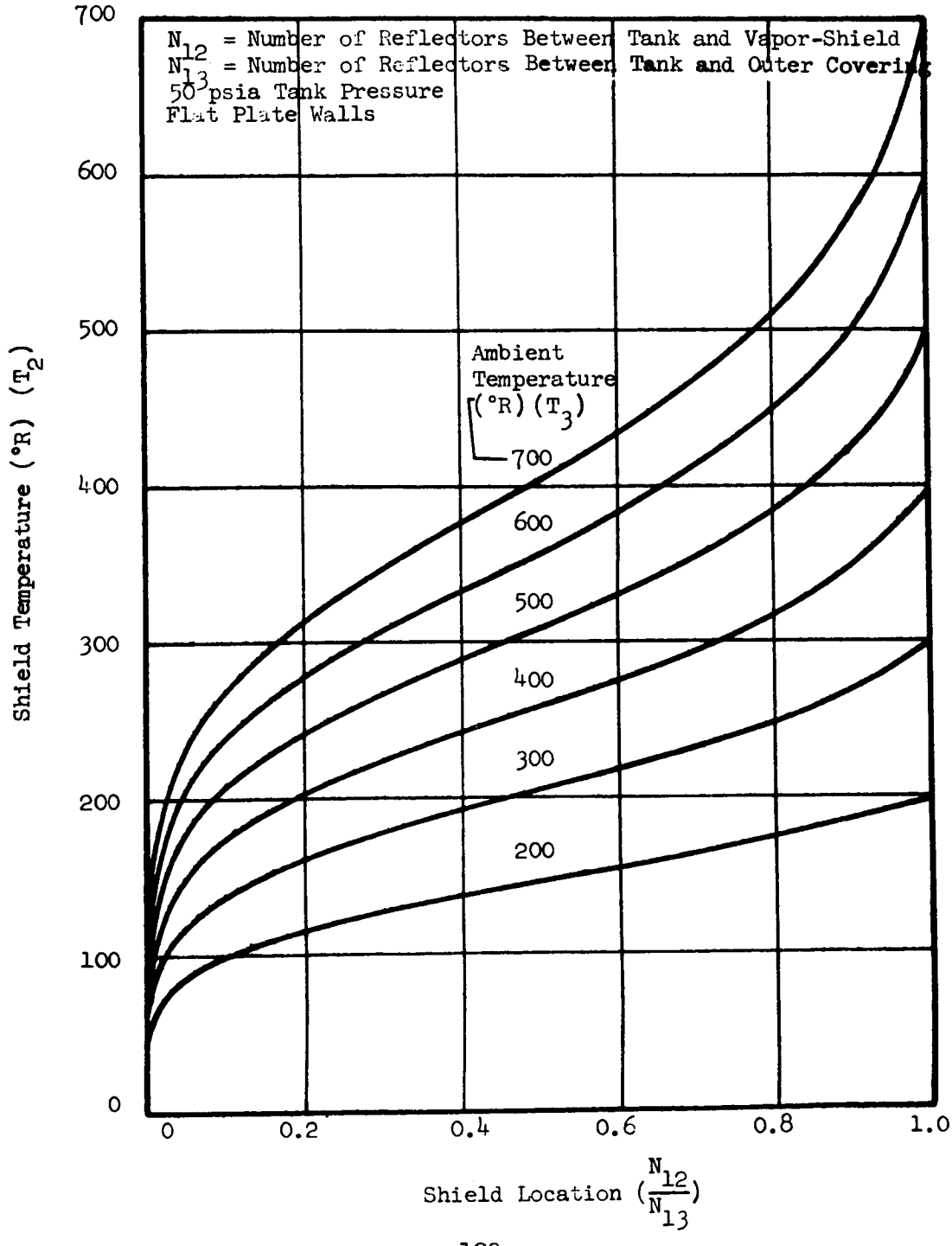

FIGURE A14
BOIL-OFF FOR VAPOR SHIELDED HYDROGEN TANKS
BASED ON STEFAN-BOLTZMANN EQUATION

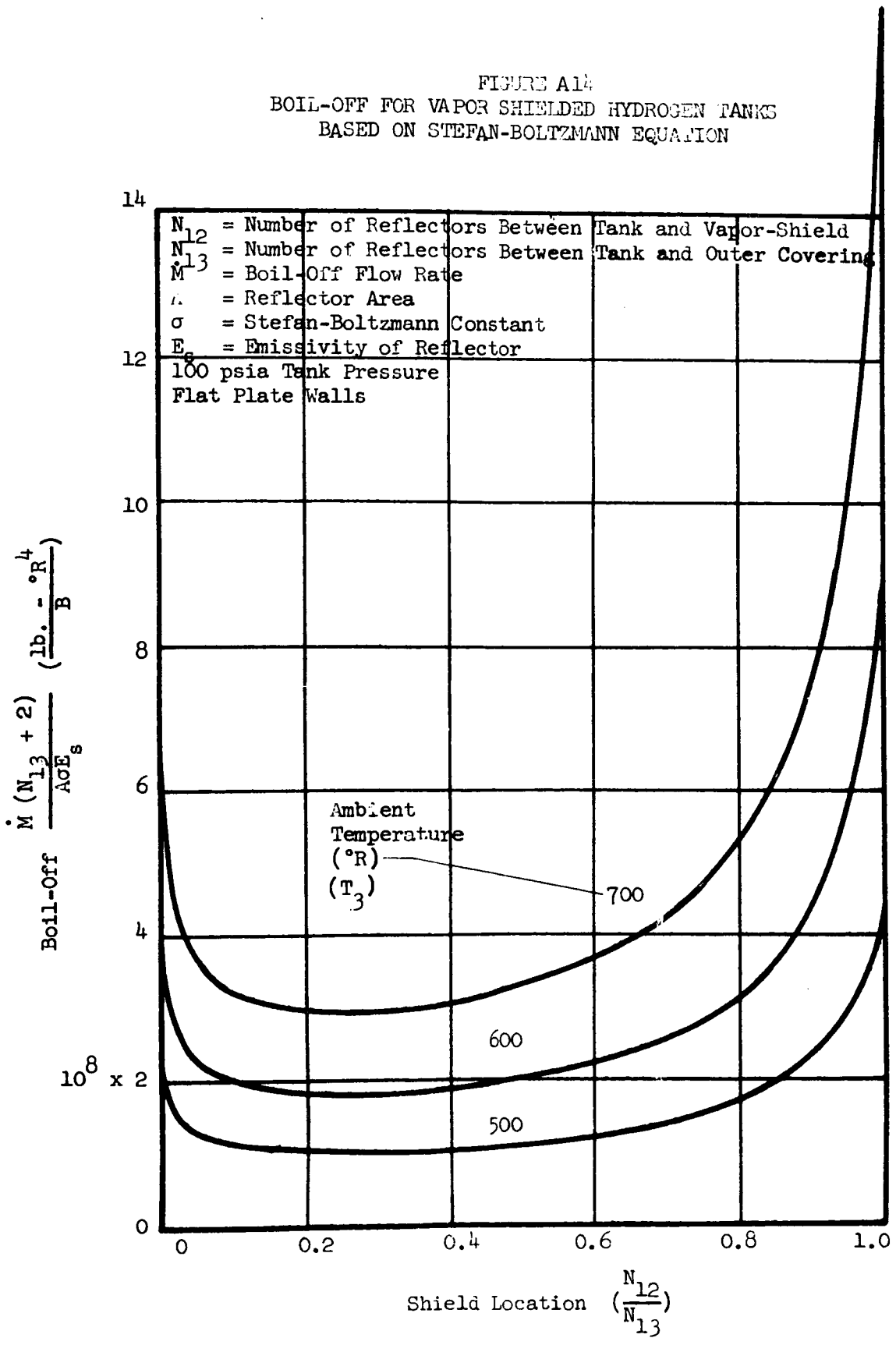

FIGURE A15
BOIL-OFF FOR VAPOR SHIELDED HYDROGEN TANKS
BASED ON STEFAN-BOLTZMANN EQUATION

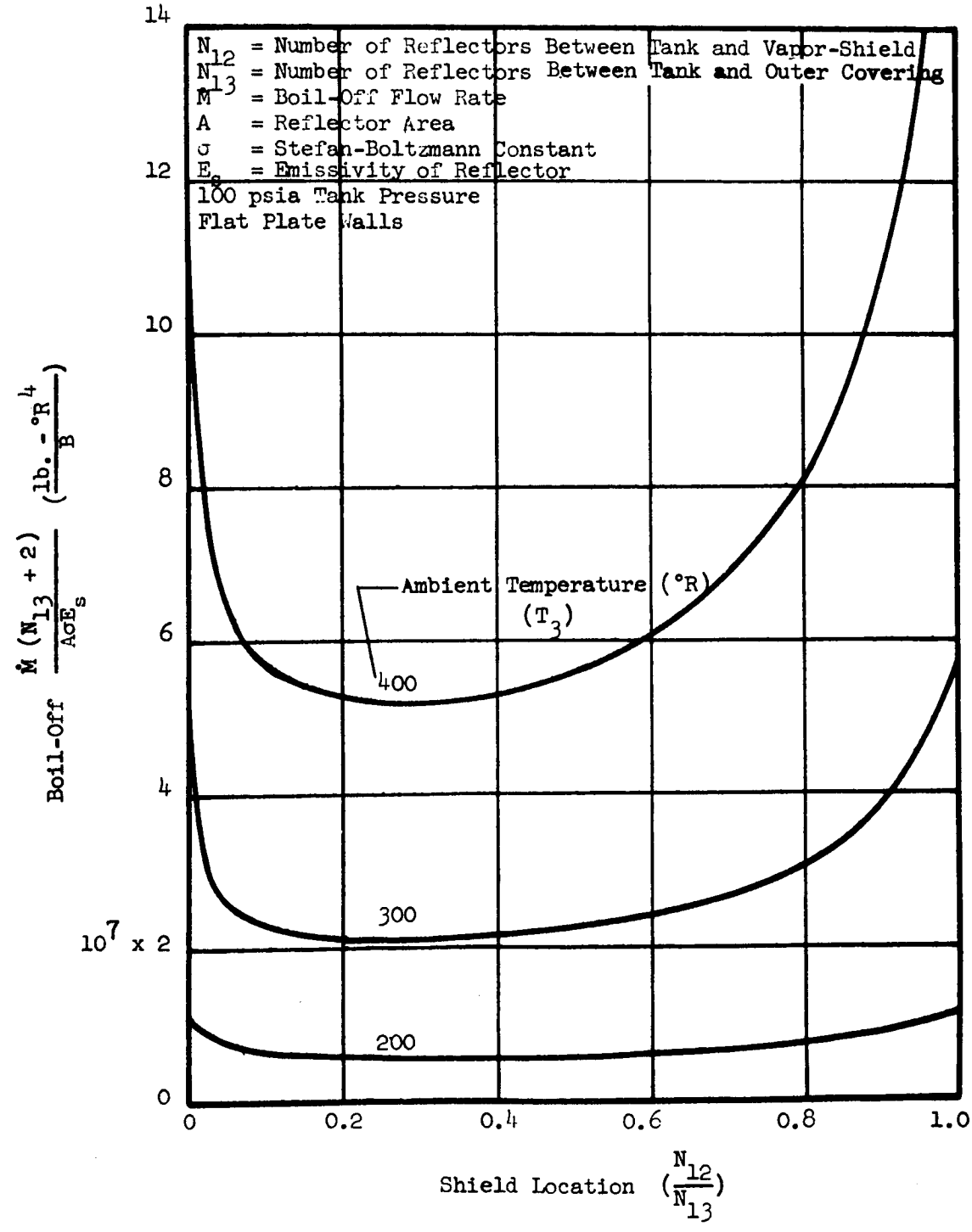

FIGURE A16
TEMPERATURE OF VAPOR-COOLED SHIELDS ON HYDROGEN TANKS
BASED ON STEFAN-BOLTZMANN EQUATION

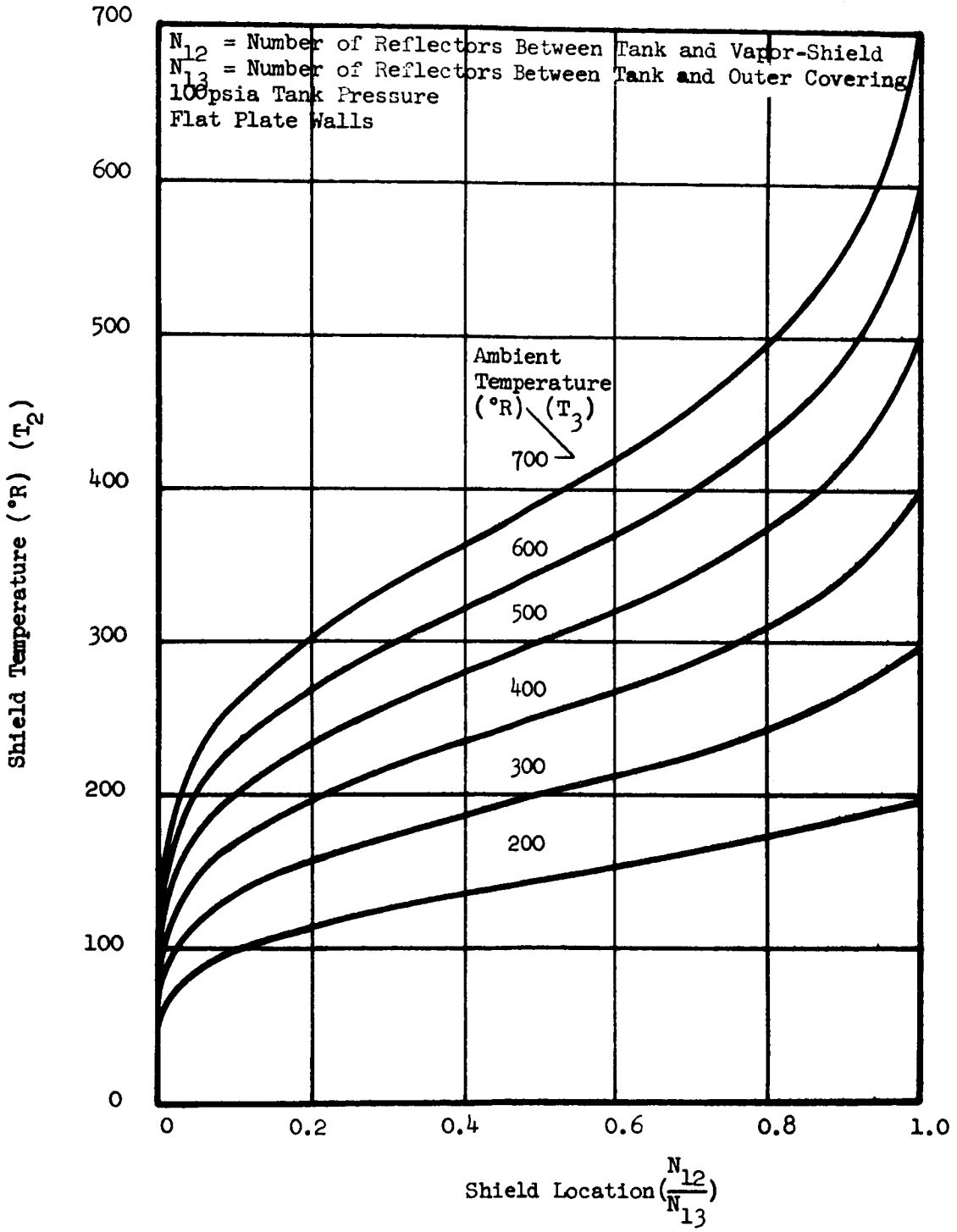

FIGURE A17
SHIELD EFFECTIVENESS FACTOR
OPTIMUM VAPOR SHIELDED HYDROGEN TANKS

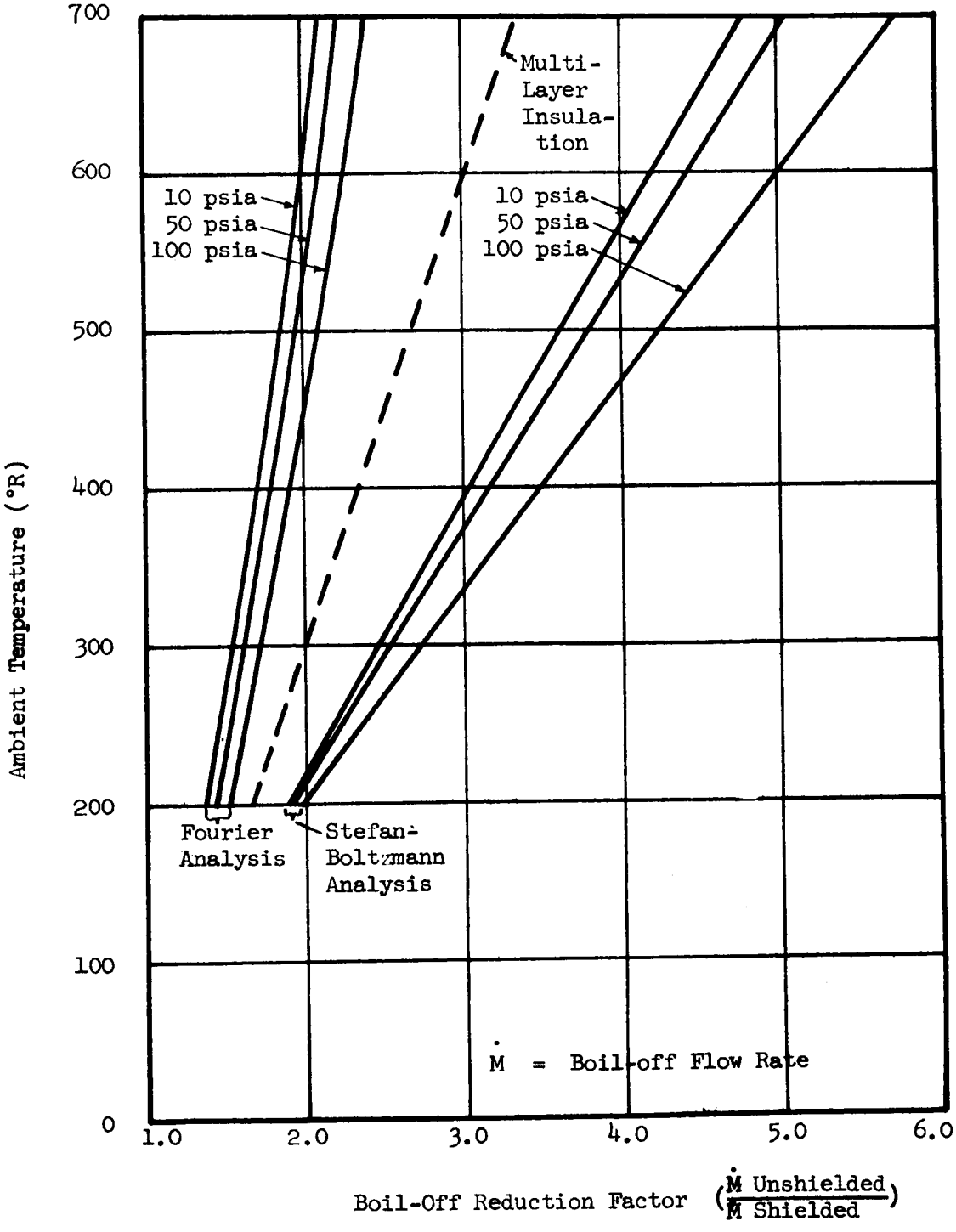

2.0 Dual Vapor-Cooled Shields

A single shield does not make fullest use of the available refrigeration from boil-off gases. The equations and curves given in this section are an indication of the improvement to be expected by placing two concentric shields in series so that the exhaust of the cold shield flows to the warm shield. The assumptions used are the same as those used in Section 1.0 of this appendix.

2.1 Dual Vapor-Cooled Shield Analysis Based on Fourier Equation

Equations and derivations are given below. The results are plotted in Figures A18 through A23. The curves should be read as follows:

1. For a given location of the warmer shield (a/c), read the ratio of the shielded boil-off to the unshielded boil-off ($\dot{M}/\dot{M}_o$) for all locations of the colder shield which lie on the colder side of the warmer shield. At all locations on the warmer side of the warmer shield, the plotted values represent one shield only.

2. The ratio of the shield temperature to the unshielded insulation temperature at that location is read from the T_3/T_1 and T_2/T_1 curves for both shields. At all locations on the warmer side of the warmer shield, the plotted values represent one shield only.

The heat per unit area reaching the liquid is expressed by:

$$Q_1 = \frac{K\,(T_2-T_1)}{(c-b)} = \dot{M}\,L_v \qquad \text{(A41)}$$

The heat reaching the colder shield is:

$$Q_2 = \frac{K\,(T_3-T_2)}{(b-a)} = \dot{M}\,L_v + \dot{M}\,(h_2-h_1) \qquad \text{(A42)}$$

The heat reaching the warmer shield is:

$$Q_3 = \frac{K\,(T_4-T_3)}{a} = \dot{M}\,L_v + \dot{M}\,(h_2-h_1) + \dot{M}\,(h_3-h_2) \qquad \text{(A43)}$$

Where:

Q_1 = Heat flow to liquid

Q_2 = Heat flow to colder shield

Q_3 = Heat flow to warmer shield

K = Thermal conductivity of insulation

a = Thickness of insulation from hot wall to warmer shield

b = Thickness of insulation from hot wall to colder shield

c = Thickness of insulation from hot wall to cold wall

T_1 = Liquid temperature

T_2 = Colder shield temperature

T_3 = Warmer shield temperature

T_4 = Temperature of outer surface of insulation (equilibrium skin temperature)

$\dot{M}$ = Shielded boil-off rate ($\dot{M}_o$ = unshielded boil-off rate)

L_v = Latent heat of vaporization

h_1 = Enthalpy of gas leaving tank at T_1

h_2 = Enthalpy of gas leaving colder shield at T_2

h_3 = Enthalpy of gas leaving warmer shield at T_3

From (A41)

$$\dot{M} = \frac{K(T_2-T_1)}{L_v(c-b)} \tag{A44}$$

Substituting (A44) into (A42)

$$\frac{K(T_3-T_2)}{(b-a)} = \frac{K(T_2-T_1)}{L_v(c-b)}(L_v + h_2 - h_1) \tag{A45}$$

Dividing by K

$$\frac{(T_3-T_2)}{(b-a)} = \frac{(T_2-T_1)}{L_v(c-b)}(L_v + h_2 - h_1) \tag{A46}$$

Substituting (A44) into (A43) and dividing by K

$$\frac{(T_4-T_3)}{a} = \frac{(T_2-T_1)}{L_v(c-b)} (L_v + h_3 - h_1) \quad (A47)$$

Working with (A46)

$$(c-b)(L_v)(T_3-T_2)-(b-a)(T_2-T_1)(L_v + h_2 - h_1) = 0 \quad (A48)$$

$$c(L_v)(T_3-T_2)-b(L_v)(T_3-T_2)-b(T_2-T_1)(L_v+h_2-h_1)+a(T_2-T_1)(L_v+h_2-h_1) = 0 \quad (A49)$$

$$c(L_v)(T_3-T_2)-b\left[(L_v)(T_3-T_2)+(T_2-T_1)(L_v+h_2-h_1)\right] +a(T_2-T_1)(L_v+h_2-h_1) = 0 \quad (A50)$$

$$\frac{a}{c} (T_2-T_1)(L_v+h_2-h_1)-\frac{b}{c} \left[(L_v)(T_3-T_2)+(T_2-T_1)(L_v+h_2-h_1)\right] +(L_v)(T_3-T_2) = 0 \quad (A51)$$

Working with (A47)

$$(c-b)(L_v)(T_4-T_3)-a(T_2-T_1)(L_v+h_3-h_1) = 0 \quad (A52)$$

$$\frac{a}{c} (T_2-T_1)(L_v+h_3-h_1)+\frac{b}{c} (L_v)(T_4-T_3)-(L_v)(T_4-T_3) = 0 \quad (A53)$$

(A51) and (A53) are of the form

$$Ax + By + C = 0 \text{ (from A51)}$$

$$Dx + Ey + F = 0 \text{ (from A52)}$$

Where

$$A = (T_2-T_1)(L_v+h_2-h_1)$$

$$B = -\left[(L_v)(T_3-T_2) + (T_2-T_1)(L_v+h_2-h_1)\right.$$

$$C = (L_v)(T_3-T_2)$$

$$D = (T_2-T_1)(L_v+h_3-h_1)$$

$$E = L_v\,(T_4-T_3)$$

$$F = -L_v\,(T_4-T_3)$$

$$x = \frac{a}{c}$$

$$y = \frac{b}{c}$$

To eliminate a term

$$ADx + BDy + CD = 0 \qquad (A54)$$

$$ADx + AEy + AF = 0 \qquad (A55)$$

Subtracting

$$(BD-AE)y + (CD-AF) = 0 \qquad (A56)$$

$$y = \frac{CD-AF}{AE-BD} \qquad (A57)$$

$$x = -\frac{(By + C)}{A} = -\frac{(Ey + F)}{D} \qquad (A58)$$

By substitution

$$\frac{b}{c} = \frac{\left[(L_v)(T_3-T_2)(T_2-T_1)(L_v+h_3-h_1)+(T_2-T_1)(L_v+h_2-h_1)(L_v)(T_4-T_3)\right]}{\{(T_2-T_1)(L_v+h_2-h_1)(L_v)(T_4-T_3)+\left[(L_v)(T_3-T_2)-(T_2-T_1)(L_v+h_2-h_1)\right](T_2-T_1)(L_v+h_3-h_1)\}} \qquad (A59)$$

$$\frac{a}{c} = \frac{\left[(L_v)(T_4-T_3)(b)-(L_v)(T_4-T_2)\right]}{(T_2-T_1)(L_v+h_3-h_1)} \qquad (A60)$$

$$\frac{a}{c} = \frac{(L_v)(T_1-T_3)(1-b)}{(T_2-T_1)(L_v+h_3-h_1)} \qquad (A61)$$

With no shield:

$$\frac{\dot{M}_o}{K} = \frac{(T_4-T_1)}{(L_v)(c)} \qquad (A62)$$

With one shield between flat plates for a unit area, the heat reaching the liquid is expressed by:

$$Q_1 = \frac{K\,(T_2-T_1)}{(c-a)} = \dot{M}\,L_v \qquad (A63)$$

The heat reaching the shield is:

$$Q_2 = \frac{K(T_4-T_2)}{a} = \dot{M}\,L_v + \dot{M}\,(h_2-h_1) \qquad (A64)$$

Where:

T_1 = Temperature of liquid

T_2 = Temperature of shield

T_3 = T_2

T_4 = Temperature of outer surface of insulation

a = Thickness of insulation between outer surface and shield

b = a

c = Thickness between hot wall and cold wall

h_1 = Enthalpy of gas leaving tank at T_1

h_2 = Enthalpy of gas leaving shield

From (A63)

$$\dot{M} = \frac{K\,(T_2-T_1)}{L_v\,(c-a)} \qquad (A65)$$

Substituting (A65) into (A64) and dividing by K

$$\frac{(T_4-T_2)}{a} = \frac{(T_2-T_1)}{L_v(c-a)}\;(L_v + h_2 - h_1) \qquad (A66)$$

$$(c-a)(L_v)(T_4-T_2)-a(T_2-T_1)(L_v+h_2-h_1) = 0 \tag{A67}$$

$$c(L_v)(T_4-T_2)-a\left[(L_v)(T_4-T_2)+(T_2-T_1)(L_v+h_2-h_1)\right] = 0 \tag{A68}$$

$$\frac{a}{c} = \frac{b}{c} = \frac{(L_v)(T_4-T_2)}{(L_v)(T_4-T_2)+(T_2-T_1)(L_v+h_2-h_1)} \tag{A69}$$

$$\frac{a}{c} = \frac{b}{c} = \frac{(L_v)(T_4-T_2)}{(L_v)(T_4-T_2)+(T_2-T_1)(L_v+h_2-h_1)} \tag{A70}$$

$$\frac{\dot{M}}{K} = \frac{(T_2-T_1)}{L_v\left(1-\frac{a}{c}\right)} \tag{A71}$$

An equilibrium temperature (T_4) of 300°R and tank pressure of 50 psia were used for the plotted curves. The method of calculation is as follows:

1. Equation A59 was solved for "b", letting c=1 and assuming a number of fixed values of T_2 while varying T_3.

   A curve of $\frac{b}{c}$ versus $\frac{T_3}{T_1}$ was plotted for each T_2.

2. Equation A61 was then solved for "a" letting c=1 and assuming a set of fixed values for T_2 while varying T_3. The values of "b" found in Step 1 were used. The same set of T_2 values were used as were used in solving A59. A curve of $\frac{a}{c}$ versus $\frac{T_3}{T_1}$ was plotted for each T_2.

3. Equation A44 was solved for $\frac{\dot{M}}{K}$ assuming the same set of fixed values for T_2 as were used to solve A59 and A61. The values of "b" found in Step 1 were used.

4. Equation A62 was solved for $\frac{\dot{M}_o}{K}$ letting c=1.

5. The results of Step 3 were divided by the results of Step 4 yielding $\dot{M}/\dot{M}_o$ values. These values were plotted versus T_3/T_1 for the same set of fixed values of T_2 as were used to solve A59 and A61.

6. From the three curves

$$\frac{b}{c} \text{ versus } \frac{T_3}{T_1}$$

$$\frac{a}{c} \text{ versus } \frac{T_3}{T_1}$$

$$\frac{\dot{M}}{\dot{M}_o} \text{ versus } \frac{T_3}{T_1}$$

it was possible to select particular values for $\frac{a}{c}$ and plot the curves shown in Figures A19 through A23.

To complete the curves for the portion to the left of the fixed $\frac{a}{c}$ which represent the one shield case, and to plot the comparison curve A18 for one shield, equations A70 and A71 were solved as follows:

1. Equation A70 was solved for $\frac{a}{c}$ for a range of T_2.
2. Equation A71 was solved for $\frac{\dot{M}}{K}$ for the same range of T_2 used in Step 1 using $\frac{a}{c}$ values from Step 1.
3. The results of Step 2 were divided by $\frac{\dot{M}_o}{K}$ from equation A62 to yield $\frac{\dot{M}}{\dot{M}_o}$. Curve A18 was plotted using this information.

2.2 Dual Vapor-Cooled Shield Analysis Based on Stefan-Boltzmann Equation

Equations and derivations are given below. The results are plotted in Figures A24 through A27. The curves should be read as follows:

1. For a given location of the warmer shield $(\frac{a}{c})$, read the ratio of the shielded boil-off to the unshielded boil-off $\frac{\dot{M}}{\dot{M}_o}$ for all locations of the colder shield which lie on the colder side of the warmer shield. At all locations on the warmer side of the warmer shield, the plotted values represent one shield only.

2. The ratio of the shield temperature to the unshielded insulation temperature at that location is read from the $\frac{T_3}{T_1}$, and $\frac{T_2}{T_1}$ curves for both shields. At all locations on the warmer side of the warmer shield, the plotted values represent one shield only.

When: $N + 1 \cong N$, shields are equally spaced. The heat per unit area reaching the liquid is expressed by:

$$Q_1 = \sigma (T_2^4 - T_1^4) \frac{\epsilon}{(c-b)(2-\epsilon)} = \dot{M} L_v \qquad (A72)$$

FIGURE A18
BOIL-OFF FOR VAPOR SHIELDED HYDROGEN TANKS
BASED ON FOURIER EQUATION

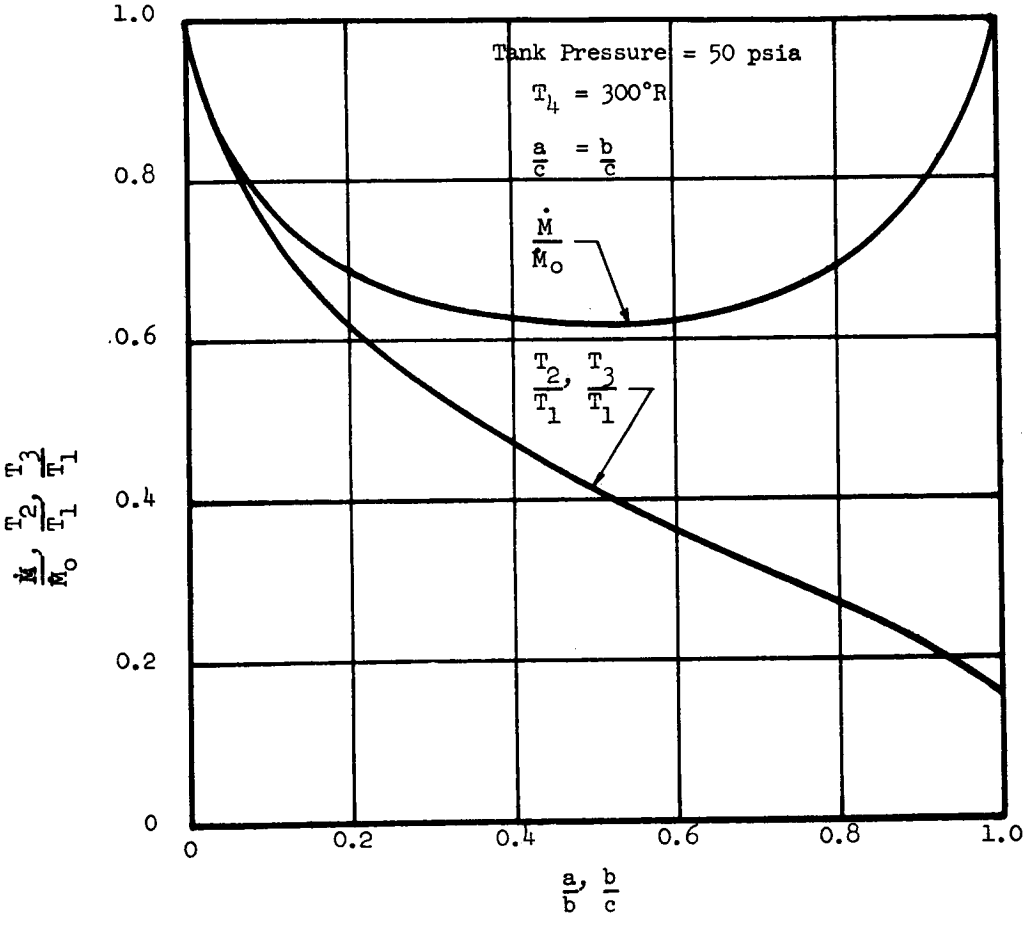

$\dot{M}_o$ = Unshielded Boil-Off Flow Rate
$\dot{M}$ = Shielded Boil-Off Flow Rate
T_1 = Stored Liquid Temperature
T_2 = Colder Shield Temperature
T_3 = Warmer Shield Temperature
a = Hot Wall to Warmer Shield Distance
b = Hot Wall to Colder Shield Distance
c = Hot Wall to Cold Wall Distance

FIGURE A19
BOIL-OFF FOR VAPOR SHIELDED HYDROGEN TANKS
BASED ON FOURIER EQUATION

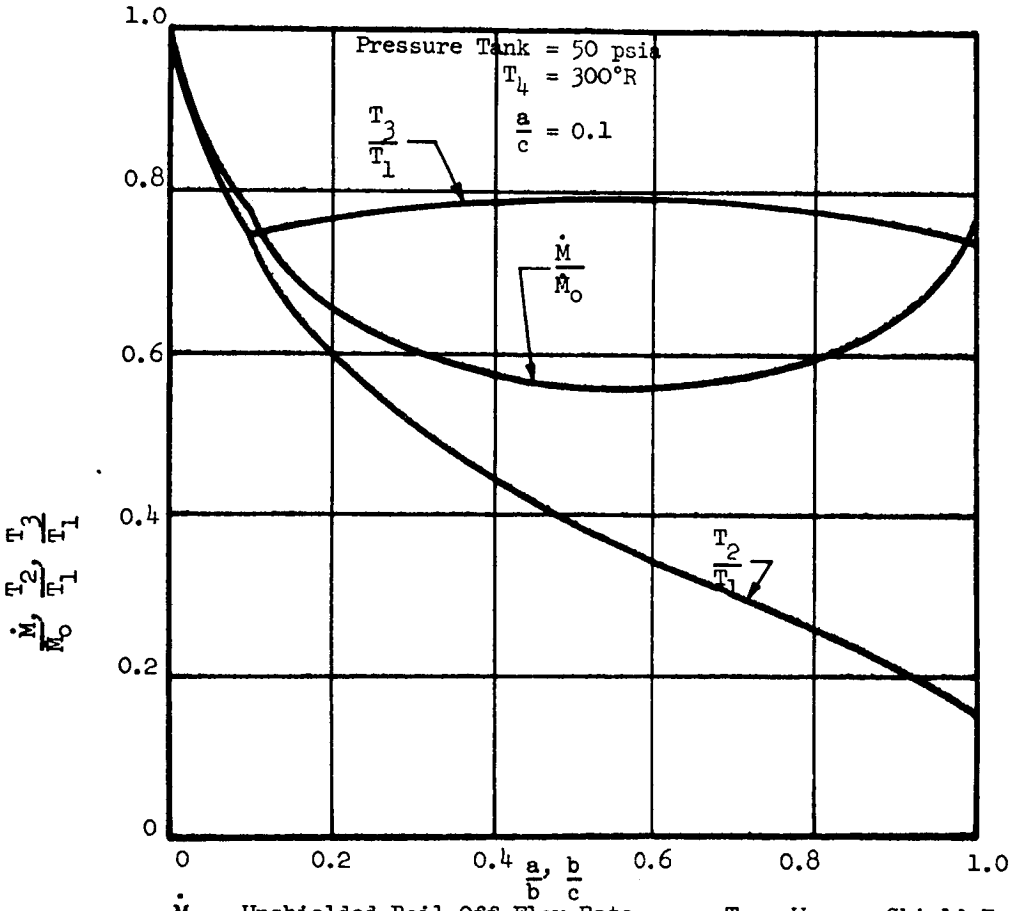

$\dot{M}_o$ = Unshielded Boil-Off Flow Rate

$\dot{M}$ = Shielded Boil-Off Flow Rate

T_1 = Stored Liquid Temperature

T_2 = Colder Shield Temperature

T_3 = Warmer Shield Temperature

a = Hot Wall to Warmer Shield Distance

b = Hot Wall to Colder Shield Distance

c = Hot Wall to Cold Wall Distance

FIGURE A20
BOIL-OFF FOR VAPOR SHIELDED HYDROGEN TANKS
BASED ON FOURIER EQUATION

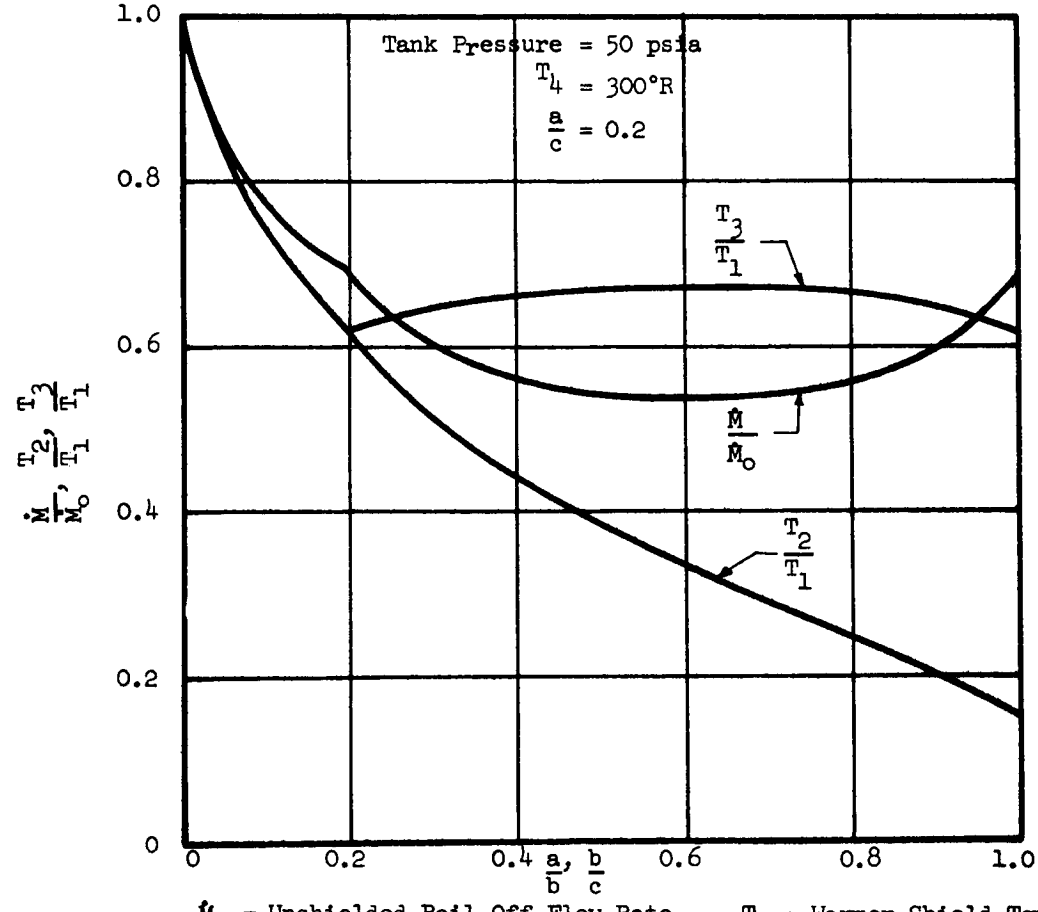

$\dot{M}_o$ = Unshielded Boil-Off Flow Rate
$\dot{M}$ = Shielded Boil-Off Flow Rate
T_1 = Stored Liquid Temperature
T_2 = Colder Shield Temperature
T_3 = Warmer Shield Temperature
a = Hot Wall to Warmer Shield Distance
b = Hot Wall to Colder Shield Distance
c = Hot Wall to Cold Wall Distance

FIGURE A21
BOIL-OFF FOR VAPOR SHIELDED HYDROGEN TANKS
BASED ON FOURIER EQUATION

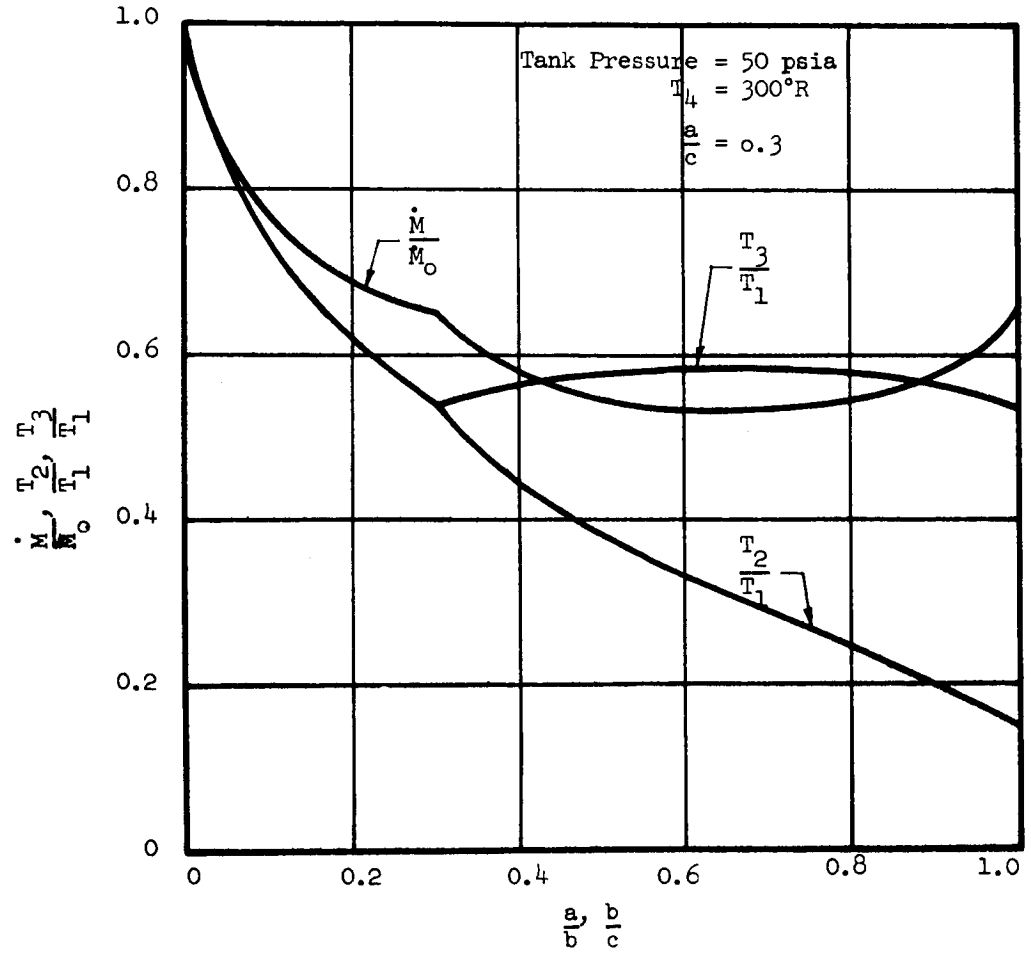

$\dot{M}$ = Unshielded Boil-Off Flow Rate
$\dot{M}_o$ = Shielded Boil-Off Flow Rate
T_1 = Stored Liquid Temperature
T_2 = Colder Shield Temperature
T_3 = Warmer Shield Temperature
a = Hot Wall to Warmer Shield Distance
b = Hot Wall to Colder Shield Distance
c = Hot Wall to Cold Wall Distance

FIGURE A22
BOIL-OFF FOR VAPOR SHIELDED HYDROGEN TANKS
BASED ON FOURIER EQUATION

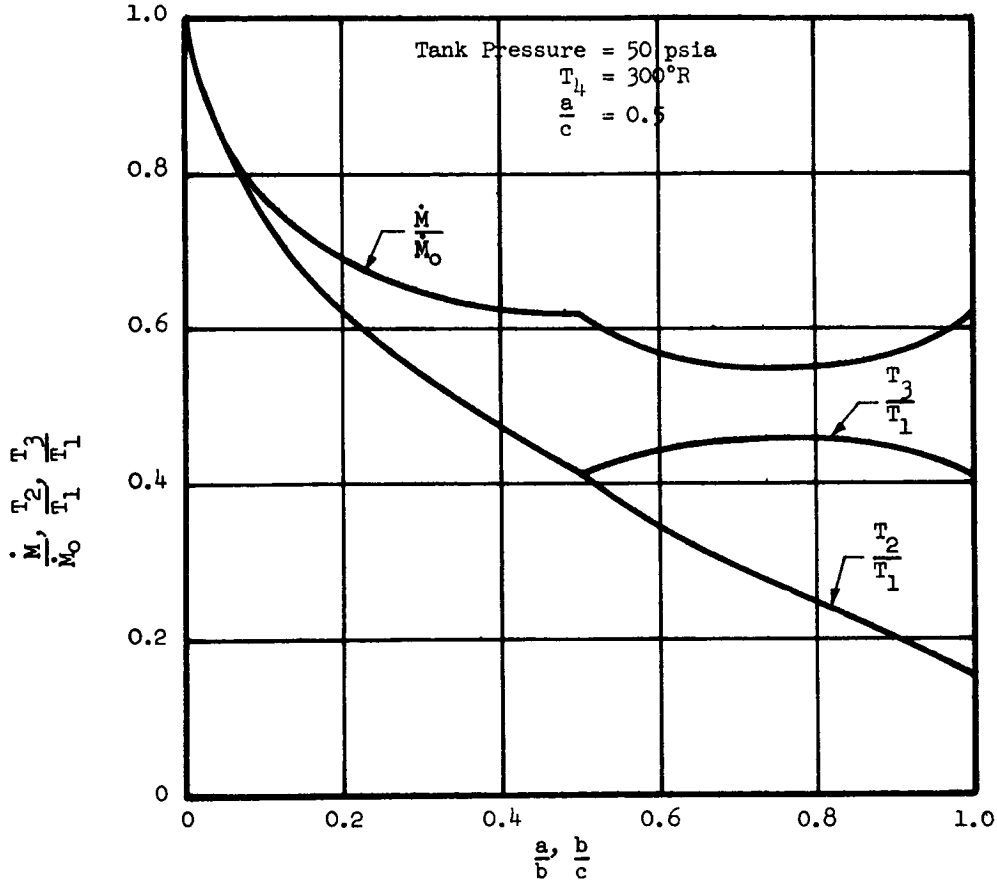

$\dot{M}$ = Unshielded Boil-Off Flow Rate
$\dot{M}^o$ = Shielded Boil-Off Flow Rate

T_1 = Stored Liquid Temperature

T_2 = Colder Shield Temperature

T_3 = Warmer Shield Temperature

a = Hot Wall to Warmer Shield Distance

b = Hot Wall to Colder Shield Distance

c = Hot Wall to Cold Wall Distance

FIGURE A23
BOIL-OFF FOR VAPOR SHIELDED HYDROGEN TANKS
BASED ON FOURIER EQUATION

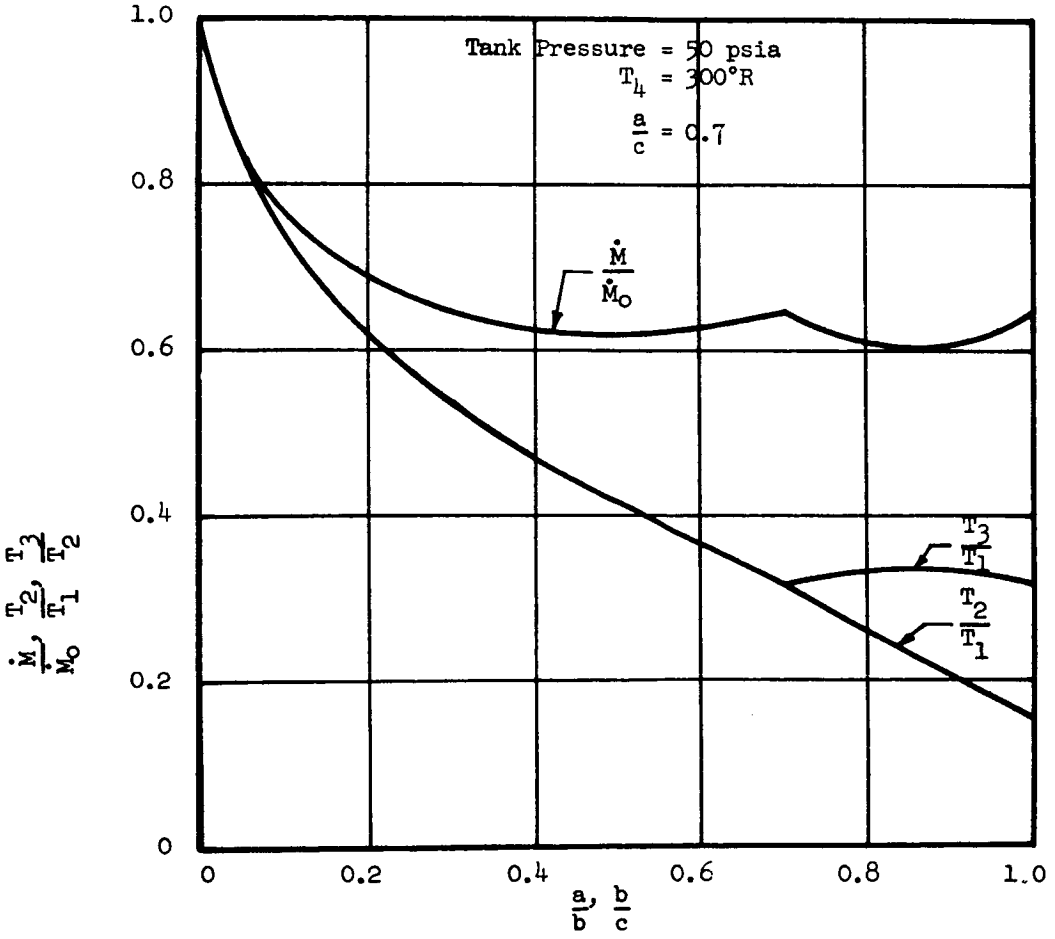

$\dot{M}$ = Unshielded Boil-Off Flow Rate
$\dot{M}^o$ = Shielded Boil-Off Flow Rate

T_1 = Stored Liquid Temperature

T_2 = Colder Shield Temperature

T_3 = Warmer Shield Temperature

a = Hot Wall to Warmer Shield Distance

b = Hot Wall to Colder Shield Distance

c = Hot Wall to Cold Wall Distance

The heat reaching the colder shield is:

$$Q_2 = \sigma (T_3^4 - T_2^4) \frac{\epsilon}{(b-a)(2-\epsilon)} = \dot{M} L_v + \dot{M} (h_2 - h_1) \qquad (A73)$$

The heat reaching the warmer shield is:

$$Q_3 = \sigma (T_4^4 - T_3^4) \frac{\epsilon}{a(2-\epsilon)} = \dot{M} L_v + \dot{M} (h_2 - h_1) + \dot{M}(h_3 - h_2) \qquad (A74)$$

Where
- σ = Stefan-Boltzmann constant
- ϵ = Emissivity of radiation barriers
- T_1 = Temperature of liquid
- T_2 = Temperature of colder shield
- T_3 = Temperature of warmer shield
- T_4 = Temperature of outer surface of insulation
- a = Thickness of insulation from warm wall to warmer shield
- b = Thickness of insulation from warm wall to colder shield
- c = Thickness of insulation from cold wall to warm wall
- $\dot{M}$ = Boil-off rate
- L_v = Latent heat of vaporization
- h_1 = Enthalpy of gas leaving tank
- h_2 = Enthalpy of gas leaving colder shield
- h_3 = Enthalpy of gas leaving warmer shield

From (A72)

$$M = \sigma (T_2^4 - T_1^4) \frac{\epsilon}{L_v (c-b)(2-\epsilon)} \qquad (A75)$$

Substituting (A75) into (A72) and cancelling terms:

$$\frac{(T_4^4 - T_3^4)}{a} - \frac{(T_2^4 - T_1^4)}{L_v (c-b)} (L_v + h_3 - h_1) = 0 \qquad (A76)$$

$$(c-b)(L_v)(T_4^4-T_3^4)-a(T_2^4-T_1^4)(L_v+h_3-h_1) = 0 \quad (A77)$$

$$(T_2^4-T_1^4)(L_v+h_3-h_1)+b(L_v)(T_4^4-T_3^4)-c(L_v)(T_4^4-T_3^4) = 0 \quad (A78)$$

$$\frac{a}{c}(T_2^4-T_1^4)(L_v+h_3-h_1)+\frac{b}{c}(L_v)(T_4^4-T_3^4)-(L_v)(T_4^4-T_3^4) = 0 \quad (A79)$$

Substituting (A75) into (A73) and cancelling terms:

$$\frac{(T_3^4-T_2^4)}{(b-a)} - \frac{(T_2^4-T_1^4)}{L_v(c-b)}(L_v+h_2-h_1) = 0 \quad (A80)$$

$$(c-b)(L_v)(T_3^4-T_2^4)-(b-a)(T_2^4-T_1^4)(L_v+h_2-h_1) = 0 \quad (A81)$$

$$a(T_2^4-T_1^4)(L_v+h_2-h_1)-b\left[(L_v)(T_3^4-T_2^4)+(T_2^4-T_1^4)(L_v+h_2-h_1)\right]+ c(L_v)(T_3^4-T_2^4) = 0 \quad (A82)$$

$$\frac{a}{c}(T_2^4-T_1^4)(L_v+h_2-h_1)-\frac{b}{c}\left[(L_v)(T_3^4-T_2^4)+(T_2^4-T_1^4)(L_v+h_2-h_1)\right]+ (L_v)(T_3^4-T_2^4) = 0 \quad (A83)$$

(A79) and (A83) are of the form:

$$Ax + By + C = 0 \quad (A84)$$

$$Dx + Ey + F = 0 \quad (A85)$$

Where:

$$A = (T_2^4-T_1^4)(L_v+h_2-h_1)$$

$$B = -\left[(L_v)(T_3^4-T_2^4)+(T_2^4-T_1^4)(L_v+h_2-h_1)\right]$$

$$C = (L_v)(T_3^4-T_2^4)$$

$$D = (T_2^4 - T_1^4)(L_v + h_3 - h_1)$$

$$E = L_v(T_4^4 - T_3^4)$$

$$F = -(L_v)(T_4^4 - T_3^4)$$

$$x = \frac{a}{c}$$

$$y = \frac{b}{c}$$

To eliminate a term:

$$ADx + BDy + CD = 0 \tag{A86}$$

$$ADx + AEy + AF = 0 \tag{A87}$$

Subtracting

$$(BD-AE)y + (CD-AF) = 0 \tag{A88}$$

$$y = \frac{CD-AF}{AE-BD} \tag{A89}$$

$$x = \frac{-(By + C)}{A} = -\frac{(Ey+F)}{D} \tag{A90}$$

Substituting terms:

$$\frac{b}{c} = \frac{(L_v)(T_3^4 - T_2^4)(T_2^4 - T_1^4)(L_v + h_3 - h_1) + (T_2^4 - T_1^4)(L_v + h_2 - h_1)(L_v)(T_4^4 - T_3^4)}{(T_2^4 - T_1^4)(L_v + h_2 - h_1)(L_v)(T_4^4 - T_3^4) + \left[(L_v)(T_3^4 - T_2^4)(T_2^4 - T_1^4)(L_v + h_2 - h_1)\right]}$$

$$\frac{1}{(T_2^4 - T_1^4)(L_v + h_3 - h_1)} \tag{A91}$$

$$\frac{a}{c} = \frac{-\left[(L_v)(T_4^4 - T_3^4)(b) - (L_v)(T_4^4 - T_3^4)\right]}{(T_2^4 - T_1^4)(L_v + h_3 - h_1)} \tag{A92}$$

$$\frac{a}{c} = \frac{(L_v)(T_4^4 - T_3^4)(1-b)}{(T_2^4 - T_1^4)(L_v + h_3 - h_1)} \qquad (A93)$$

With no shield:

$$Q_o = \sigma (T_4^4 - T_1^4) \frac{\epsilon}{c(2-\epsilon)} = \dot{M}_o L_v \qquad (A94)$$

$$\dot{M}_o = \frac{\sigma (T_4^4 - T_1^4) \epsilon}{(L_v)(c)(2-\epsilon)} \qquad (A95)$$

An equilibrium temperature T_4 of 300°R and tank pressure of 50 psia were used for the plotted curves. The method of calculation is as follows:

1. Equation A91 was solved for "b", letting c=1 and assuming a number of fixed values of T_2 while varying T_3.

   A curve of $\frac{b}{c}$ versus $\frac{T_3}{T_1}$ was plotted for each T_2.

2. Equation A93 was then solved for "a" letting c=1 and assuming a set of fixed values for T_2 while varying T_3. The values of "b" found in Step 1 were used. The same set of T_2 values were used as were used in solving A91. A curve of $\frac{a}{c}$ versus $\frac{T_3}{T_1}$ was plotted for each T_2.

3. Equation A75 was solved for $\dot{M}$ assuming the same set of fixed values for T_2 as were used to solve A91 and A93. The values of "b" found in Step 1 were used.

4. Equation A95 was solved for $\dot{M}_o$ letting c=1.

5. The results of Step 3 were divided by the results of Step 4 yielding $\frac{\dot{M}}{\dot{M}_o}$ values. These values were plotted versus $\frac{T_3}{T_1}$ for the same set of fixed values of T_2 as were used to solve A91 and A93.

6. From the three curves

   $\frac{b}{c}$ versus $\frac{T_3}{T_1}$

$\frac{a}{c}$ versus $\frac{T_3}{T_1}$

$\frac{\dot{M}}{\dot{M}_o}$ versus $\frac{T_3}{T_1}$

it was possible to select particular values for $\frac{a}{c}$ and plot the curves shown in Figures A24 through A27.

To complete the curves for the portion to the left of the fixed $\frac{a}{c}$ which represent the one shield case, and to plot the comparison curve A24 for one shield the data of Appendix A, Section 1.2 was used (See Figures A12 and A13).

FIGURE A24
BOIL-OFF FOR VAPOR SHIELDED HYDROGEN TANKS
BASED ON STEFAN-BOLTZMANN EQUATION

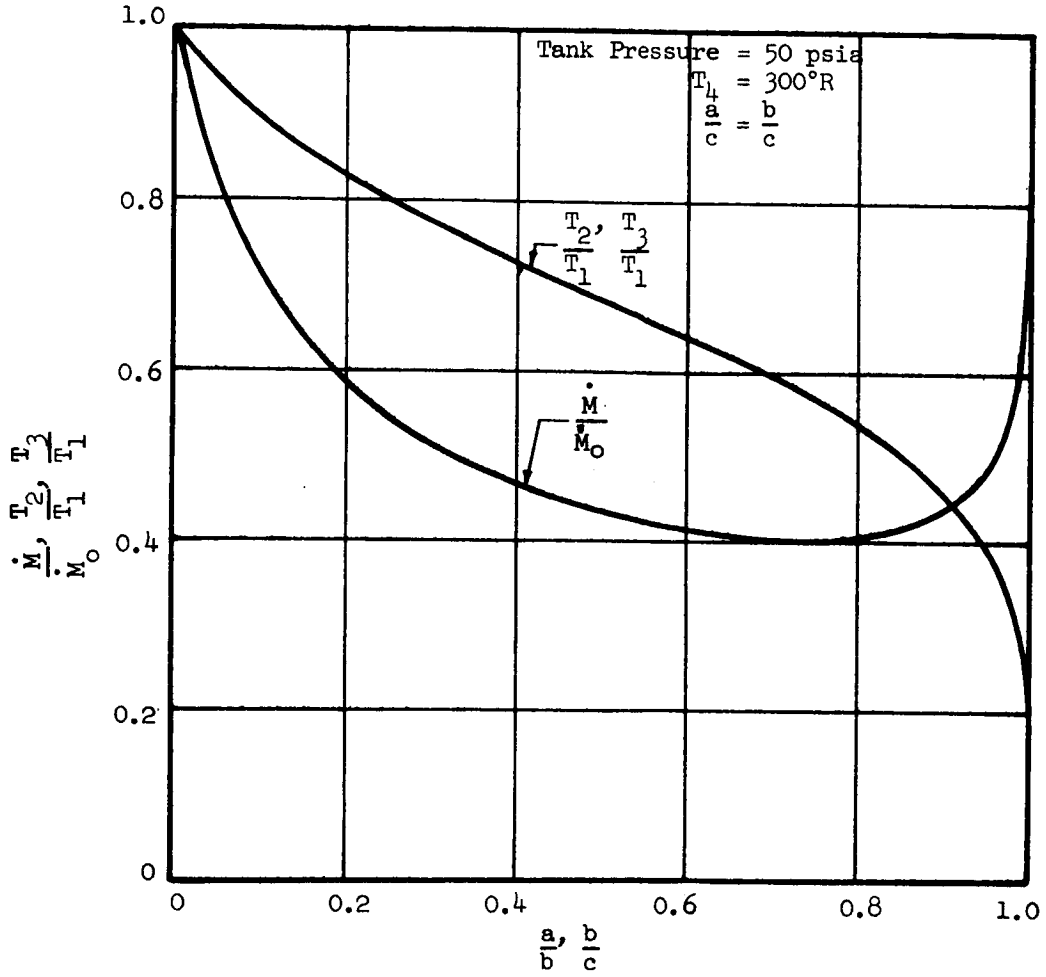

$\dot{M}_o$ = Unshielded Boil-Off Flow Rate
$\dot{M}$ = Shielded Boil-Off Flow Rate
T_1 = Stored Liquid Temperature
T_2 = Colder Shield Temperature
T_3 = Warmer Shield Temperature
a = Hot Wall to Warmer Shield Distance
b = Hot Wall to Colder Shield Distance
c = Hot Wall to Cold Wall Distance

FIGURE A25
BOIL-OFF FOR VAPOR SHIELDED HYDROGEN TANKS
BASED ON STEFAN-BOLTZMANN EQUATION

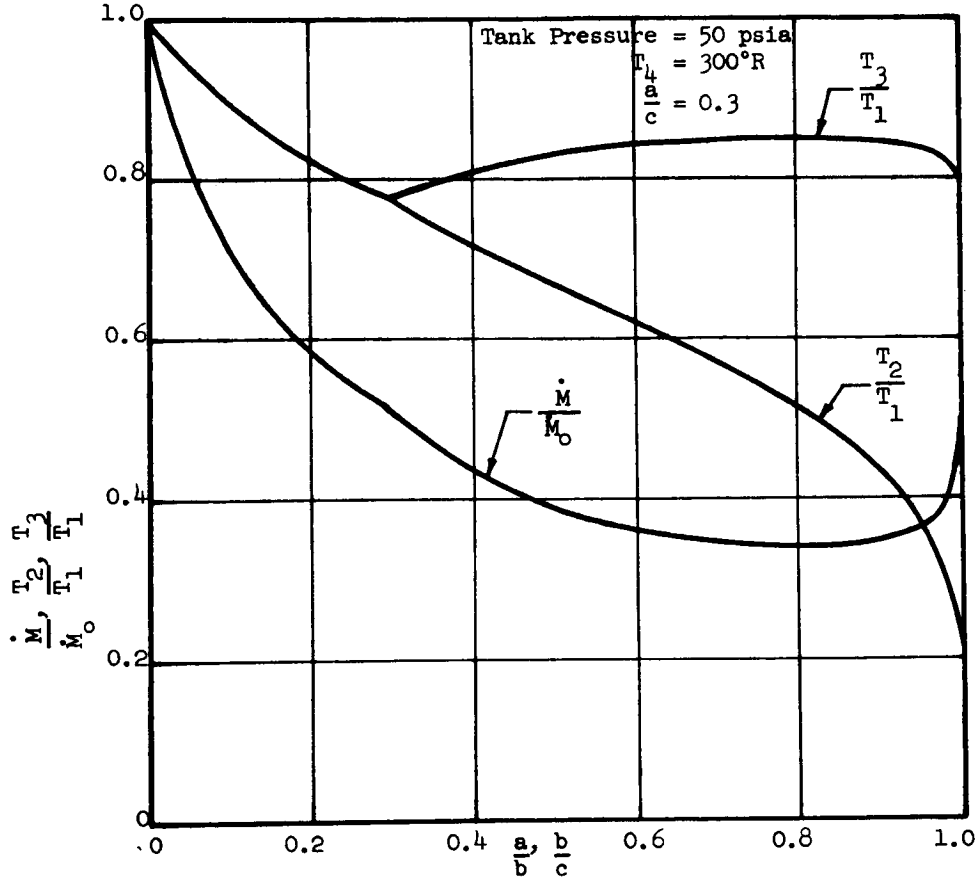

$\dot{M}_o$ = Unshielded Boil-Off Flow Rate

$\dot{M}$ = Shielded Boil-Off Flow Rate

T_1 = Stored Liquid Temperature

T_2 = Colder Shield Temperature

T_3 = Warmer Shield Temperature

a = Hot Wall to Warmer Shield Distance

b = Hot Wall to Colder Shield Distance

c = Hot Wall to Cold Wall Distance

FIGURE A26
BOIL-OFF FOR VAPOR SHIELDED HYDROGEN TANKS
BASED ON STEFAN-BOLTZMANN EQUATION

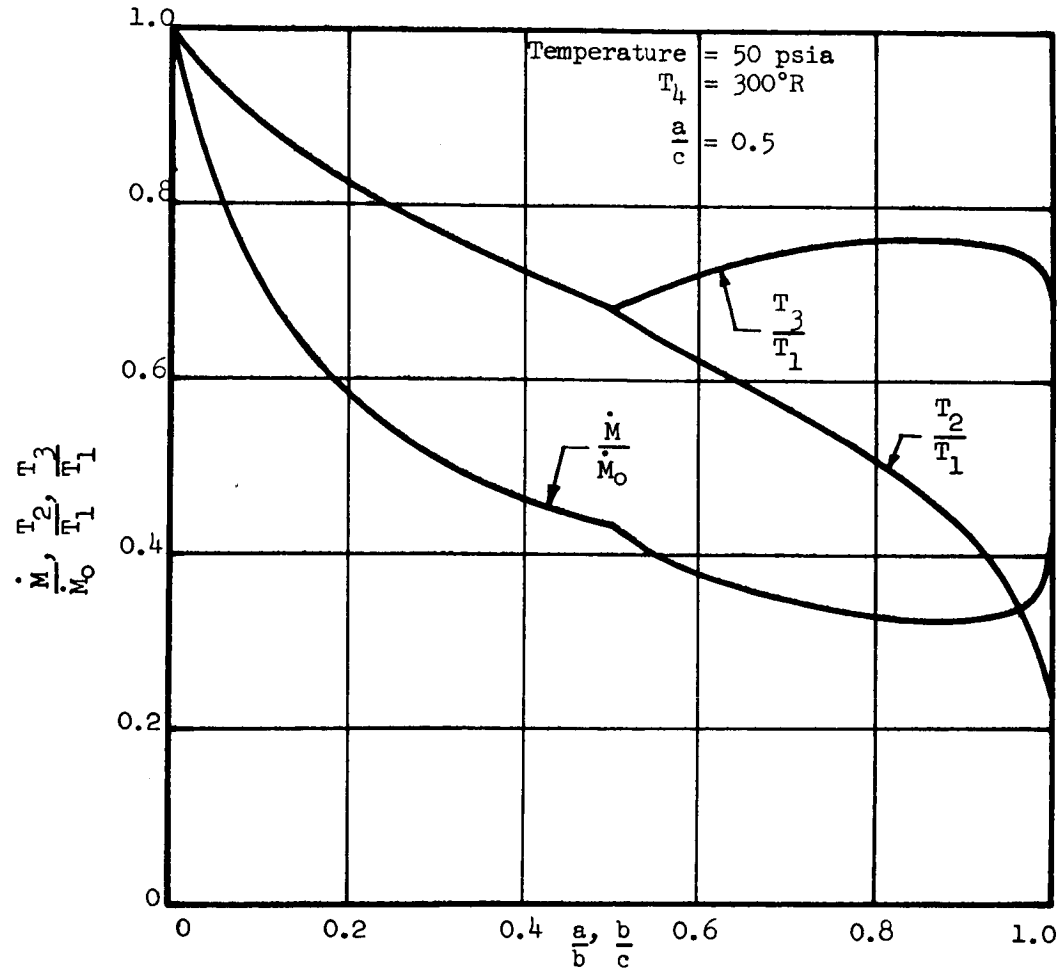

$\dot{M}$ = Unshielded Boil-Off Flow Rate
$\dot{M}_o$ = Shielded Boil-Off Flow Rate
T_1 = Stored Liquid Temperature
T_2 = Colder Shield Temperature
T_3 = Warmer Shield Temperature
a = Hot Wall to Warmer Shield Distance
b = Hot Wall to Colder Shield Distance
c = Hot Wall to Cold Wall Distance

FIGURE A27
BOIL-OFF FOR VAPOR SHIELDED HYDROGEN TANKS
BASED ON STEFAN-BOLTZMANN EQUATION

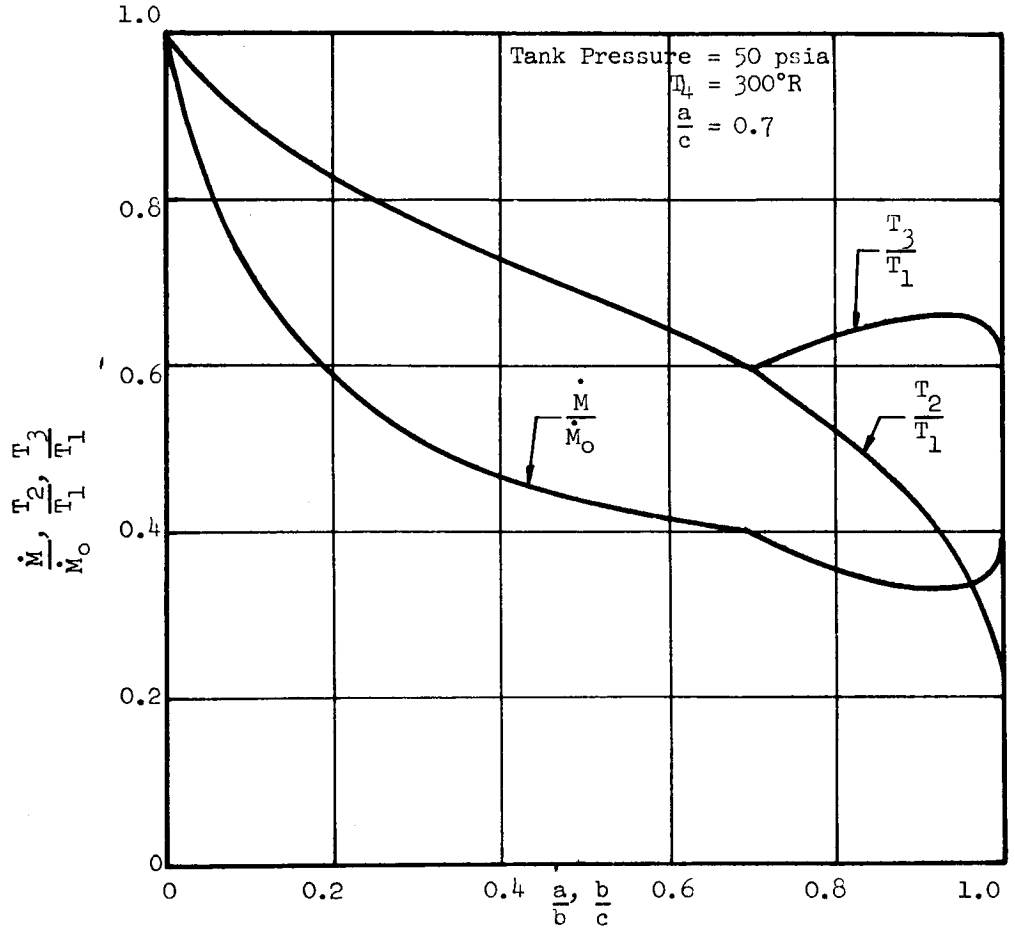

$\dot{M}$ = Unshielded Boil-Off Flow Rate
$\dot{M}_o$ = Shielded Boil-Off Flow Rate
T_1 = Stored Liquid Temperature
T_2 = Colder Shield Temperature
T_3 = Warmer Shield Temperature
a = Hot Wall to Warmer Shield Distance
b = Hot Wall to Colder Shield Distance
c = Hot Wall to Cold Wall Distance

APPENDIX B

1.0 Regenerative Gas Feed System Test Request

2.0 Test Description

The electrothermal tankage feed system will be qualitatively tested.

3.0 Schedule

1. Begin tests by May 2.
2. Complete tests by June 1.

4.0 Test Setup

5.0 Installation

1. Transport equipment to bunker where all tests shall be performed.
2. Install equipment into oxygen tank.
3. Evacuate vacuum space to at most 300 microns when the entire tank is heated to 200°F. A vacuum of less than 10 microns is required when the tank contains liquid hydrogen.
4. Connect readout equipment to pressure transducers. A strip chart record is desired in addition to pressure gages.
5. Connect liquid sensing resistors to ohm meters.
6. Attach helium bottle with regulator to solenoid valve container.
7. Charge valve container to 70 psig. An internal pressure between 60 and 80 psig is required during test runs.
8. Connect wet test flowmeters to gas delivery line.

6.0 Test Procedures

1. Purge the system by standard methods.
2. Fill tank with liquid hydrogen and close all valves except feed valve.
3. Close feed valve after tank is full and allow tank pressure to build up to operating pressure of 60 psi.
4. Adjust feed valve and fill valve, if necessary, for a flow of 0.07 pounds per hour through the feed line. The solenoid valve should be in the gas feed position.

5. Observe and record the following system operating characteristics during feed:

   a. Tank pressure
   b. Line pressure
   c. Liquid indication
   d. Relief valve operation
   e. Mass flow
   f. Solenoid valve operation

6. Change the position of the solenoid valve to the liquid feed position and observe any fluctuations in tank and line pressures and liquid indicators.

7. Switch from gas to liquid feed several times until the general system characteristics are known. By this time it should be possible to outline the exact test procedure for obtaining useful recorded data.

8. Perform tests flowing alternately liquid and gas as directed by Engineering. Record line and tank pressures and liquid sensor indications.

9. Test Precaution:

   Do not close the feed line valve all the way for more than a few seconds. A trap exists between the control valve and feed relief valve which can cause high line pressure due to heat leak.

APPENDIX C

1.0 General Structural Equations

1.1 Inner Radius of Pressure Vessel

The tank radius may be related to the mass of contained fluid by the equation:

$$R_1 = \left(\frac{3M_f}{4\pi\rho_f} \right)^{1/3} \qquad (C1)$$

1.2 Pressure Vessel Thickness

With the low pressures involved in this study the tank skin thickness is small so the following equation may be used with sufficient accuracy.

$$t_1 = \frac{P_1 R_1}{2\sigma_a} \qquad (C2)$$

A manufacturing tolerance and a corrosion allowance must be added to this value.

1.3 Inner Radius of Insulation

The insulation lies directly on the outer surface of the pressure vessel and this radius is:

$$R_2 = R_1 + t_1 \qquad (C3)$$

1.4 Outer Radius of Insulation

For this analysis both the load-bearing and non-load-bearing insulation are assumed to have equal thermal conductivity. Only a small error is introduced here because the non-load-bearing insulation thickness is a small percentage of the total insulation thickness. The influence of the support shell thickness is neglected. The equation for the outer radius is:

$$R_3 = \frac{R_2}{1 + \frac{4\pi k R_2 (T_1 - T_2)}{\dot{M} L_v} \left(\frac{\dot{M} \text{ (Shielded)}}{\dot{M} \text{ (Unshielded)}} \right)} \qquad (C4)$$

The section on vapor-cooled shields (Section 2.1.1.1) in this report explains the use of $\frac{\dot{M} \text{ (Unshielded)}}{\dot{M} \text{ (Shielded)}}$, the shield boil-off reduction factor.

1.5 Support Shell Radius and Thickness

In this study the support shell is placed a constant distance, L, from the pressure vessel. The inner radius of the support shell is:

$$R_4 = R_2 + L \qquad (C5)$$

The support shell must be able to resist buckling caused by all inertial loads. From Section (C1) with a factor of two on pressure the thickness to resist buckling is:

$$t_2 = R_4 \left(\frac{P_2}{E} \right)^{1/2} [3(1-\nu^2)]^{1/4} \qquad (C6)$$

Based on inertial loads the thickness is:

$$t_2 = \frac{(M_f + W_1 + W_i)\, g}{2\pi R_4 (\sigma_a - R_4 \rho_t g)} \qquad (C7)$$

The larger of these two values is chosen for the support shell thickness.

1.6 Retracting Support Pins

The worst condition for the support pins is to treat them as cantilever beams with the support ring end being treated as the free end. For a beam:

FIGURE C1
CANTILEVER BEAM

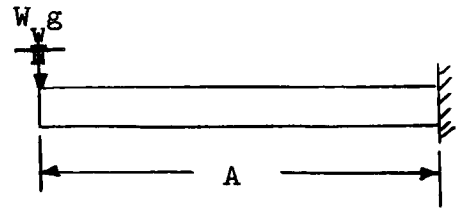

$$\sigma_a = \frac{Mc}{I} \tag{C8}$$

Where

$$M = \frac{W_w g A}{N} \tag{C9}$$

or

$$\frac{I}{c} = \frac{W_w g A}{N \sigma_a} \tag{C10}$$

The pin size may be calculated from $\left(\frac{I}{c}\right)$, the section modulus term.

2.0 Contact Stresses Between Retracting Pin and Support Lug

FIGURE C2
CONTACT STRESSES

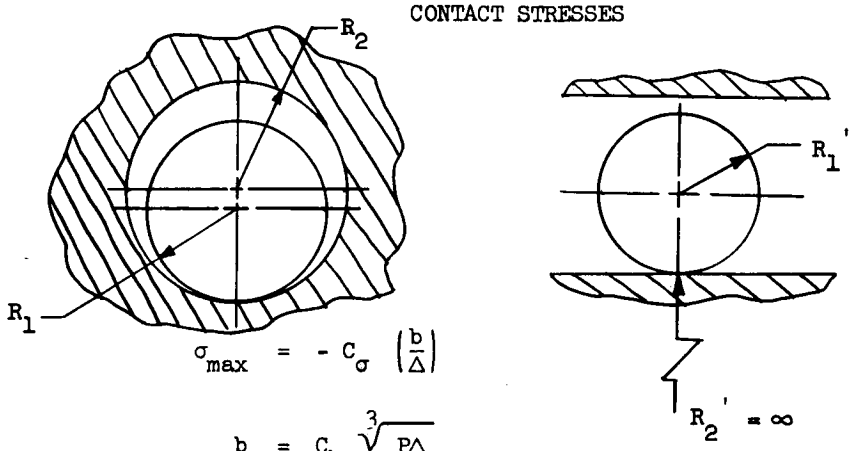

$$\sigma_{max} = - C_\sigma \left(\frac{b}{\Delta}\right) \tag{C11}$$

$$b = C_b \sqrt[3]{P\Delta} \tag{C12}$$

$$C_\sigma = f\left(\frac{B}{A}\right) \tag{C13}$$

$$C_b = f\left(\frac{B}{A}\right) \tag{C14}$$

$$\Delta = \frac{1}{A+B} \left(\frac{1-\nu_1^2}{E_1} + \frac{1-\nu_2^2}{E_2}\right) \tag{C15}$$

$$A = \frac{1}{4} \left(\frac{1}{R_1} + \frac{1}{R_2} + \frac{1}{R_1'} + \frac{1}{R_2'}\right) + \tag{C16}$$

$$\frac{1}{4}\sqrt{\left[\left(\frac{1}{R_1} - \frac{1}{R_1'}\right) + \left(\frac{1}{R_2} - \frac{1}{R_2'}\right)\right]^2 - 4\left(\frac{1}{R_1} - \frac{1}{R_1'}\right)\left(\frac{1}{R_2} - \frac{1}{R_2'}\right)\sin\alpha}$$

$$B = \frac{1}{4}\left(\frac{1}{R_1} + \frac{1}{R_2} + \frac{1}{R_1'} + \frac{1}{R_2'}\right) - \frac{1}{4}\sqrt{\left[\left(\frac{1}{R_1} - \frac{1}{R_1'}\right) + \left(\frac{1}{R_2} - \frac{1}{R_2'}\right)\right]^2 - 4\left(\frac{1}{R_1} - \frac{1}{R_1'}\right)\left(\frac{1}{R_2} - \frac{1}{R_2'}\right)\sin\alpha} \qquad (C17)$$

Where $R_1 = R_1'$

$R_2 = -R_2$

$R_2' = \infty$

$\alpha = 0$

$$A = \frac{1}{4}\left(\frac{1}{R_1} - \frac{1}{R_2} + \frac{1}{R_1}\right) + \frac{1}{4}\left[\left(\frac{1}{R_1} - \frac{1}{R_1}\right) + \left(-\frac{1}{R_2}\right)\right]$$

$$= \frac{1}{4}\left(\frac{2}{R_1} - \frac{1}{R_2} - \frac{1}{R_2}\right) \qquad (C18)$$

$$A = \frac{1}{2}\left(\frac{1}{R_1} - \frac{1}{R_2}\right) \qquad (C19)$$

$$B = \frac{1}{4}\left(\frac{1}{R_1} - \frac{1}{R_2} + \frac{1}{R_1}\right) - \frac{1}{4}\left[\left(\frac{1}{R_1} - \frac{1}{R_1}\right) - \frac{1}{R_2}\right]$$

$$= \frac{1}{4}\left(\frac{2}{R_1} - \frac{1}{R_2} + \frac{1}{R_2}\right) \qquad (C20)$$

$$B = \frac{1}{2}\left(\frac{1}{R_1}\right) \qquad (C21)$$

$$\frac{B}{A} = \frac{\frac{1}{2}\left(\frac{1}{R_1}\right)}{\frac{1}{2}\left(\frac{1}{R_1} - \frac{1}{R_2}\right)} = \frac{\frac{1}{R_1}}{\frac{R_2 - R_1}{R_1 R_2}} \qquad (C22)$$

$$\frac{B}{A} = \frac{R_2}{R_2 - R_1} \tag{C23}$$

$$\Delta = \frac{1}{\frac{1}{2}\left(\frac{1}{R_1} - \frac{1}{R_2}\right)} + \frac{1}{2}\left(\frac{1}{R_1}\right)\left(\frac{1 - \nu_1^2}{E_1} + \frac{1 - \nu_2^2}{E_2}\right) \tag{C24}$$

$$= \frac{1}{\frac{1}{2}\left(\frac{2}{R_1} - \frac{1}{R_2}\right)} \left(\frac{1 - \nu_1^2}{E_1} + \frac{1 - \nu_2^2}{E_2}\right)$$

$$= \frac{2}{2\,\frac{R_2 - R_1}{R_1 R_2}} \left(\frac{1 - \nu_1^2}{E_1} + \frac{1 - \nu_2^2}{E_2}\right)$$

$$\Delta = \frac{2 R_1 R_2}{2 R_2 - R_1} \left(\frac{1 - \nu_1^2}{E_1} + \frac{1 - \nu_2^2}{E_2}\right) \tag{C25}$$

Values for C_σ and C_b, as a function of B/A, may be found in Section C2.

3.0 Discontinuity Stresses

The preceding equations for the shells have been only for those areas which are in the pure membrane condition. Additional analysis is required in areas where discontinuities exist. The following sections show the equations which are required to determine the discontinuity stresses.

3.1 Shell-Support Ring Juncture

Discontinuity Stress

FIGURE C3
SHELL-RING JUNCTURE

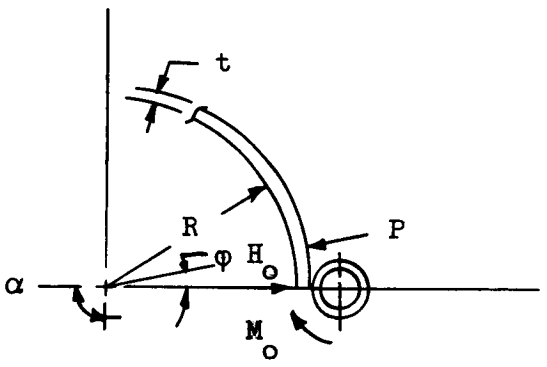

From Section C3

$$\sigma_\varphi = -\left[\frac{2\lambda}{Rt}\cot(\alpha-\varphi)\,\Omega(\lambda\varphi) \mp \frac{6}{t^2}\,\Phi(\lambda\varphi)\right]\left[\frac{PR^2(1-\nu)}{4\lambda^2}\right]$$

$$-\left[\frac{1}{t}\cot(\alpha-\varphi)\,\Psi(\lambda\varphi) \pm \frac{6}{\lambda t^2}\,\Omega(\lambda\varphi)\right]\left[\frac{PR(1-\nu)}{2\lambda}\sin\alpha\right] \quad (C26)$$

$$\sigma_\theta = \left[\frac{2\lambda^2}{Rt}\,\Psi(\lambda\varphi) \pm \frac{6}{t^2}\,\Phi(\lambda\varphi)\right]\left[\frac{PR^2(1-\nu)}{4\lambda^2}\right]$$

$$-\left[\frac{2\lambda}{t}\,\theta(\lambda\varphi) \pm \frac{6\nu R}{\lambda t^2}\,\Omega(\lambda\varphi)\right]\left[\frac{PR(1-\nu)}{2\lambda}\right] \quad (C27)$$

Where

$$\lambda = \left[3(1-\nu^2)\frac{R_2}{t^2}\right]^{1/4} \quad (C28)$$

3.2 Change in Thickness of Spherical Shell

Discontinuity Stress

FIGURE C4
CHANGE IN THICKNESS

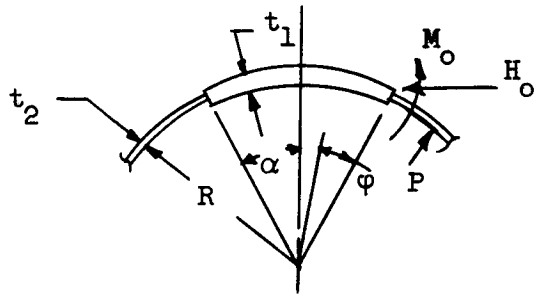

$$H_o = \frac{(1-\nu)\,R}{2\lambda_1 \sin\alpha}\left[\frac{(1-C)(1+C^{5/2})}{(1+C^2)^2 + 2C^{3/2}(1+C)}\right] P \qquad (C29)$$

$$M_o = \frac{(1-\nu)\,R}{4\lambda_1^{\,2}}\left[\frac{(1-C)(1-C^2)}{(1+C^2)^2 + 2C^{3/2}(1+C)}\right] P \qquad (C30)$$

$$C = \frac{h_1}{h_2} \qquad (C31)$$

$$\sigma_\varphi = -\left[\frac{2\lambda}{Rt_1}\cot(\alpha-\varphi)\,\Omega(\lambda\varphi) \mp \frac{6}{t_1^{\,2}}\,\Phi(\lambda\varphi)\right] M_o$$

$$-\left[\frac{1}{t_1}\cot(\alpha-\varphi)\,\Psi(\lambda\varphi) \pm \frac{6R}{\lambda t_1^{\,2}}\,\Omega(\lambda\varphi)\right]\left[H_o \sin\alpha\right] \qquad (C32)$$

$$\sigma_\theta = \left[2\lambda^2\,\Psi(\lambda\varphi) \pm \frac{6\nu}{t_1^{\,2}}\,\Phi(\lambda\varphi)\right] M_o$$

$$-\left[\frac{2\lambda}{t_1}\,\theta(\lambda\varphi) \pm \frac{6\nu R}{\lambda t_1^{\,2}}\,\Omega(\lambda\varphi)\right]\left[H_o \sin\alpha\right] \qquad (C33)$$

$$\lambda = \left[3\,(1-\nu^2)\,\frac{R^2}{t_1^{\,2}}\right]^{1/4} \qquad (C34)$$

3.3 Small Openings in Shell

FIGURE C5
SMALL HOLE

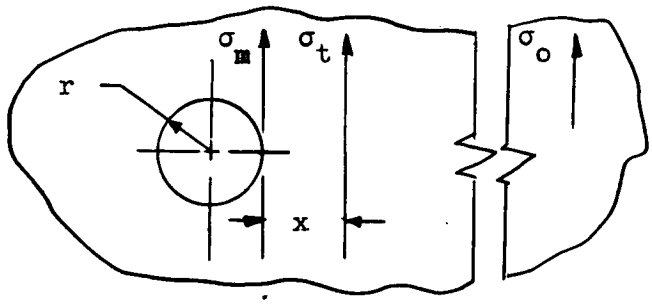

$$\sigma_t = \frac{\sigma_o}{2}\left(2 + \frac{r^2}{x^2} + \frac{3r^4}{x^4}\right) \qquad (C35)$$

when x = r

$$\sigma_t = \sigma_m = 3\sigma_o \qquad (C36)$$

For biaxial stress

$$\sigma_1 = -\nu\sigma_2 \qquad (C37)$$

$$\sigma_m = 3\,(\sigma_o - \nu\sigma_o) \qquad (C38)$$

$$\sigma_m = 3\sigma_o\,(1-\nu) \qquad (C39)$$

$$\sigma_t = \frac{\sigma_o}{2}\,(1-\nu)\left(2 + \frac{r^2}{x^2} + \frac{3r^4}{x^4}\right) \qquad (C40)$$

4.0 Support Ring

In sizing the support ring, a value for the outer radius, r_1, is chosen and from this the inner radius is determined from the equation:

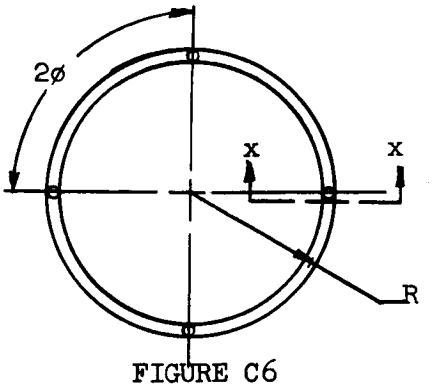

FIGURE C6
SUPPORT RING

$$r_2 = \left\{ r_1^4 - \frac{2r_1}{\pi\sigma_a} \left[M + (M^2+T^2)^{1/2} \right] \right\}^{1/4} \qquad \text{(C41)}$$

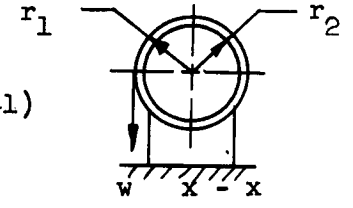

Where

$$M = WR^2 \, (M/WR^2) + WrR \, (M/WrR)$$

$$T = WR^2 \, (T/WR^2) + WrR \, (T/WrR)$$

$$\frac{M}{WR^2} = 1 - \left[\frac{\sin \phi \, (2G+E) - \phi \cos \phi \, (E)}{\frac{\phi}{2}(2G+E) + \frac{\sin 2\phi}{4}(2G-E)} \right] \cos \phi \qquad \text{(C42)}$$

$$\frac{T}{WR^2} = \phi - \left[\frac{\sin \phi \, (2G+E) - \phi \cos \phi \, (E)}{\frac{\phi}{2}(2G+E) + \frac{\sin 2\phi}{4}(2G-E)} \right] \sin \phi \qquad \text{(C43)}$$

$$\frac{M}{WrR} = \frac{G \sin 2\phi}{\frac{\phi}{2}(2G+E) + \frac{\sin 2\phi}{4}(2G-E)} - 1 \qquad \text{(C44)}$$

$$\frac{T}{WrR} = \frac{2G \sin^2 \phi}{\frac{\phi}{2}(2G+E) + \frac{\sin 2\phi}{4}(2G-E)} \qquad \text{(C45)}$$

The deflection of the ring at the midpoint between supports may be found from the equation:

$$\delta = \frac{WR^4}{4GEI}\left\{2G\,(1-\cos\phi)^2 + E\,(\phi-\sin\phi)^2 - [2G\sin^2\phi + E\,(1-\cos\phi)^2]\left[\frac{\sin\phi(2G+E)-\phi\cos\phi(E)}{\frac{\phi}{2}(2G+E)+\frac{\sin2\phi}{4}(2G-E)} - 1\right]\right\}$$

$$+ \frac{WrR^3}{4GEI}\left\{-(2G-E)(1-\cos\phi)^2 + [E(1-\cos\phi)^2 + 2G\sin^2\phi]\left[\frac{2G\sin\phi}{\frac{\phi}{2}(2G+E)+\frac{\sin2\phi}{4}(2G-E)} - 1\right]\right\} \quad (C46)$$

The rotation of the ring at the midpoint is:

$$\theta = \frac{WR^3}{4GEI}\left\{2E(\phi\sin\phi) - 2\,(2G+E)(1-\cos\phi) + (2G-E)\sin^2\phi + (2G-E)\sin^2\phi\left[\frac{\sin\phi\,(2G+E) - \phi\cos\phi\,(E)}{\frac{\phi}{2}(2G+E) + \frac{\sin 2\phi}{4}(2G-E)} - 1\right]\right\}$$

$$+ \frac{WrR^2}{4GEI}\left\{2G(1-\cos\phi)^2 + E\sin^2\phi - (2G-E)\sin^2\phi\left[\frac{2\,G\sin\phi}{\frac{\phi}{2}(2G+E) + \frac{\sin 2\phi}{4}(2G-E)} - 1\right]\right\} \quad (C47)$$

This analysis assumes the load, W, to be uniform and the support lugs to be fixed.

SYMBOLS

R_1 = Inner radius of pressure vessel

R_2 = Outer radius of pressure vessel

R_3 = Outer radius of insulation

R_4 = Inner radius of support shell

P_1 = Inner pressure

P_2 = Outside pressure

T_1 = Inside temperature

T_2 = Outside temperature

E = Modulus of elasticity

G = Transverse modulus of elasticity

W_1 = Weight of pressure vessel

W_2 = Weight of support shell

W_i = Weight of insulation

W_w = Total wet weight of tank

M_f = Total weight of fluid

L = $R_4 - R_2$

I = Moment of inertia

k = Thermal conductivity of insulation

M = Moment

N = Number of supports

L_v = Latent heat of vaporization

t_1 = Thickness of pressure vessel

t_2 = Thickness of support shell

c = Distance to outer fiber

g = Acceleration in gravity units

$\dot{M}$ = Mass flow rate

$\frac{\dot{M}\ (\text{Unshielded})}{\dot{M}\ (\text{Shielded})}$ = Boil-off reduction factor

w_i = Weight of load-bearing insulation

ρ_f = Density of fluid

ρ_t = Density of shells

ρ_i = Density of insulation

ν = Poisson's ratio

σ_a = Allowable stress

σ_φ = Meridional stress

σ_θ = Circumferential stress

$\Omega(\lambda\varphi) = e^{-\lambda\varphi} \sin \lambda\varphi$

$\Phi(\lambda\varphi) = e^{-\lambda\varphi} (\cos \lambda\varphi + \sin \lambda\varphi)$

$\theta(\lambda\varphi) = e^{-\lambda\varphi} \cos \lambda\varphi$

$\Psi(\lambda\varphi) = e^{-\lambda\varphi} (\cos \lambda\varphi - \sin \lambda\varphi)$

Additional symbols are shown on Figures C1 through C6.